Parameterization of Knotted Surfaces Arising from Classical and Welded Knots

विद्या वाचस्पति की
उपाधि की अपेक्षाओं की आंशिक पूर्ति में प्रस्तुत शोध प्रबंध

A thesis submitted in partial fulfillment of the requirements
of the degree of Doctor of Philosophy

द्वारा / By

टुम्पा माहातो / Tumpa Mahato

पंजीकरण सं. / Registration No.: 20183612

शोध प्रबंध पर्यवेक्षक / Thesis Supervisor:

Prof. Rama Mishra

भारतीय विज्ञान शिक्षा एवं अनुसंधान संस्थान पुणे
INDIAN INSTITUTE OF SCIENCE EDUCATION AND RESEARCH
PUNE
2024

Dedicated to Maa, Babu, Didi and Bhai

Certificate

Certified that the work incorporated in the thesis entitled "Parameterization of Knotted Surfaces Arising from Classical and Welded Knots", submitted by Tumpa Mahato was carried out by the candidate, under my supervision. The work presented here or any part of it has not been included in any other thesis submitted previously for the award of any degree or diploma from any other University or institution.

Rama Mishra

Prof. Rama Mishra

Date: 27/11/2024

Declaration

Name of Student: Tumpa Mahato
Reg. No.: 20183612
Thesis Supervisor(s): Prof. Rama Mishra
Department: Department of Mathematics
Date of joining program: 1st August, 2018
Date of Pre-Synopsis Seminar: 21st June, 2024

Title of Thesis: Parameterization of Knotted Surfaces Arising from Classical and Welded Knots

I declare that this written submission represents my idea in my own words and where others' ideas have been included; I have adequately cited and referenced the original sources. I declare that I have acknowledged collaborative work and discussions wherever such work has been included. I also declare that I have adhered to all principles of academic honesty and integrity and have not misrepresented or fabricated or falsified any idea/data/fact/source in my submission. I understand that violation of the above will be cause for disciplinary action by the Institute and can also evoke penal action from the sources which have thus not been properly cited or from whom proper permission has not been taken when needed.

The work reported in this thesis is the original work done by me under the guidance of Prof. Rama Mishra.

Date: 27/11/2024

Tumpa Mahato.

Tumpa Mahato

Acknowledgments

First and foremost, I would like to express my deep gratitude to Prof. Rama Mishra, my research supervisor, for her patient guidance, enthusiastic encouragement, and useful critiques of this research work. Additionally, I wish to thank Dr. Tejas Kalelkar and Prof. P. Ramadevi for their advice and assistance in keeping my progress on schedule. I am also grateful to Prof. Louis Kauffman for all the helpful discussions and suggestions. Also, my seniors, Visakh and Sahil, thank you for guiding and encouraging me.

My sincere thanks also go to the members of my thesis committee for their insightful comments and suggestions, which were invaluable in improving the quality of this document. I also acknowledge the support received from my funding agency, CSIR. Without this support the research journey would not have been feasible.

I am deeply grateful to my family: Babu, Maa, Didi and Bhai. Their love, prayers, and sacrifices, without which I would not have been able to be in this position where I am. Their trust in my abilities kept me going even when I was not confident. I come from a middle-class family where money was always an issue. However, my father and sister always ensured that it would not be a problem in my academic journey. I am feeling blessed to have you as my family. I also want to thank two persons, Ravi and Rahul, who have always been there for me as a family and guided me to make decisions.

I cannot forget to thank all my friends, Sujeet, Pavan, Dhruv, Mitesh, Visakh, Namrata, Ramya, Keerti, Rashi, Maheswari, Abhishek, Shreerang, Shivshankar, Pranjal, Jewel, Sushant, Veer, Aniruddha, Shumyla, Latika, Bhavna, all players of Oceans' Eleven. I was truly overwhelmed by all the support and love I received from them.

I would like to thank my teachers, Rajib Basu, Prof. Hridoy Kumar Mondol, Kalyan Halder, Prof. Samit Bhattacharyya, Dr Vivek Mallick, Dr Debargha Banerjee, Dr Tejas Kalelkar, Prof. Akhil Ranjan, Prof. Amit Hogadi, Prof. Anupam Singh.

I also want to thank my institute, IISER Pune. This campus will always be in my heart. Joining this institute was a dream come true. I found a new version of me and learned so many things. Specifically, participating in IISM, IPL was a life-changing experience for a person who had never played anything before coming to IISER.

I also want to thank the Mathematics office staff, Suvarna and Yogesh. They have been extremely helpful and nice to me. I also want to thank Sayalee from the academic office for her service and polite behaviour.

Contents

List of Figures

List of Tables

Abstract

In this thesis we discuss how to parameterize certain two dimensional knots in four space using simple polynomial functions. More specifically we have taken up 2 dimensional sphere S^2 and the torus T^2 embedded inside S^4 or $\mathbb{R}^4$ as examples of knotted surfaces. We also touch upon knotted planes of special type, as non-compact 2 dimensional knots referred as the long 2 knots.

It is difficult to provide a general scheme to parameterize all surface knots since a structural classification of surface knots is still not well understood. We have chosen those knotted surfaces which arise from some known 1 dimensional knot theories such as of the classical knots, long knots and the welded knots. For example, given a classical knot one can obtain knotted spheres using spun and twist spun constructions. Similarly using a result of S. Satoh, knotted tori can be obtained as a tube of some welded knot. Likewise, knotted planes can be obtained using the theory of long knots and also from slice knots. In this thesis, we have used a polynomial parameterization of a long knot K to parameterize the spun of K and the d twist spun of K for all $d \geq 1$. To parameterize ribbon torus knots, trigonometric parameterizations of classical knots are utilized. Knotted planes are constructed using a parameterization of a long knot. In each case we have described a method to explicitly construct a parametrization. We have also demonstrated our results by examples and included the plots of their 3 dimensional projection obtained using *Mathematica*.

In knot theory one of the main questions is to detect if a given knot is non-trivial. We have answered this for the ribbon torus knots by ensuring the associated welded knots have their fundamental groups not isomorphic to $\mathbb{Z}$. In this thesis, we have discussed some invariants of welded knots that are un-knot detectors. We have examined for few families of classical knots (such as torus knots of type $(2, 2n + 1)$ and twist knots) how to obtain different non-trivial ribbon torus knots by welding few of the crossings in their standard diagrams.

Chapter 1

Introduction

Classical knot theory focuses on studying knots in 3-dimensional space and it helps in understanding 3-manifolds. It is natural to wonder if knots in higher dimensional spaces could help understanding higher dimensional manifolds. The question now is: if the ambient space is chosen to be $\mathbb{R}^n$ for $n \geq 4$, how do we see knots there? It is known that one can certainly obtain knots when an $(n-2)$ dimensional submanifold is embedded inside a manifold of dimension n [**Vir**]. Thus after learning about knots in $\mathbb{R}^3$ the next case would be to study 2 dimensional manifolds embedded in $\mathbb{R}^4$. In order to develop a good understanding of these embedded submanifolds, it will be helpful to find their defining functions so that we can see their 3-dimensional projections on different hyper surfaces. We call these embeddings as parametrizations of the embedded manifolds. This thesis discusses the methods of obtaining a parametrization for some 2-dimensional manifolds such as sphere, torus and plane embedded inside $\mathbb{R}^4$ or S^4. Once we have an embedding of a manifold inside $\mathbb{R}^4$, how do we ensure that it is non-trivial (truly knotted!). This thesis also answers this question for each situation. The embeddings of manifolds such as S^2 and T^2 inside $\mathbb{R}^4$ come under the surface knots which are compact, whereas the embeddings of $\mathbb{R}^2$ in $\mathbb{R}^4$ are long 2-knots which are non-compact. The theory of surface knots in 4-space was initiated with a paper by Artin [**Art**] in 1925 where he defined a method to construct knotted spheres, called *Spinning*. By the late 1950s and early 1960s, surface knot theory had undergone a significant development, and its beauty and richness were soon realized. Many variations of spinning construction [**Lit**] were defined to obtain knotted surfaces. Also

diagrammatic surface knot theory, surface braid theory and various invariants for surface knots were subsequently defined [**Kam**],[**CarSai**]. Some of the numerical invariants such as the *sheet number* [**Sat09**] and the *triple point number* [**Sat01**] can be estimated if an embedding that represents the surface knot is produced, i.e., if we can parameterize the knot. Also as three dimensional beings, we are unable to perceive objects in the four-dimensional space. Thus, visualizing and understanding knotted surfaces can be quite challenging. Therefore, parameterizing the knotted surfaces is not only useful from a combinatorial or computational perspective, but it also helps us develop our intuition and visual understanding of higher dimensional objects by stretching the limits of our imagination. Additionally, creating a computer program based on these parameterizations provides a practical way to engage with these abstract mathematical objects.

In classical knot theory, several parameterizations are studied, and the knots are referred to as Parameterized knots, e.g. *Polynomial knots, Fourier knots* [**Kau98**], *Lissajous Knots* [**Bog**] etc. Polynomial knots actually represent *long knots* which are embeddings of $\mathbb{R}$ in $\mathbb{R}^3$. It is known that polynomial parameterization exists for every long knot [**Sha**],[**Shu**]. It was easier to parameterize classical knots because there is an enumeration based on crossing numbers, and each knot can be represented by various preferred diagrams that help in guessing the functions that parameterize the knot. On the other hand, a meaningful enumeration or classification for knotted surfaces is hardly known. However, there are ways to obtain knotted surfaces from classical knots. The first geometric construction, called *Spinning*, was introduced by Artin [**Art**] and was later generalized by Zeeman's *Twist spinning* [**Zee**]. These two constructions give knotted spheres in 4-space called *Spun 2-knot* and *d-Twist Spun 2-knot*, respectively. Many other constructions for knotted spheres are also introduced later, e.g. Roll spinning, Super spinning, and Deform spinning [**Lit**]. We have used the polynomial parameterization of long knots to generate a parametrization for spun 2-knots and d-twist spun 2-knots, which, upon using a suitable polynomial approximation, results in a polynomial parameterization of these knotted spheres.

Moving on with the next surface, torus, we consider a particular class of knotted tori, known as the *ribbon torus knots* , that are related to another 1 dimensional knot theory known as the *welded knot theory*. We show that these can be parameterized using the known parameterization of classical knots. In 1999, the combinatorial per-

spective of classical knots took a new direction when L. Kauffman defined a more general type of knots, termed virtual knots [**Kau99**]. New generalized moves were defined for virtual knot diagrams. Additionally, there are two other diagrammatic moves, referred to as "over" and "under forbidden moves". Allowing both these moves in a virtual knot diagram results in a trivial diagram, hence the term "forbidden" is justified. But allowing only over forbidden move with generalized virtual moves results in a new non-trivial knot theory, called *welded knot theory* which is distinct from the virtual knot theory. In this thesis, while working with welded knots a virtual crossing is referred as a welded crossing.

Yajima [**Yaj**] showed that to each classical knot diagram, one can associate a ribbon torus-knot in $\mathbb{R}^4$ constructed by means of a tube map. Later S. Satoh extended the domain to the set of all virtual knot diagrams and proved the converse showing that every ribbon torus-knot T corresponds to a virtual knot diagram K such that $\text{Tube}(K) \cong T$. This pair (T, K) is referred to as a virtual knot presentation of T. Naturally, we will want the corresponding tubes of two isotopic virtual knot diagrams to be isotopic. That is true only if two virtual knot diagrams are welded equivalent i.e they are related by finite sequence of generalized Reidemeister moves and the over forbidden move. It is important to note that the tube map fails to be injective, as pointed out by Winter [**Win**]. This means that the non-triviality of a welded knot does not guarantee the non-triviality of a ribbon torus knot. At the surface knot level, we have the *unknotting conjecture* which states that a surface knot F is topologically unknotted if and only if $\pi_1(S^4 \setminus F)$ is isomorphic to $\mathbb{Z}$. However the unknotting conjecture has been proved only for 2-spheres [**Fre**], and for surfaces of genus g when $g \neq 1, 2$ [**Hil-Kaw**],[**Con-Pow**]. Despite the unknotting conjecture being open, a knotted torus T will certainly be non-trivial if $\pi_1(S^4 \setminus T)$ turns out to be not isomorphic to $\mathbb{Z}$. Here, the following results of Satoh that show the connection between welded knots and ribbon torus knots on a knot group level become crucial in the study of non-triviality of ribbon torus knots.

Theorem. [**Sat00**] Let T be a ribbon torus knot in $\mathbb{R}^4$ and K be the associated virtual knot such that $T = Tube(K)$.

Proposition. [**Sat00**] Let $\pi_1(\mathbb{R}^4 \setminus T)$ be the fundamental group of the complement of T in $\mathbb{R}^4$ and $G(K)$ be the fundamental group of the virtual knot K. Then

$$\pi_1(\mathbb{R}^4 \setminus T) \cong G(K).$$

Corollary. [**Sat00**] If K and K' are welded equivalent, i.e, isotopic up to all generalized Reidemeister moves and over forbidden move, then $G(K) \cong G(K')$.

Therefore, even though a non-trivial welded knot is not sufficient to produce a non-trivial ribbon torus knot, a welded knot with a knot group that is not isomorphic to $\mathbb{Z}$ will definitely correspond to a non-trivial ribbon torus knot. To produce examples of non-trivial ribbon torus knots, we have taken few families of classical knots and converted them into welded knots by marking few crossings to be welded. We compute the knot group of these welded knots and prove that these groups are not isomorphic to $\mathbb{Z}$.

At present very few invariants are known for welded knots. Knot group is one invariant which is generalized for both virtual and welded knots in a completely combinatorial sense. In the case of classical knots, it is proved to be an unknot detecter i.e a knot K is trivial iff $\pi_1(S^3 \setminus K) \cong \mathbb{Z}$. For virtual knots it does not detect virtual unknot. There exist non-trivial virtual knots with knot group $\mathbb{Z}$. For example, trefoil knot diagram with one of the crossings as virtual crossing is non-trivial as the jones polynomial is non-trivial but the knot group is isomorphic to $\mathbb{Z}$ [**Kau99**]. But it is still unknown if the knot group of a welded knot can detect unknot. Therefore, it is crucial to define and compute new invariants in order to study welded knots. In this thesis, we will study one invariant of welded knots, called the "*welded unknotting number*," which is defined as the minimum number of crossings needed to be changed from classical to welded to obtain a trivial welded diagram across all diagrams of a welded knot. We will also explore its relation with other invariants, such as the warping degree [**LiLeiWu**] and classical unknotting number.

A smooth embedding of S^2 in S^4 naturally produces a smooth embedding of $\mathbb{R}^2$ in $\mathbb{R}^4$ which is proper. These are known as *long 2-knots* in the literature. For a general long 2-knot, a generic projection may have double point curves and triple points as its singularity and one has to keep track of these singularities to write a parameterization. In this thesis, we have taken the simplest situation in which a long 2-knot has a projection into some hyper surface having only double point curves as singularities. We call them as *simple long 2-knots*. In [**Mis14**] the author has defined an invariant for classical knots known as the singularity index and related it with the unknotting number of knots. In this thesis we extend the notion of singularity index for long 2-knots and show that a polynomial parameterization of a long knot can be

used to produce a parameterization of a simple, long 2-knot and the singularity index of the polynomial knot provides a bound on the singularity index of the resulting long 2-knot.

Here is the outline of the thesis:

This thesis is divided into seven chapters with Chapter 1 as the Introduction. Chapter 2 covers all the basic definitions and materials necessary for this thesis. It is divided into 6 sections. Section 2.1 has several subsections and it reviews 1 dimensional combinatorial knots and some of their important invariants. 2.1.1 introduces classical knot theory briefly. 2.1.2 introduces virtual and welded knots and discusses fundamental group or knot group for these knots. Next, 2.1.3 discusses results involving unknotting number, crossing number and triviality of welded knots. 2.1.4 discusses "warping degree" of a welded knot which is used as a tool to understand unknotting number of welded knots. Section 2.2 contains all concepts that is necessary to introduce the theory of knotted surfaces in 4-dimensional space. Section 2.3 focuses on constructions of some knotted spheres, called spun 2-knots and d-twist spun 2-knots. In Section 2.4 we discuss ribbon torus knots which are related to welded knot theory by a special construction called *Tube map*. Section 2.5 discusses the *Tube map* in detail. We include some known results regarding parameterization of long knots and classical knots in Section 2.6.

In Chapter 3, we present methods of finding some functions for the parameterizations of spun 2-knots and d-twist spun 2-knots. In Section 3.1 we study the spun 2-knots and prove the following theorem:

Theorem (3.1.1)**.** Given a classical knot, there exist polynomials $f(t,s)$, $g(t,s)$, $h(t,s)$ and $p(t,s)$ in two variables t and s such that for some interval $[a,b]$ the image of $[a,b]\times[0,2\pi]$ under the map $\Phi:\mathbb{R}^2\to\mathbb{R}^4$ defined by

$$\Phi((t,s)) = (f(t,s), g(t,s), h(t,s), p(t,s))$$

is isotopic to the spun of K.

As a demonstration of our method we include explicit examples and figures generated using *Mathematica*.

In Section 3.2, we discuss d-twist spun 2-knots. The twist-spun construction

involves two types of rotations: one is around $\mathbb{R}^2$ in $\mathbb{R}^4$, called *spinning* and the other is around the axis of a 3-ball in $\mathbb{R}^3$ that contains the knotted part of the arc, called *twisting*. For the twist rotation, we use the Rodrigues rotation formula [**Rod**] and to restrict the rotation inside the 3-ball, we use bump functions. As these rotation formula involves various smooth functions, we replace all cosine, sine, bump functions with their Chebyshev approximations to get the final polynomial parameterization leading to the following :

Theorem (3.2.1)**.** Given a classical knot, there exist polynomials $f(t,\theta)$, $g(t,\theta)$, $h(t,\theta)$ and $p(t,\theta)$ in two variables t and θ such that for some interval $[a,b]$ the image of $[a,b]\times[0,2\pi]$ under the map $\Psi:\mathbb{R}^2\to\mathbb{R}^4$ defined by

$$\Psi(t,\theta)=\big(\bar{f}(t,\theta),\bar{g}(t,\theta),\bar{h}(t,\theta),\bar{p}(t,\theta)\big)$$

is isotopic to the d-twist spun 2-knot obtained from the given classical knot.

In Appendix A.1, A.2, A.4, the *Mathematica* programs of Chebyshev approximations and the examples of spun and d-twist spun knots are provided.

Chapter 4 discusses the welded knot invariants. It is divided in three sections. In Section 4.1, we find relations of the *welded unknotting number*, denoted by $u_w(K)$ with other invariants like warping degree $d(K)$ and classical unknotting number $u(K)$, given by the following theorems:

Theorem (4.1.2)**.** For every welded knot K, the welded unknotting number does not exceed the warping degree, i.e., $u_w(K)\leq d(K)$.

Theorem (4.1.3)**.** For every welded knot K, the welded unknotting number does not exceed twice of the unknotting number, i.e., $u_w(K)\leq 2u(K)$.

We also prove the following results regarding the welded unknotting number for two specific families of classical knot:

1. Torus knot family $K(2,2n+1)$ of type $(2,2n+1)$,
2. Twist knot family T_n with n number of half twists.

Theorem (4.1.4)**.** T_n has welded unknotting number 1 for all n.

Theorem (4.1.5)**.** Let $K(2,2n+1)$ denote the torus knot of type $(2,2n+1)$. Then

$$u_w(K(2,2n+1))\leq u(K(2,2n+1))=n.$$

In Section 4.2, we examine how welded knot groups help in finding non-trivial ribbon torus knots. In order to do this we weld few crossings in the standard classical diagrams of $K(2, 2n+1)$ and T_n and explore when the welded knot groups are not isomorphic to $\mathbb{Z}$. Here are the results we prove for the family $K(2, 2n+1)$. Let us denote the standard diagram of $K(2, 2n+1)$ with one welded crossing by $K_{n,1}$ and the standard diagram of $K(2, 2n+1)$ with two welded crossings with m_1 gap by $K_{n,2,m_1}$ respectively. Then we prove the following results for the knot groups of $K_{n,1}$ and $K_{n,2,m_1}$:

Theorem (4.2.1)**.** $G(K_{n,1}) \cong \mathbb{Z}$.

Theorem (4.2.3)**.**

$$G(K_{n,2,m_1}) \cong \mathbb{Z} \quad \text{when} \quad m_1 = n-1,$$
$$G(K_{n,2,m_1}) \ncong \mathbb{Z} \quad \text{when} \quad 1 \leq m_1 < n-1.$$

Using the connection of welded knots with ribbon torus knots as discussed in Section 2.5 we conclude that the corresponding ribbon torus knots in $\mathbb{R}^4$ are non-trivial as stated in the following:

Corollary (4.2.4)**.**

1. (a) $\pi_1\left(\mathbb{R}^4 - \text{Tube}(K_{n,2,m_1})\right) \cong \mathbb{Z}$ if $m_1 = n-1$.
   (b) $\pi_1\left(\mathbb{R}^4 - \text{Tube}(K_{n,2,m_1})\right) \ncong \mathbb{Z}$ if $1 \leq m_1 < n-1$.
2. The number of non-trivial ribbon torus knots obtained from the $K(2, 2n+1)$ with two weldings does not exceed $n-1$.

Now, for the twist knot family T_n, denote T_n with one welded crossing at the clasp region by $T_{n,1}$ and T_n with two welded crossings at the twist region with one gap by $T_{n,2,1}$ respectively. Then we prove the following results.

Theorem (4.2.5)**.**

$$G(T_{n,1}) = \left\langle a, b \;\middle|\; \begin{array}{c} (ab^{-1})^{\frac{n-2}{2}} a (ba^{-1})^{\frac{n-2}{2}} b = b(ab^{-1})^{\frac{n-4}{2}} a (ba^{-1})^{\frac{n-2}{2}}, \\ b(ab^{-1})^{\frac{n-2}{2}} = (ab^{-1})^{\frac{n-4}{2}} a \end{array} \right\rangle \cong \mathbb{Z}.$$

Theorem (4.2.6)**.** Let $G(T_{n,2,1})$ be the knot group of $T_{n,2,1}$. Then

$$G(T_{n,2,1}) \ncong \mathbb{Z} \quad \text{when } n \text{ is odd.}$$

Corollary (4.2.7)**.** If n is odd, then $\pi_1(\mathbb{R}^4 - \text{Tube}(T_{n,2,1})) \ncong \mathbb{Z}$.

We also have the following conjecture.

Conjecture (4.2.8)**.** If n is even, then $G(T_{n,2}) \ncong \mathbb{Z}$.

To prove the knot groups to be not isomorphic to $\mathbb{Z}$ we produce an epimorphism from these groups to some dihedral group and use the fact that the dihedral groups are non-abelian. Also in Section 4.3, we include a table of knot groups of all the welded knots that can be obtained from classical knots with six crossings.

After discussing the non-triviality of ribbon torus knots, we describe the methods to parameterize the ribbon torus knots by finding functions that represent the tube map in Chapter 5. As the tube map is defined in a manner that near a classical crossing the lower tube goes through the upper tube and to have a ribbon singularity the lower tube should be shrunk near the crossing. Also near a welded crossing, two tubes do not touch each other. So to parameterize ribbon torus knots we define two functions $S_c(t)$ and $S_w(t)$ for shrinking and displacing the tubes respectively. Using these functions, we have the following

Theorem (5.0.1)**.** Given a classical knot K with given trigonometric parameterization $\phi' : [0, 2\pi] \to \mathbb{R}^3$ given by

$$\phi'(t) = (f(t), g(t), h(t))$$

there exists functions $S_c(t)$ and $S_w(t)$ such that the image of $[0, 2\pi] \times [0, 2\pi]$ under the map $\tilde{\Psi} : \mathbb{R}^2 \to \mathbb{R}^4$ defined by

$$\tilde{\Psi}(t, s) = (f(t),\ (r - d_1 S_c(t))\, g(t) + \cos s,\ (r - d_1 S_c(t))\, g(t) + \sin s + d_2 S_w(t),\ h(t))$$

where $r, d_1, d_2 \in \mathbb{R}^+$, is isotopic to the $Tube(K)$.

We provide an explicit non-trivial example with *Mathematica* for a ribbon torus knot obtained from the torus knot $T(2, 7)$ in which two crossings are welded with a gap. The corresponding *Mathematica* program is included in Appendix A.5.

In Chapter 6, we extend the results related to polynomial representation of long knots ($\mathbb{R}$ in $\mathbb{R}^3$) for the case of long 2-knots ($\mathbb{R}^2$ in $\mathbb{R}^4$). We prove the following:

Theorem (6.0.1)**.** Every smooth long 2-knot ($\mathbb{R}^2 \to \mathbb{R}^4$) has a polynomial representation.

Theorem (6.0.5)**.** Let $\psi_0 \equiv (x_0, y_0, z_0, w_0)$ and $\psi_1 \equiv (x_1, y_1, z_1, w_1)$ be two polynomial embeddings of $\mathbb{R}^2$ in $\mathbb{R}^4$ which represent the isotopic 2-knots. Then ψ_0 and ψ_1 are polynomially isotopic.

A long 2-knot represented by a polynomial embedding is referred as a polynomial 2-knot. We introduce the term P-homotopy between two polynomial 2-knots and prove the following.

Theorem (6.0.7)**.** For every polynomial 2-knot F, there exists a P-homotopy that transforms F to a trivial surface knot.

We define the *Singularity Index* of long 2-knots and prove the following theorem.

Theorem (6.0.11)**.** Given a polynomial knot K, with singularity index n there exists a simple polynomial 2-knot P_K with singularity index less than or equal to n.

At the end of this chapter we present two constructions to obtain a long 2-knot from a polynomial knot using spun knot construction. In the first one, we construct a knotted disc bounded by $K \sharp K^*$, the connected sum [**Kaw**] of a knot K and its mirror image K^*. Then using a homotopy of long knots, we extend this disc to a plane as stated in the following.

Theorem (6.0.15)**.** For every polynomial knot K, there exists a knotted plane that contains a knotted disc bounded by $K \sharp K^*$.

In the second construction, we provide a method to place a knotted arc in $\mathbb{R}^3_+$ so that after spinning it in $\mathbb{R}^3$, we can obtain a polynomial 2-knot in $\mathbb{R}^4$. This is given by the following result.

Theorem (6.0.18)**.** For a polynomial knot K given by $\big\{(f(t), g(t), h(t)) \,|\, t \in \mathbb{R}\big\}$, there exists a polynomial 2-knot obtained from spinning operation with parameterization given by $\psi' : [a, \infty] \times [0, 2\pi] \to \mathbb{R}^4$ which is defined by

$$\psi'(t, s) = (f_1(t), g_1(t), h_1(t)\, S(s), h_1(t)\, C(s))\,.$$

Chapter 7 includes some concluding remarks and open problems. At the end, we have included the *Mathematica* notebooks for every example of parameterization. A detailed list of references is provided in the Bibliography.

Chapter 2

Preliminaries

In this chapter, we discuss the concepts that are necessary for this thesis. As there are notions used from various topics, we divide this chapter into several sections. If required, an individual section may have subsections.

2.1 Knotting, as a placement problem and 1-dimensional knot theories

Definition 2.1.1. Let M be a smooth manifold. An isotopy of M is a diffeomorphism $h : M \times I \to M \times I$ such that

(i) $h(M \times \{t\}) = M \times \{t\}$ for $0 \leq t \leq 1$, therefore for each t, there is a diffeomorphisms $h_t : M \to M$ such that $h(m, t)) = (h_t(m), t)$ for all $m \in M$.

(ii) h_0 is the identity on M.

Definition 2.1.2. Let M and N be two smooth manifolds. Let f and g be two smooth embeddings of $N \to M$. We say that f and g are isotopic if there exists an isotopy of M such that $h_1 \circ f = g$.

Isotopy is an equivalence relation on the set of smooth embeddings of N to M. Let $ISO(N \subset M)$ denote the set of isotopy classes of smooth embeddings from N to M. Let $HOM(N \subset M)$ denote the set of smooth homotopy classes of maps from

N to M. Clearly there is a natural onto map $F : ISO(N \subset M) \to HOM(N \subset M)$ since isotopic maps are clearly homotopic.

Definition 2.1.3. [**Zee61**] If the map $F : ISO(N \subset M) \to HOM(N \subset M)$ is also injective, we say that N unknots in M, otherwise we say N can get knotted.

Example 2.1.4.

(a) S^1 knots in S^3 as there are many isotopy classes of embeddings of S^1 in S^3 but there is only one homotopy class.

(b) A point unknots in any closed manifold but knots in a manifold with boundary, because there is one isotopy class for the interior of the manifold, and one for each boundary component.

Definition 2.1.5. [**EMB**] Let N be an embedded submanifold of M and $i : N \to M$ is the standard embedding of N given by the inclusion map. An embedding $f : N \to M$ represents an unknot if there exists a diffeomorphism $h : M \to M$ such that $h(f(N)) = i(N)$, i.e., we can place $f(N)$ in the same embedded position of N with the help of a diffeomorphism h.

One of the classical problems in topology is the *knotting problem*, i.e., classify embeddings of a manifold inside another manifold [**MAP**]. It has been shown that submanifolds of codimension 2 can get knotted [**Vir**]. Thus, we can obtain knotted embeddings of 1-dimensional closed manifolds inside any 3-manifold. If the 3-manifold happens to be S^3, it is the *classical knot theory*. Knots inside thickened surfaces are studied in *virtual knot theory*.

Both the classical knot theory and the virtual knot theory have been studied by several mathematicians. For a detailed exposition, one can refer to [**Kaw**] for the classical knot theory and [**Man**] for the virtual knot theory. There is a combinatorial improvement in virtual knot theory, which is known as the *welded knot theory*. Virtual knots are conceptualized as knots that lie on a thickened surface, but no such explanation is known for welded knots. In Section 2.1.1, we briefly introduce the classical knot theory. Sections 2.1.2 through 2.1.4 are devoted to the virtual and welded knot theories.

2.1.1 Classical knot theory

Definition 2.1.6. Ambient isotopy classes of 1-dimensional, closed submanifolds of S^3 are known as classical links. Single component links are called knots.

Definition 2.1.7. A long knot is an isotopy class of a proper, smooth embedding $\phi : \mathbb{R} \to \mathbb{R}^3$ such that as $|t| \to \infty$, $||\phi(t)|| \to \infty$.

We are going to use the term "knot" to refer to both knots and links. Classical knot theory is about classifying knots and links. Knot theorists have been discovering better and better invariants to solve this. Some invariants are numerical, e.g., crossing number, unknotting number, bridge number [**Sch**], and super bridge number [**Kui**]. Some are algebraic structures such as $\pi_1(S^3 \setminus K)$, and some are polynomials such as Jones polynomial. There are various approaches for defining invariants. One is the diagrammatic knot theory, in which knots are represented by a diagram drawn on paper. There can be several diagrams for the same knot, but the famous Reidemeister theorem takes care of it.

In another approach, knots are represented as the closure of a braid, and this representation is also not unique, but Markov's theorem resolves this issue. In this approach, the representation theory of braid groups is used to define many sophisticated quantum invariants.

The biggest challenge lies in computing these invariants. Diagrammatic knot theory has been very useful in providing simple combinatorial descriptions of many invariants. For example, the knot group $\pi_1(S^3 \setminus K)$ has a nice presentation (Wirtinger Presentation) describing generators and relations from any knot diagram. Also, finding a concrete embedding that represents a given knot (up to isotopy) turns out to be helpful in estimating some of the numerical invariants. These are known as parameterized knots. Fourier knots and polynomial knots are some examples of parameterized knots.

2.1.2 Virtual and welded knot theories

Louis Kauffman introduced the theory of virtual knots [**Kau99**] as a combinatorial generalization of classical knot theory. Virtual knots are studied by virtual diagrams in which a new type of crossing is introduced, called virtual crossing (Figure 2.1). When we project a classical knot on a plane, we get a 4-valent planar graph in which the vertices are the crossings of the knot, and we remove a part of the lower arc to provide the over/under crossing information at each vertex. A virtual diagram or a diagram of a virtual link is the image of an immersion of a 4-valent graph in $\mathbb{R}^2$ with a finite number of intersections of edges. Moreover, each intersection is a transverse double point, which we call a *virtual crossing* and is marked by a small circle, and each vertex of the graph is a classical crossing (with over/under information specified).

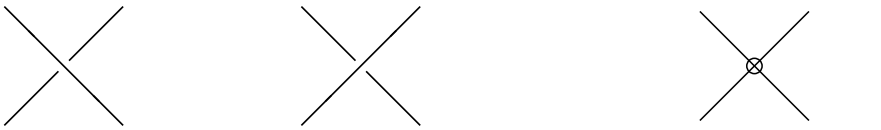

(a) Classical crossings (b) Virtual crossing

Figure 2.1: Two types of crossing

The virtual link diagrams are classified using the following moves:

1. classical Reidemeister moves involving only classical crossings (Figure 2.2),
2. virtual Reidemeister moves involving only virtual crossings, and
3. mixed Reidemeister moves connecting classical and virtual crossings (Figure 2.3).

Definition 2.1.8. Two virtual link diagrams K and K' are said to be *equivalent* if one can be transformed into the other by a finite sequence of classical Reidemeister moves R_1, R_2, R_3 (see Figure 2.2) and virtual Reidemeister moves vR_1, vR_2, vR_3, vR_4 (see Figure 2.3). We denote it by $K \overset{v}{\sim} K'$.

Definition 2.1.9. A virtual link is an equivalence class of virtual link diagrams under the equivalence relation generated by classical and virtual Reidemeister moves. A virtual link with one component is called a virtual knot.

The idea behind the virtual crossings is that these crossings are actually not

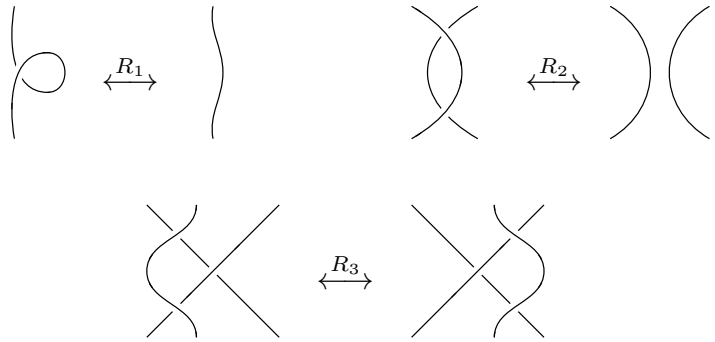

Figure 2.2: Classical Reidemeister moves

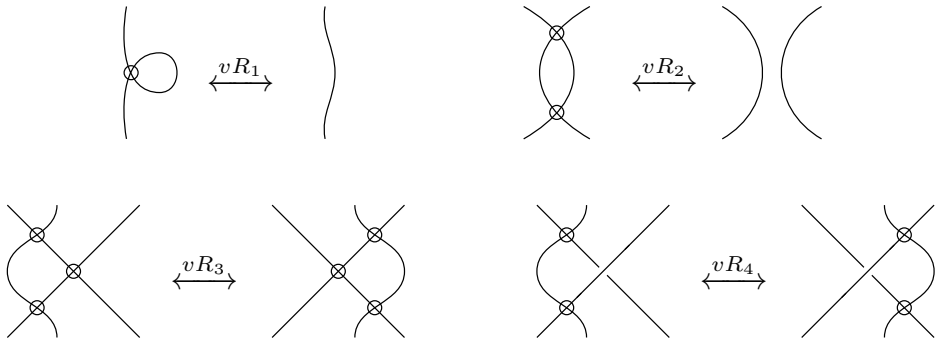

Figure 2.3: Virtual and mixed Reidemeister moves.

there and should not be treated as two arcs going over another. Instead, they represent two parts of the knot, which are very far away from each other and can move freely. The crossing appears because of the projection of the knot on a plane. This is explained by the *detour move* (Figure 2.4). Here, one branch of the knot diagram with multiple consecutive virtual crossings (not containing classical crossings) can be moved to any part of the knot diagram and all new intersections and self-intersections are marked as virtual crossings.

There are two other local moves: the over-forbidden move F_o and the under-

Figure 2.4: Detour move

forbidden move F_u (see Figure 2.5). These moves are not allowed on a virtual knot diagram together due to the following result independently proved by Kanenobu [**Kan**] and Nelson [**Nel**].

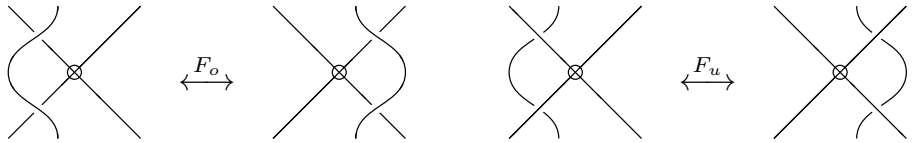

Figure 2.5: Forbidden moves

Theorem 2.1.10. [**Kan**] *For any virtual knot K, there exists a finite sequence of generalized Reidemeister moves and F_o and F_u-moves that takes K to a trivial knot.*

In the collection of virtual knots, if we allow only one forbidden move, say the over forbidden move F_o , then we obtain another non-trivial theory, known as *welded knot theory.*

Definition 2.1.11. A welded knot is an equivalence class of all those virtual knot diagrams, which are related by a finite sequence of classical and virtual Reidemeister moves and the over forbidden move. We denote this equivalence between two welded knot diagrams K and K' by $K \overset{w}{\sim} K'$.

Note.

1. Throughout this thesis, we refer to the non-classical crossings in a welded knot diagram as *welded crossings*, and it is marked by a circle at the crossing.
2. The set of moves allowed in virtual knot theory is referred to as virtual moves, and the ones for welded knot theory are referred to as welded moves.

Definition 2.1.12. By a trivial virtual (resp. welded) knot diagram, we mean a diagram that can be transformed into an unknot by finitely many virtual (resp. welded) moves. Here unknot refers to the knot with no classical, virtual or welded crossings.

Example 2.1.13. The virtual knot diagram K in Figure 2.6 is a trefoil with one virtual crossing. This is shown to be non-trivial as a virtual knot by [**Kau99**]. However, if we allow the over forbidden move F_o, and treat it as a welded knot diagram then it is equivalent to a trivial knot diagram as shown in the Figure 2.6 (Figure is taken from [**Sat00**]).

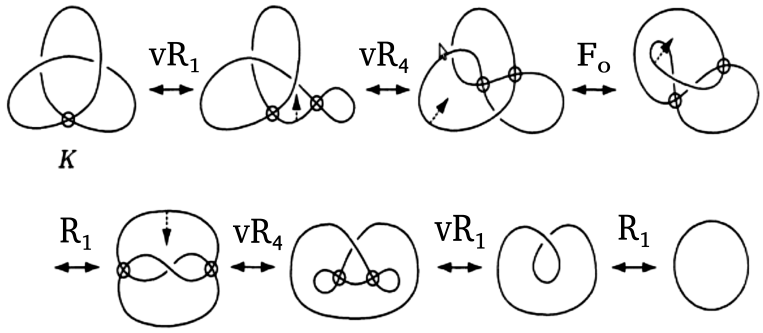

Figure 2.6: Trefoil with one welded crossing is equivalent to a trivial welded knot

.

Fundamental group of virtual and welded knots:

The fundamental group $\pi_1(S^3 \setminus K)$ of a classical knot K can be described by a group presentation at the diagram level, with one generator for each arc and one relation for each crossing of the knot diagram [**CroFox**]. The relations are of two forms $a = x^{-1}\, y\, x$ or $z = x\, y\, x^{-1}$ depending on the sign or type of the crossing as shown in Figure 2.7. This group is a classical knot invariant. It is known that K is trivial if and only if $\pi_1(S^3 \setminus K) \cong \mathbb{Z}$. This combinatorial presentation of the group written using a knot diagram can be extended for virtual and welded knots. In this case, one *arc* of a virtual diagram starts from a classical undercrossing and ends at a classical undercrossing (ignore the virtual crossings in between).

Figure 2.7: Relations for each type of crossings

Definition 2.1.14. The fundamental group or knot group $G(K)$ for an oriented virtual knot K is defined by taking one generator for each arc, and relations are defined only for the classical crossings in the same manner as the classical case. No generator or relation is added for the virtual crossings.

Remark 2.1.15.

(a) $G(K)$ is a virtual knot invariant since it is invariant under all the classical and generalized Reidemeister moves [**Kau99**].

(b) $G(K)$ also does not change under the over-forbidden move F_o and therefore it is an invariant for welded knots [**Kau99**].

(c) A non-trivial virtual knot can have a trivial knot group. For example, a trefoil knot with one welded crossing is a non-trivial virtual knot, but the knot group is isomorphic to $\mathbb{Z}$ [**Kau99**].

(d) It is not known if $G(K)$ can detect trivial welded knots or not.

2.1.3 Some results on welded knots

Definition 2.1.16. An oriented welded knot diagram D is said to be *descending* if there is a base point, and while walking along D from the base point following the orientation, we meet each crossing as an over-crossing on the first encounter.

Proposition 2.1.17. [**Sat18**] *Any descending diagram can be transformed into a trivial diagram by a finite sequence of* R_1, vR_1–vR_4, *and* F_o.

S.Satoh [**Sat18**] also proved that crossing change is an unknotting operation for welded knots.

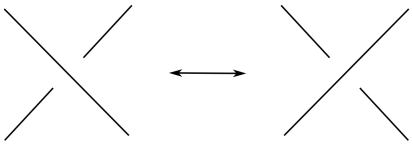

Figure 2.8: Crossing change

Theorem 2.1.18. [**Sat18**] *For any diagram D of a welded knot K, there is a diagram D' , such that*

1. *D' is obtained from D by changing some classical crossings from over to under (or vice-versa), and*
2. *D' is welded equivalent to the unknot.*

Let $c(K)$ be the minimal number of classical crossings for all diagrams of a welded knot K. Now, for a welded knot diagram D, let $u(D)$ be the minimal number

of crossing changes in D needed to obtain a diagram of the trivial welded knot. The number $u(D)$ is well defined by Theorem 2.1.18. The unknotting number of a welded knot K is defined by

$$u(K) := \min_{D} \{u(D) \mid D \text{ is a diagram of } K\}.$$

Lemma 2.1.19. [**Sat18**] *For any non-trivial welded knot K, $c(K) \geq 3$.*

Proposition 2.1.20. [**Sat18**] *For any non-trivial welded knot K, $u(K) \leq \dfrac{(c(K)-1)}{2}$.*

2.1.4 Warping degree of a welded knot

The concept of the warping degree of welded knots [**LiLeiWu**] is used as a tool to understand the unknotting number of welded knots. Let D be an oriented welded knot diagram of a welded knot K. Let a be a point on D, which is not a crossing point. We call it a base point of D. Denote the diagram D with a base point a as D_a.

Definition 2.1.21. A classical crossing point of D_a is called a *warping crossing point* if we encounter the crossing point first at the undercrossing while going along the diagram following the orientation, starting at the base point a.

Definition 2.1.22. The *warping degree* of D_a, denoted by $d(D_a)$, is the number of warping crossing points of D_a. The warping degree of D, denoted by $d(D)$, is the minimal warping degree for all base points of D.
Then, the warping degree of a welded knot K is defined by

$$d(K) \coloneqq \min_{D}\{d(D), d(-D) \mid D \text{ is a diagram of } K\},$$

where $-D$ be the inverse of D.

Let $c(D)$ be the classical crossing number of D.

Lemma 2.1.23. [**LiLeiWu**] *Let D_a be a welded knot diagram with base point a. Then*

$$d(D_a) + d(-D_a) = c(D).$$

Proposition 2.1.24. [**LiLeiWu**] *Let D^* be the mirror image of D. Then*

$$d(D^*) = d(-D).$$

Theorem 2.1.25. [**LiLeiWu**] *Let D be an oriented welded knot diagram with $c(D) \geq 3$. Then*

$$d(D) + d(-D) + 1 \leq c(D).$$

Further, the equality holds if D is an alternating diagram.

Example 2.1.26. Let D be a diagram of a welded figure-eight knot K with one welded crossing as in Figure 2.9. Here, we have $d(D_b) = 0, d(D_a) = 1, d(D_c) = 1$. Hence, we have $d(D) = 0$. For the inverse $-D$ of D (see Figure 2.10), we have $d(-D_a) = 2, d(-D_b) = 3, d(-D_c) = 2$. So, $d(-D) = 2$. And therefore $d(K) = 0$.

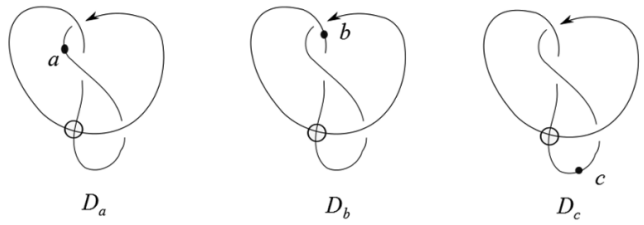

Figure 2.9: The welded figure-eight knot diagram D

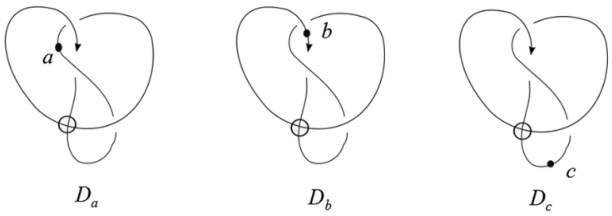

Figure 2.10: The welded figure eight knot diagram $-D$

Lemma 2.1.27. [**LiLeiWu**] *The unknotting number of a welded knot is less or equal to its warping degree, i.e, $u(K) \leq d(K)$.*

Corollary 2.1.28. [**LiLeiWu**] *A welded knot is trivial if and only if $d(K) = 0$.*

Example 2.1.29. From the Example 2.1.26 we see that the welded figure eight knot K with one weldinng has a diagram D_b with base point b (Figure 2.9) such that

$d(D_b) = 0$ which implies $d(K) = 0$. This means D_b is a descending diagram and by Proposition 2.1.17, D_b can be transformed into a trivial diagram by a finite sequence of $R_1, vR_1 - vR_4$, and F_o.This verifies the fact that this is a welded unknot.

2.2 Surface knots

We discussed in the previous section that the set of isotopy classes of embeddings of a surface inside a 4-dimensional manifold has the possibility of containing one that is knotted. Conventionally, the surface knots are studied inside S^4 or $\mathbb{R}^4$. In order to understand surface knots in detail, we present some definitions here.

Let N be an n-dimensional manifold embedded in an m-dimensional manifold M $(n \leq m)$.

Definition 2.2.1. We call an embedding $f : N \to M$ to be *proper* if, every compact subset $K \subset f(N)$ has a compact preimage $f^{-1}(K) = \{x \in N | f(x) \in K\}$.
In other words, the manifold $f(N)$ is proper if $\partial f(N) = f(N) \cap \partial M$.

Example 2.2.2. The first figure of Figure 2.11 shows an example of a properly embedded 1-manifold in a 3-ball. The second one is not proper because one of the interior points of the 1-manifold is on the boundary of the 3-ball. The third one is not proper because one of the boundary points of the 1-manifold is an interior point of the 3-ball.

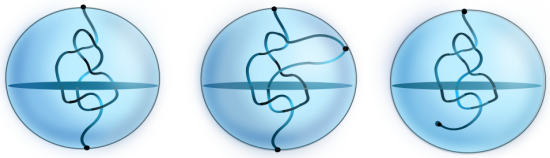

Figure 2.11: Examples of proper and non-proper manifold

Definition 2.2.3. Let N be a properly embedded submanifold in M. N is said to be *locally flat* at a point $x \in M$ if there exists a neighborhood U of x in M such that the pair $(U, U \cap f(N))$ is homeomorphic to the standard ball pair (D^m, D^n), where D^k is the unit ball in $\mathbb{R}^k$, centred at origin. We say that N is *locally flat* if it is locally flat at every point of M.

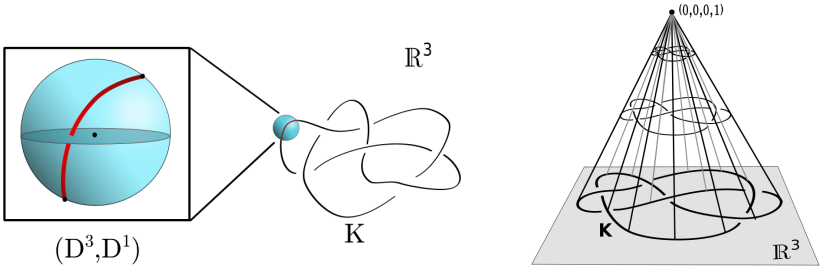

(a) Locally flat property

(b) Non-locally flat surface in $\mathbb{R}^4$

Figure 2.12: Locally flat and non-locally flat

Example 2.2.4 (Non-locally flat)**.** Let K be a classical knot embedded in the hyperspace $\mathbb{R}^3 \cong \{(x, y, z, 0) \,|\, (x, y, z) \in \mathbb{R}^3\}$ in $\mathbb{R}^4$. Now take a point in $\mathbb{R}^4$ outside that hyperspace, say $(0, 0, 0, 1)$ (Figure 2.12(b)). Now, joining each point on K with $(0, 0, 0, 1)$, we get a *Cone* over K. This is a 2-manifold embedded in $\mathbb{R}^4$. But it is not locally flat at $(0, 0, 0, 1)$ since any regular neighbourhood of $(0, 0, 0, 1)$ has K as its boundary and, therefore, not homeomorphic to D^2.

Definition 2.2.5. A *surface link* is a proper, locally flat embedding of a closed surface F in $\mathbb{R}^4$ or S^4.

- When $F = S^2$, it is called a *2-knot* or 2-dimensional knot.
- If F is a connected surface then it is called a *surface knot*.
- If $F = S^2 \bigsqcup S^2 \bigsqcup \cdots \bigsqcup S^2$ then it is called a *2-link* or 2-dimensional link.

Definition 2.2.6. A proper, locally flat embedding of R^2 in R^4 is referred as a *long 2-knot*.

Definition 2.2.7. Two surface links F and F' are *equivalent* if and only if they are ambient isotopic, i.e. there exists an ambient isotopy $\{h_t\}$ of $\mathbb{R}^4$ such that $h_1(F) = F'$. When F and F' are oriented, then $h_1|_F : F \to F'$ is assumed to be an orientation-preserving homeomorphism.

The notion of connected sum and split sum for the surface knots are similar to the classical knots.

Definition 2.2.8. A surface knot is *trivial or unknotted* if it is a connected sum of trivial standard surfaces (e.g. standard sphere, standard tori or standard projective

planes) in $\mathbb{R}^4$.
A *surface link* is *trivial* or *unknotted* if it is a split sum of trivial surface knots. Equivalently, a closed orientable surface link F is trivial or unknotted iff

- F is the boundary of a 3-manifold M embedded in $\mathbb{R}^4$ with all connected components as handlebody. Or,
- F is equivalent to a surface link which can be embedded in some 3-dimensional hyperplane of $\mathbb{R}^4$.

Classical links are studied by projecting them into a suitable plane. Similarly, surface links are studied by projecting them into a suitable hypersurface.

2.2.1 Generic projection of a surface link:

Let $g : F \to \mathbb{R}^3$ be a map from a closed surface F in $\mathbb{R}^3$. Now, let D_1, D_2, D_3 be 2-disks obtained by restricting the cube $[-1,1] \times [-1,1] \times [-1,1]$ on the co-ordinate planes. Denote the origin as O.

- Regular point: A point $y \in g(F)$ is defined to be a *regular point* if there is a regular 3-ball neighborhood $N(y)$ of y such that $g|_{g^{-1}(g(F)\cap N(y))}$ is an immersion and the triple $(N(y), N(y) \cap g(F), y)$ is homeomorphic to the triple (D^3, D_1, O) (Figure 2.13(a)).
- Double point: A point $y \in g(F)$ is defined to be a *double point* if there is a regular 3-ball neighborhood $N(y)$ of y such that $g|_{g^{-1}(g(F)\cap N(y))}$ is an immersion and the triple $(N(y), N(y) \cap g(F), y)$ is homeomorphic to the triple $(D^3, D_1 \cup D_2, O)$ (Figure 2.13(b)).
- Triple point: A point $y \in g(F)$ is defined to be a *triple point* if there is a regular 3-ball neighborhood $N(y)$ of y such that $g|_{g^{-1}(g(F)\cap N(y))}$ is an immersion and the triple $(N(y), N(y) \cap g(F), y)$ is homeomorphic to the triple $(D^3, D_1 \cup D_2 \cup D_3, O)$ (Figure 2.13(c)).
- Branch point: A point $y \in g(F)$ is defined to be a *branch point* if there is a regular 3-ball neighborhood $N(y)$ of y such that $g^{-1}(y)$ is a single point $x \in F$ and $g|_{g^{-1}(g(F)\cap N(y))}$ is an immersion everywhere except at x. Also, the triple $(N(y), N(y) \cap g(F), y)$ is homeomorphic to the triple (D^3, cone over a figure eight curve, O) i.e $N(y)$ has a figure eight curve as its boundary (Figure 2.13(d)).

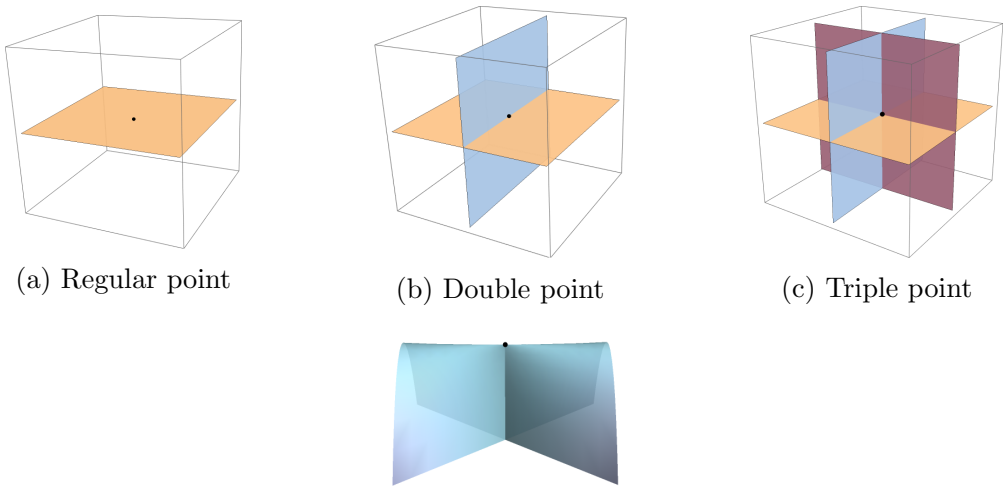

(a) Regular point

(b) Double point

(c) Triple point

(d) Branch point

Figure 2.13: Neighborhood of singular points

Definition 2.2.9. A map $g : F \to \mathbb{R}^3$ is called a *generic map* or a map in a *general position* if every point in $g(F)$ is either a regular point, a double point, a triple point or a branch point.

Definition 2.2.10. Choose a vector $v \in \mathbb{R}^4$ and let us take a projection of $\mathbb{R}^4$ onto some hyperplane H orthogonal v by a projection map $\pi : \mathbb{R}^4 \to H$. A surface link F is in general position with respect to π or π is a *generic projection* of F if $\pi|_F : F \to H$ is a generic map.

We denote by $\Gamma(F)$ the set of double points, triple points and branch points of $\pi(F)$, and call it the multiple point set. We can consider the multiple point set $\Gamma(F)$ as a disjoint union of connected graphs and embedded circles in $\mathbb{R}^3$ with vertices of valency one (for branch points) or six (for triple points). See Figure 2.14. By connecting the edges which are diagonal at triple points, we obtain double point curves (arcs and circles) such that the endpoints of a double point arc are a pair of branch points, and the curves pass through each triple point three times. Figure 2.15 shows neighborhoods of a double point arc and a double point circle. If a double point curve does not pass through any triple point then we call it simple.

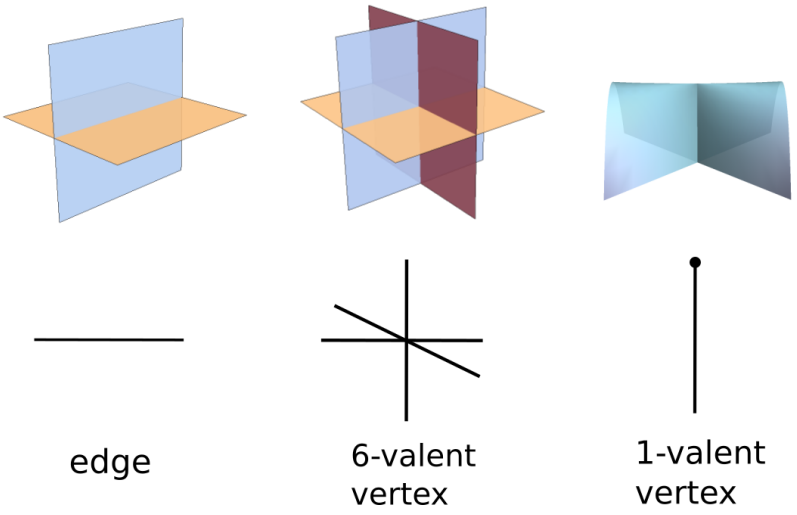

Figure 2.14: Edge and vertices of $\Gamma(F)$

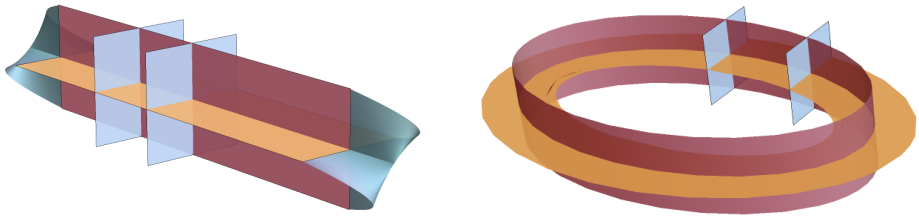

(a) For a double point arc

(b) For a double point circle

Figure 2.15: Neighborhood of double point sets

2.2.2 Broken surface diagram:

Definition 2.2.11. A *surface link diagram* of F is the image under a generic projection map π equipped with the over/under information at all multiple points with respect to the direction of the vector v.

When y ia a singular point, we can distinguish the sheets (i.e. the 2-disks) in $N(y)$ by the relative height with respect to the direction of the vector v as upper-lower (for double point and branch point), upper-middle-lower (for triple point). In case of branch point, two sheets converge at the branch point. Define the set of preimages by

$$\left\{x \in F \,\middle|\, \pi|_F(x) = \pi|_F(y) \text{ for some } y\,(\neq x) \in F\right\}.$$

Let D, T, B be the set of double, triple, branch points and $T \subset D$ and $B \subset D$. Two preimages of double points on K are denoted by D_a and D_b where a, b represents above and below respectively. This means that D_a is higher with respect to the direction of v than D_b. D_a and D_b are called the upper decker and lower decker set respectively. The transverse components of D_a and D_b are the arcs that intersect at the preimages of the triple points or the branch points. The preimage of a branch point on K is the boundary of both D_a and D_b.

In classical knot theory, we draw a knot diagram by taking a knot projection on some plane and then by removing a small neighborhood of the under crossing point we give the over/under information. We generalize this idea of broken lower arc at a crossing for surface links. Let N be a thin open neighborhood of $D_b \setminus B$ such that the branch points are in the closure of N i.e $B \subset \overline{N}$. So, we take a thin strip along D_b in F and whenever some arc in D_b has a branch point as an end point then that branch point will be on the boundary of the strip.

Definition 2.2.12. For N defined as above, $\pi|_F(F \setminus N)$ gives us the surface link projection with a strip removed, i.e. broken from lower sheets consistently along all double point curves. This we call a *broken surface diagram* of the surface link F.

The neighborhood of the singular points after removing a strip from the lower sheet is shown in Figure 2.16 and a broken surface diagram of a knotted sphere is shown in Figure 2.17.

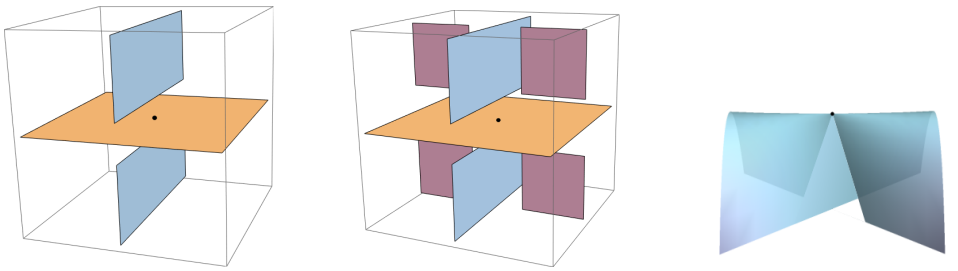

(a) Near a double point (b) Near a triple point (c) Near a branch point

Figure 2.16: Broken surface diagram near a singular points

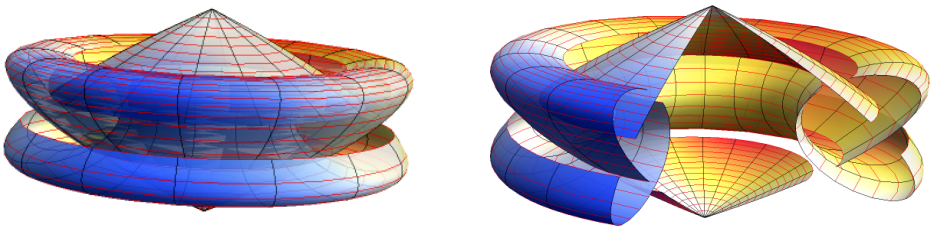

(a) Broken surface diagram (b) Inside view

Figure 2.17: Broken surface diagram of a knotted sphere

2.2.3 Motion pictures or movies

It is sometimes hard to draw the whole surface diagram as some parts are behind other parts. To avoid that we can use movies or motion pictures where we cut the surface diagram by parallel hyperplanes. Then each intersection gives a 1-dimensional manifold.

Let $F \subset \mathbb{R}^4$ be a given knotted surface and take a vector $v \in \mathbb{R}^4$. Let $\{\mathbb{R}^3_t\}_{t\in\mathbb{R}}$ be family of parallel hyperplanes, each of which is orthogonal to the vector v, containing the point tv. Now, $F_t = F \cap \mathbb{R}^3_t$ ia always a 1-dimenisonal manifold i.e a classical link or empty. Since, F is compact, there exists an interval $[a, b]$ such that $F \subset \cup_{t\in[a,b]} \mathbb{R}^3_t$.

Let $p_v : \mathbb{R}^4 \to \mathbb{R}_v$ be the projection map onto the line $\mathbb{R}_v = \{tv \in \mathbb{R}^4 \,|\, t \in \mathbb{R}\}$. Consider the restriction map $p_v|_F : F \to \mathbb{R}_v$. By Morse theory, non-degenrate critical points of $p_v|_F$ are isolated and the intersections at those points are of our interest as the knot type does not change at any point other than the critical points. Now, A critical point of index 0 and 1 are a minimal and a maximal point respectively and they corresponds to birth and collapse of a simple unknotted curve. A critical point t_i of index 2 is a saddle point and $F_{t_i+\epsilon}$ can be obtained from $F_{t_i-\epsilon}$ by attaching a 1-handle or a band.

Definition 2.2.13. For the Morse function on F defined above by restricting the projection of $\mathbb{R}^4$ onto $\mathbb{R}_v$, the one parameter family $\{F_t \subset \mathbb{R}^3_t\}_{t\in[a,b]}$ is called the *motion picture* or a *movie* of the surface link F. And each F_t for a $t \in \mathbb{R}$ is called a *still* of the movie.

Remark 2.2.14. Since the knot type changes at only at finitely many critical points, a finite number of stills are sufficient to describe the surface link. Therefore, although

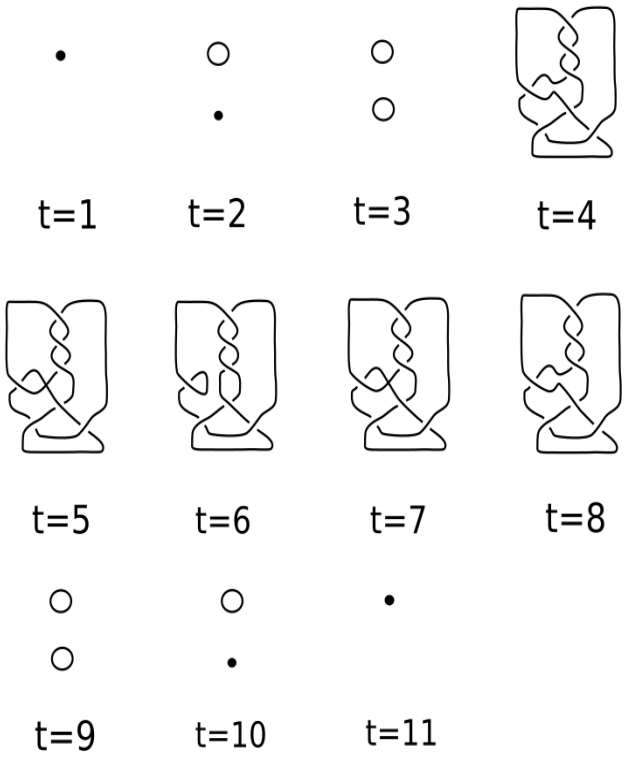

Figure 2.18: Motion picture of a knotted sphere

the whole famliy $\{F_t \subset \mathbb{R}^3_t\}_{t\in[a,b]}$ is called the movie, we can take only a finite set of stills as the motion picture or a movie of the surface link.

2.2.4 Roseman moves for broken surface diagram:

Here, we introduce a set of moves called Roseman moves [**Ros**] which connects two isotopic surface knots. There are seven types of Roseman moves:

- Move in the top left corner in Figure 2.19 is called *type I bubble move*. On the top, two branch points are connected by a double point arc. So, this move removes the pair of branch points and the double point arc or introduce them.
- Move in the bottom left corner in Figure 2.19 is called a *type II bubble move* which introduces or removes a closed double point curve.
- Move on the right colomn in Figure 2.19 is called *type III bubble move* which introduces or removes a pair of triple points. There should be three double

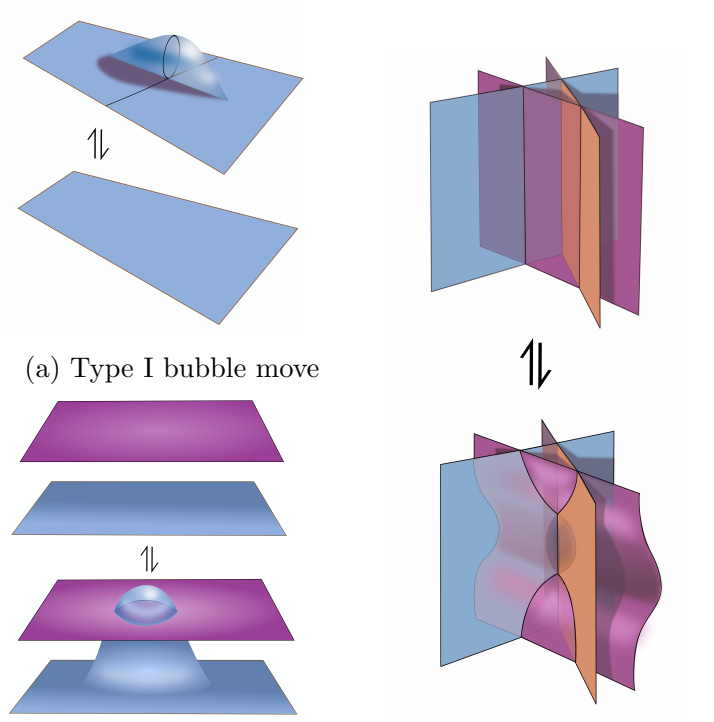

(a) Type I bubble move

(b) Type II bubble move

(c) Type III bubble move

Figure 2.19: Bubble moves

point arcs connecting the triple points for the cancellation to happen.

- Move on the left in Figure 2.20 is called *type I saddle move*. This move cancels a pair of branch points by connecting the double point arcs which terminates at those branch points. Also, a pair of branch points can be introduced. The pair of branch point should have consistent crossing information so that the broken diagram after the move remains well defined.
- Move on the right in Figure 2.20 is called *type II saddle move* which joins or separates two double point arcs. The crossing information on all four arcs are same.
- Move in Figure 2.21(a) introduces or cancels a triple point by *passing a branch point through a sheet*.
- Figure 2.21(b) illustrates the move called *tetrahedral move*. Here four sheets of the surface makes a tetrahedron. The sheets look like three co-ordinate planes and the plane $x + y + z = 1$ before the move and the plane $x + y + z = -1$

along with the co-ordinate planes after the move. So this move passes a sheet through a triple point.

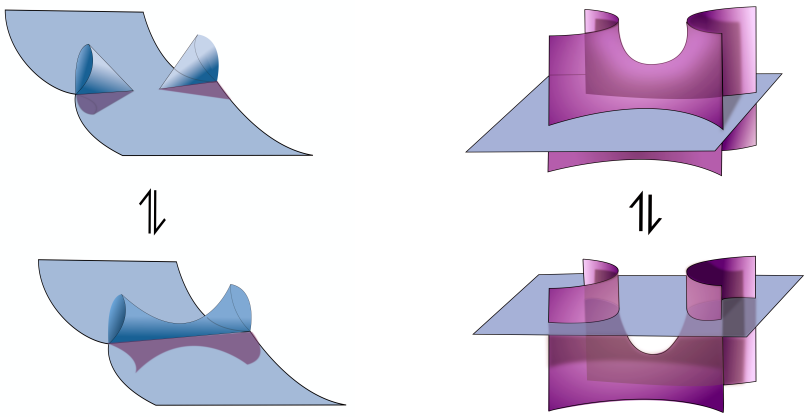

(a) Type I saddle move (b) Type II saddle move

Figure 2.20: Saddle moves

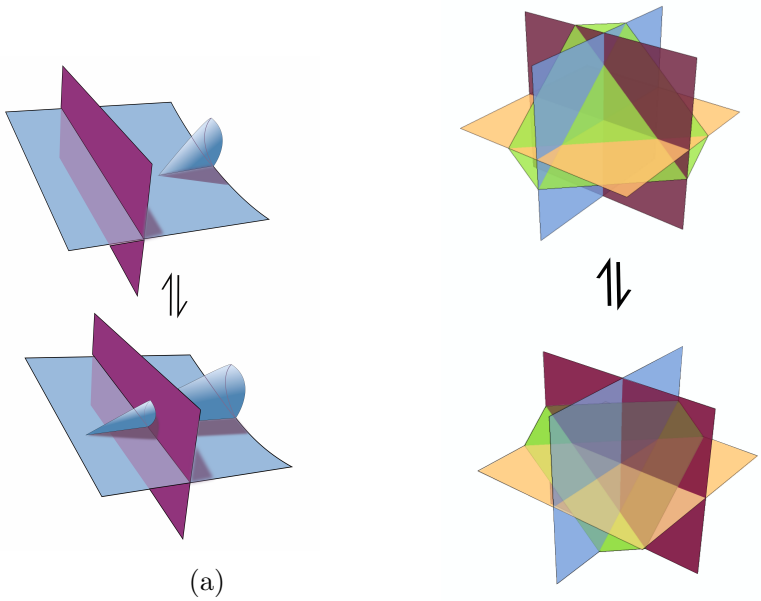

(a)

(b)

Figure 2.21: (a) Passing a branch point, (b) Tetrahedral move

Remark 2.2.15. In the above Figures, the moves are shown in the projection, not in the broken diagram. For every move in the projection there are more than one move

corresponding to the over/under information. The over/under information has to be consistant when we go from one side of the move to the other.

Theorem 2.2.16. [**Ros**] *Two broken surface diagrams represent equivalent knotted surfaces if and only if one can be obtained from the other by a finite sequence of moves from the list illustrated in the above figures and ambient isotopy of the diagrams in 3-space.*

2.3 Construction of knotted surfaces

In this section, we discuss few ways to obtain knotted surfaces in 4-space such as spun knots, twist spun knots, and ribbon surface knots.

2.3.1 Spinning

Artin [**Art**] introduced a way to construct 2-knots by spinning a knotted arc embedded in the half-space $\mathbb{R}^3_+$ around $\mathbb{R}^2$. The resulting 2-knots are called *Spun Knots*. Spun knots represent the simplest class of 2-knots. Their construction is described as follows: In $\mathbb{R}^4$, consider the upper half space

$$\mathbb{R}^3_+ = \{(x_1, x_2, x_3, 0) : x_3 \geq 0\}$$

with the boundary

$$\partial\mathbb{R}^3_+ = \mathbb{R}^2 = \{(x_1, x_2, 0, 0)\}.$$

Now, locus of a point $x = (x_1, x_2, x_3, 0)$ in $\mathbb{R}^3_+$ rotated in 4-space about $\mathbb{R}^2$ is given by

$$\{(x_1, x_2, x_3 \cos\theta, x_3 \sin\theta) \,|\, 0 \leq \theta \leq 2\pi\}.$$

To construct a spun knot, we choose a properly embedded arc k in $\mathbb{R}^3_+$ i.e k is embedded in $\mathbb{R}^3_+$ locally flatly and intersects $\partial\mathbb{R}^3_+$ transversely only at the endpoints (Figure 2.22(a)). Then we spin $\mathbb{R}^3_+$ along $\mathbb{R}^2$ by 360^o and the continuous locus of the arc gives a 2-knot given by

$$\{(x_1, x_2, x_3 \cos\theta, x_3 \sin\theta) \,|\, (x_1, x_2, x_3) \in k, 0 \leq \theta \leq 2\pi\}.$$

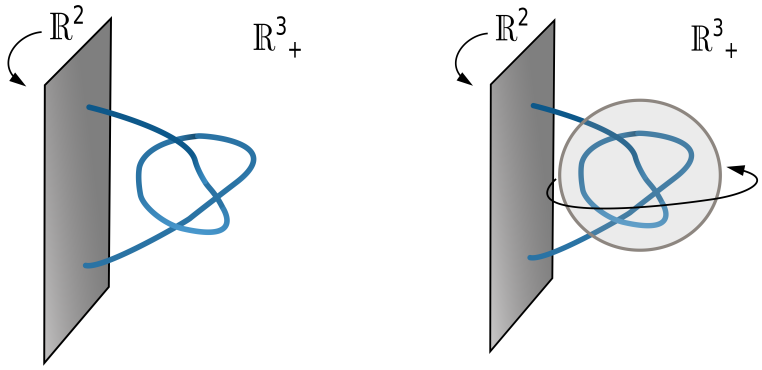

(a) Spun knot (b) d-twist spun knot

Figure 2.22: Knotted sphere constructions

2.3.2 Twist-spinning

E.C. Zeeman in 1965 [**Zee65**] generalized Artin's spinning construction to *twist spinning*. In this case, we imagine the knotted part of k inside a 3-ball as in Figure 2.22(b). Now, to include twisting in the spinning construction we rotate the ball d times around its own axis while rotating $\mathbb{R}^3_+$ around $\mathbb{R}^2$ once. Position of the knotted arc after d twists should match its initial position after completing the rotation around $\mathbb{R}^2$. This way we get a 2-sphere in $\mathbb{R}^4$, called *d-twist spun knot*. By definition, for $d = 0$ we get a spun knot.

Theorem 2.3.1. [**Zee65**] *Let F be d-twist spun knot obtained from a classical knot K in S^3. Let $M_d(K)$ denote a d-fold cyclic branch covering space of S^3 with K as a branch set. Then F is a fibered 2-knot whose fiber is the punctured $M_d(K)$.*

Remark 2.3.2. The above theorem implies that for the values $d = \pm 1$, d-twist spun knot obtained from any clssical knot K, is fibered and the fiber is homeomorphic to a standard 3-ball. Therefore, the ± 1-twist spun knots are unknotted as they bound a standard 3-ball [**Zee65**].

2.4 Ribbon Surface Knots

Definition 2.4.1. Let M be an compact 3-manifold immersed in $\mathbb{R}^4$ and $f : M \to \mathbb{R}^4$ be the immersion map. A connected component D of the double point set is called a

ribbon singularity if the preimage $f^{-1}(D)$ is the union of 2-disks D_1 and D_2 such that D_1 is a properly embedded 2-disk in M and D_2 is an embedded 2-disk in the interior of M.

Definition 2.4.2. Let $\Delta = \Delta_1 \sqcup \cdots \sqcup \Delta_k$ and $\mathcal{B} = \mathcal{B}_1 \sqcup \cdots \sqcup \mathcal{B}_l$ be two disjoint collections of 3-balls embedded in $\mathbb{R}^4$, with each component of Δ and $\mathcal{B}$ is called a base and a band respectively. We parameterize each band by $h_i : D^2 \times [0,1] \to \mathbb{R}^4$ such that

1. for each $i = 1, 2, \cdots, l$,
$$\partial\Delta \cap h_i(D^2 \times [0,1]) = h_i(D^2 \times \partial[0,1]), \quad \text{and}$$

2. If $h_i(D^2 \times [0,1])$ intersects a base, then it intersects this base in meridional 2-disks that are prpoerly embedded in the band and contained in the interior of the base:
$$h_i(D^2 \times [0,1]) \cap \Delta_j = h_i(D^2 \times \{t\})$$
for $t \in (0,1)$. And all these intersections are ribbon singularities (Figure 2.23).

Now, the surface given by

$$F = \left[\partial\Delta \setminus \cup_{i=1}^{l} h_i(D^2 \times [0,1])\right] \bigcup \cup_{i=1}^{l} h_i(\partial D^2 \times [0,1]),$$

is called a *ribbon surface knot* (Figure 2.24).

- If $l = k - 1$ then F is homeomorphic to a 2-sphere and F is called a *ribbon 2-knot* or a *ribbon sphere*.
- If F is homeomorphic to a torus then we call it a *ribbon torus-knot*.
- The pair $(\Delta, \mathcal{B})$ is called a *ribbon presentation* of F with l fusion bands.

The intersections of type (1) and (2) are depicted in Figure 2.23 for classical case (bottom) and surface case (top). Figure 2.24 indicates that ribbon surface knots has a natural projection and there is a diagram to represent ribbon surface knot with simple closed curves of double points.

Equivalently, we can define ribbon surface knot as follows:

Definition 2.4.3. A *ribbon surface knot* is an embedded surface F in $\mathbb{R}^4$ which bounds a 3-manifold immersed in $\mathbb{R}^4$, each component of which is a handlebody and

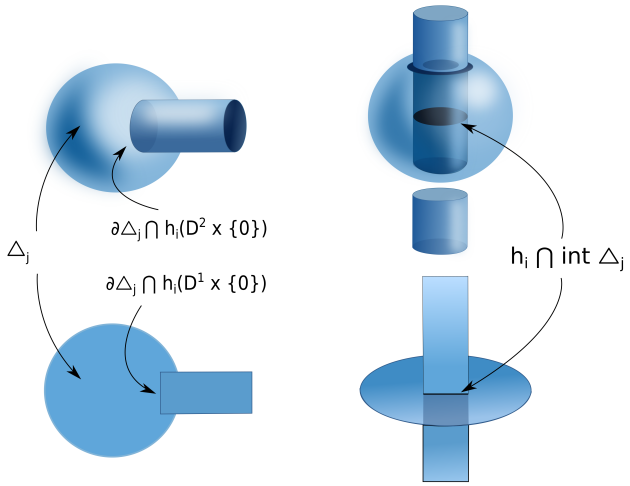

Figure 2.23: Ribbon presentation in dimension one and two

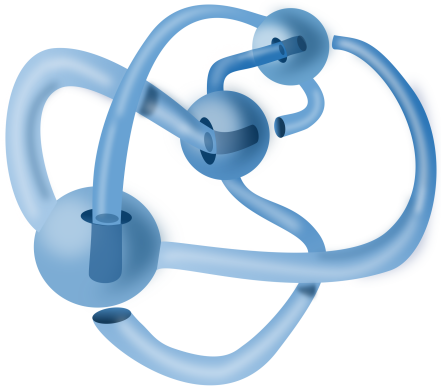

Figure 2.24: A broken surface diagram of a ribbon surface knot

each singularity is a ribbon singularity.

2.5 Relation between ribbon torus knots and welded knots

S. Satoh showed a correspondence between ribbon torus knots and virtual knots by defining a map called *Tube* map [**Sat00**]. Let K be a virtual knot diagram on XY-plane. We construct a surface diagram corresponding to K in the following way:

- At every point of the diagram we put a circle in the z direction (Figure 2.26).

- At a classical crossing, the tube corresponding to the under arc penetrates through the tube corresponding to the over-arc (Figure 2.25(a)).
- At the virtual crossings the tubes are free from the over/under information of the diagram in $\mathbb{R}^3$ and they can move independently (Figure 2.25(b)).

(a) Near the classical crossing (b) Near the virtual crossing

Figure 2.25: Tube map near the crossings

So, Tube(K) is defined as the ribbon torus knot with surface diagram as described above for K (Figure 2.26).

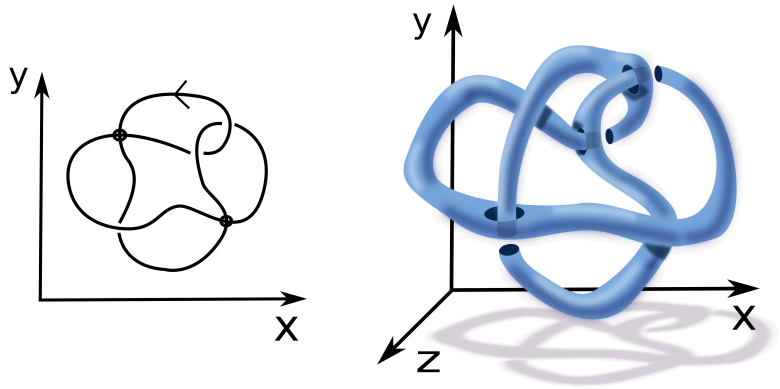

Figure 2.26: Tube map

Remark 2.5.1. The image of the Tube map for a virtual and a welded crossing will be same since welded crossings are just virtual crossings of a virtual diagram with over forbidden move allowed along with the classical and virtual Reidemeister moves.

Theorem 2.5.2. [**Sat00**] *For every ribbon torus knot T, there exists a virtual knot diagram K such that T is homeomorphic to the Tube(K), i.e. $T \cong Tube(K)$.*

Proposition 2.5.3. [**Sat00**] *Let K and K' be two virtual knot diagrams related by generalized Reidemeister moves and over forbidden move i.e K and K' are equivalent*

as welded knot diagrams then their corresponding tubes are also equivalent as surface knots, i.e.,

$$K \overset{w}{\sim} K' \implies Tube(K) \cong Tube(K').$$

This is how ribbon torus knots are associated with welded knots.

Remark 2.5.4.

(a) A trivial welded knot always corresponds to a trivial ribbon torus knot. For example, the *Tube* of the welded trefoil knot diagram in Example 2.1.13 is equivalent to a trivial surface knot.

(b) It is already proved that the Tube map is not injective [**Win**]. Therefore, a non-trivial welded knot can correspond to a trivial ribbon torus knot.

Theorem 2.5.5. [**Sat00**] *If we take a classical knot K instead of a welded knot then*

$$Tube(K) \cong Spun(K).$$

Theorem 2.5.6. [**Sat00**] *Let T be a ribbon torus knot in $\mathbb{R}^4$ and K be the associated virtual knot such that $T = Tube(K)$. Also let $\pi_1(\mathbb{R}^4 \setminus T)$ be the fundamental group of the complement of T in $\mathbb{R}^4$ and $G(K)$ be the fundamental group of the virtual knot K. Then*

$$\pi_1(\mathbb{R}^4 \setminus T) \cong G(K).$$

Corollary 2.5.7. [**Kau99**] *If $K \overset{w}{\sim} K'$ then $G(K) \cong G(K')$.*

This result brings a topological meaning to the fundamental group of a welded knot which is defined purely combinatorially.

2.6 Parameterization of knots

Parameterization of a geometric object is a mathematical expression as a function of some independent quantities called parameters. In knot theory, parameterization of knots is a way to present a knot, defining its coordinates using elementary functions, such as trigonometric or polynomial functions. They are referred to as trigonometric knots or polynomial knots. Fourier knots [**Kau98**] and Lissajous knots [**Bog**] are examples of trigonometric knots. One example of trigonometric parameterization of

torus knot $T(2,7)$ is given by (Figure 2.27). Fourier knots have a parameterization of the form

$$x(t) = \cos 2t(\cos 7t + 3)$$
$$y(t) = \sin 2t(\cos 7t + 3)$$
$$z(t) = \sin 7t.$$

Trigonometric parameterization provides a compact classical knot embedding, whereas polynomial parameterization presents long knots, i.e., embeddings of $\mathbb{R}$ in $\mathbb{R}^3$.

In this thesis, we are interested in parameterizing 2-dimensional knots. From the earlier sections, it is clear that a parameterization of long knots can be used to construct a parameterization of spun 2-knots and d- twist spun 2-knots. Furthermore, we can use trigonometric parameterization to parameterize ribbon torus knots. A detailed discussion of this is provided in Chapters 3 and 5. We use some concepts

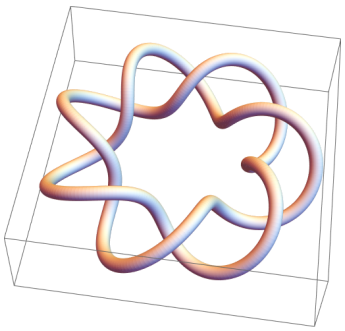

Figure 2.27: Trigonometric parameterization

related to polynomial knots to parameterise certain knotted planes. To develop a better understanding of polynomial knots, we provide a brief exposition below.

2.6.1 Polynomial knots

It is already known that the ambient isotopy classes of classical knots ($S^1 \subset S^3$) are in bijection with the ambient isotopy classes of long knots, i.e., the smooth embeddings of $\mathbb{R}$ in $\mathbb{R}^3$, which are proper and have asymptotic behaviour outside a closed interval. In 1994, the following theorems regarding long knots were proved.

Theorem 2.6.1. [**Sha**], [**Shu**] *For every long knot K there exists a polynomial embedding $t \to (f(t), g(t), h(t))$ from $\mathbb{R}$ to $\mathbb{R}^3$ which is isotopic to K.*

Theorem 2.6.2. [**Shu**] *If two polynomial embeddings* $\phi_0 : \mathbb{R} \to \mathbb{R}^3$ *and* $\phi_1 : \mathbb{R} \to \mathbb{R}^3$ *represent isotopic knots, then there exists a one-parameter family of polynomial embeddings* $\phi_t : \mathbb{R} \to \mathbb{R}^3$ *for each* $t \in [0, 1]$. *We say that* ϕ_0 *and* ϕ_1 *are polynomially isotopic.*

Example 2.6.3. As a demonstration, here is the embedding

$$t \to \left(t^3 - 3t, t^4 - 4t^2, -t^6 + 2t^5 + 4.24t^4 - 8.48t^3 - 3.24t^2 + 6.48t + 12\right)$$

whose Mathematica plot is shown in Figure 2.28.

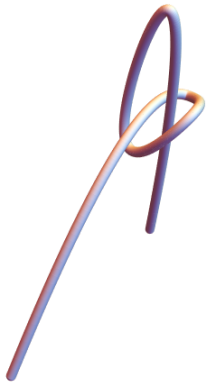

Figure 2.28: Mathematica plot of a polynomial embedding

Both of these theorems were proved using Weierstrass' Approximation [**Rud**]. Later, concrete polynomial embeddings representing a few classes of knots were constructed, and their degrees were estimated ([**PraMis**], [**Mis09**]).

In all the constructions, the main idea is to fix a suitable knot diagram and find real polynomials $f(t)$ and $g(t)$ such that the plane curve $(x(t), y(t)) = (f(t), g(t))$ provides the projection of the diagram. For this curve, one can explicitly find the parameter pairs (s_i, t_i) for which $f(s_i) = f(t_i)$ and $g(s_i) = g(t_i)$ for each i. Then, depending upon the over/under crossing information, we can construct a polynomial $h(t)$ which provides $h(s_i) < h(t_i)$, at an undercrossing and $h(s_i) > h(t_i)$, at an overcrossing. Note that in our construction, we always project the knot on the XY plane, and the Z co-ordinate provides the height function. All the crossings of the

knot lie in the image of a closed interval $[a, b]$. We prove the following lemma, which will be useful in Chapter 3.

Lemma 2.6.4. *Given a long knot K, there exists a polynomial embedding from $\mathbb{R} \to \mathbb{R}^3$ defined by $t \to (x(t), y(t), z(t))$ such that for some interval $[a, b]$, $z(a) = z(b) = 0$, $z(t) > 0$ for $t \in (a, b)$ and there are no crossings outside $[a, b]$.*

Proof. We construct polynomials $f(t)$ and $g(t)$ such that the curve, defined by $(x, y) = (f(t), g(t))$ represents a projection of K on XY plane. We choose the polynomial $h_0(t)$, which provides the over/under crossing information. Note that we can choose $h_0(t)$ as an even degree polynomial. Now by adding a sufficiently large real number R, we can show that $h(t) = h_0(t) + R$ has exactly two real roots a and b, $h(t) > 0$ for $t \in (a, b)$ and all the double points of the projection lie inside $[a, b]$ (Figure 2.29). This completes the proof. □

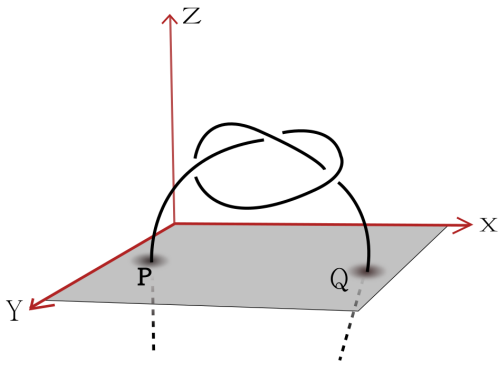

Figure 2.29: A long trefoil knot

In [**Mis14**], using polynomial parameterization, it is shown that a polynomial knot diagram can be transformed into a trivial knot diagram through a homotopy, which represents the unknotting operation of switching over/under information of a knot diagram. An invariant arises from this homotopy called the *singularity index* of a long knot.

Definition 2.6.5. Let $\phi_0, \phi_1 : \mathbb{R} \to \mathbb{R}^3$ be two polynomial knots. ϕ_0, ϕ_1 are said to be strongly P-regular homotopic if there exists a one parameter family $\{\psi_s | 0 \leq s \leq R\}$ of polynomial maps from $\mathbb{R}$ in $\mathbb{R}^3$ such that $\psi_0 = \phi_0$ and $\psi_R = \phi_1$ and for each $0 \leq s \leq R$, the projection maps $t \to (f_s(t), g_s(t))$ have the same crossing data, i.e., the pairs (t_1, t_2) for which $f_s(t_1) = f_s(t_2)$ and $g_s(t_1) = g_s(t_2)$ is same for all $s \in [0, R]$.

Proposition 2.6.6. [**Mis14**] *Every polynomial knot is strongly P-regular homotopic to a polynomial unknot.*

The proof of this proposition goes by defining the homotopy as the one parameter family

$$\left\{\psi_s : \left(f(t) + s, g(t) + s, h(t) + s^2 t\right) \mid s \in \mathbb{R}\right\}$$

which are immersions for each $s \in \mathbb{R}$ such that ψ_0 is the original polynomial knot $\{f(t), g(t), h(t)\}$ and for $s > R \in \mathbb{R}$, ψ_s represents trivial knot diagrams. Now, the number of values of $s \in [0, R]$ for which ϕ_s is not an embedding is said to be the Singularity index of the polynomial knot ϕ denoted by SI_ϕ.

Definition 2.6.7. Let D be a knot diagram with n crossings. The *singularity index*, $SI(D)$ of the diagram D is defined as:

$$SI(D) = \min_{\phi} \{SI_\phi | \phi \text{ is a polynomial knot that represents } D\}.$$

Singularity index of a knot K can be defined as the minimum value of $S(D)$ minimized over all possible diagrams of K.

The singularity index of a long knot provides a bound on the unknotting number of a long knot, given by the following result.

Theorem 2.6.8. [**Mis14**] *The singularity index of a knot diagram is less than or equal to its unknotting number.*

Chapter 3

Polynomial parameterization of spun knots and d twist spun knots

In this chapter, we describe a method to write a polynomial parameterization for two classes of knotted spheres obtained from spun knot and twist spun knot constructions, denoted by $Spun(K)$ and the $d\text{-}twistspun(K)$, respectively. Section 2.3 shows how these knotted spheres are constructed with the help of certain rotation operations performed on a knotted arc. Hence, this chapter focuses on finding functions representing the rotation operations involved in constructing these knotted spheres. Both of these knotted spheres require a locally flat, properly embedded knotted arc k in ${\mathbb{R}^3}_+$ with endpoints on the boundary $\mathbb{R}^2$. By Lemma 2.6.4, we can choose a polynomial parameterization of a long knot given by

$$\phi(t) \to (f(t), g(t), h(t))$$

such that $h(a) = 0 = h(b)$ and $h(t) > 0$ for all $t \in (a, b)$. Therefore, $\phi([a, b])$ represents the required knotted arc k. We use this parameterization for the knotted arc k.

The rotation operations applied on k result in embeddings represented by smooth functions, not all of which are polynomials. Therefore, to get a polynomial parameterization, we use the Chebyshev approximation [**Abu**] of these smooth functions inside a suitable compact domain. In Appendix A.1, a *Mathematica* program is pro-

vided that is used to compute the Chebyshev approximations of $\cos dx$ and $\sin dx$ in any closed interval where $d \in \mathbb{N}$. For example, the Chebyshev approximations $C(x)$ and $S(x)$ of $\cos x$ and $\sin x$ in $[0, 2\pi]$ respectively are as follows:

$$\begin{aligned} C(x) = & -0.0000193235x^8 + 0.000485652x^7 - 0.00399024x^6 + 0.0081095x^5 \\ & + 0.0265068x^4 + 0.0163844x^3 - 0.509175x^2 + 0.00205416x + 0.999921, \\ S(x) = & \ 8.73651067430188 \times 10^{-19}x^8 + 0.000144829x^7 - 0.00318496x^6 \\ & + 0.0220637x^5 - 0.0322337x^4 - 0.125592x^3 - 0.0257364x^2 \\ & + 1.00614x - 0.000238495. \end{aligned}$$

For better clarity, we present the constructions of the spun knots and the d-twist spun knots in separate sections.

3.1 Polynomial parameterization of spun 2-knot

Theorem 3.1.1. *Given a classical knot K, there exist polynomials $f(t,s)$, $g(t,s), h(t,s)$ and $p(t,s)$ in two variables t and s such that for some interval $[a,b]$ the image of $[a,b] \times [0,2\pi]$ under the map $\Phi : \mathbb{R}^2 \to \mathbb{R}^4$ defined by*

$$\Phi((t,s)) = (f(t,s), g(t,s), h(t,s), p(t,s))$$

is isotopic to the spun of K.

Proof. For the classical knot K, up to isotopy, let us choose a polynomial representation ϕ of K such that $\phi : [a,b] \to \mathbb{R}^3_+$ of the knotted arc k is given by

$$\phi(t) \to (f(t), g(t), h(t))$$

such that $h(a) = 0 = h(b)$ and $h(t) > 0$ for $t \in (a,b)$. Now, the spinning construction gives a map $\bar{\Phi} : [a,b] \times [0,2\pi] \to \mathbb{R}^4$ defined by

$$\bar{\Phi}(t,s) = (f(t),\ g(t),\ h(t)\cos s,\ h(t)\sin s)$$

that represents $Spun(K)$. Using the point set topology argument, one can prove that

the image of $\bar{\Phi}$ in $\mathbb{R}^4$ is homeomorphic to S^2. Now, we replace the trigonometric functions $\cos s$ and $\sin s$ with their Chebyshev approximations inside the interval $[0, 2\pi]$. Let the Chebyshev approximation of $\cos s$ and $\sin s$ inside the interval $[0, 2\pi]$ be denoted by $C(s)$ and $S(s)$, respectively. Then by choosing $f(t, s) = f(t)$, $g(t, s) = g(t)$, $h(t, s) = h(t)\, C(s)$ and $p(t, s) = h(t)\, S(s)$, we obtain a polynomial parameterization of $Spun(K)$. This completes the proof. □

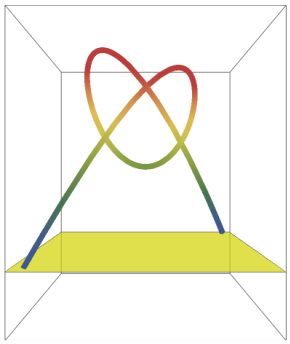

Figure 3.1: Knotted arc of long trefoil knot

Example 3.1.2 (Spun trefoil knot)**.** Let us take the following polynomial representation of the long trefoil knot given by $\phi : \mathbb{R} \to \mathbb{R}^4$ where

$$\phi(t) = \left(t^3 - 3t, t^5 - 10t, t^4 - 4t^2\right)$$

We change the function $(t^4 - 4t^2)$ to $(-t^4 + 4t^2 + 3)$ which has only two real roots $t = -2.1554$ and $t = 2.1554$. This ensures that the knotted part of the long knot is in the upper half space and intersects the boundary of $\mathbb{R}^2$ only at two points. Therefore, the knotted arc k (Figure 3.1) is given by $\phi : [-2.1554, 2.1554] \to \mathbb{R}^4$ where

$$\phi(t) = \left(t^3 - 3t, t^5 - 10t, -t^4 + 4t^2 + 3\right).$$

The spun trefoil knot is given by the parameterization $\bar{\Phi} : [-2.1554, 2.1544] \times [0, 2\pi] \to \mathbb{R}^4$ where

$$\bar{\Phi}(t, s) = \left((t^3 - 3t), (t^5 - 10t), (-t^4 + 4t^2 + 3)\, \cos s, (-t^4 + 4t^2 + 3)\, \sin s\right).$$

After replacing cosine and sine functions with $C(s)$ and $S(s)$ respectively, we get the

final polynomial parameterization $\Phi : [-2.1554, 2.1544] \times [0, 2\pi] \to \mathbb{R}^4$ defined by

$$\Phi(t, s) = \left((t^3 - 3t), (t^5 - 10t), (-t^4 + 4t^2 + 3)\, C(s), (-t^4 + 4t^2 + 3)\, S(s)\right).$$

Mathematica plots for a projection of the spun trefoil are shown in Figure 3.2(a). In Figure 3.2(b), an inside view is also given where it can be seen that the knotted arc does not deform while spinning around $\mathbb{R}^2$.

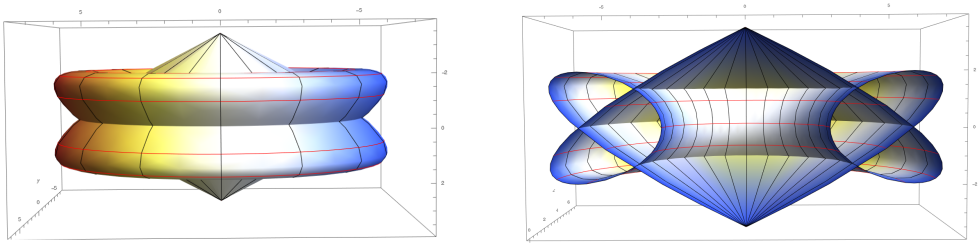

(a) Projection on a hyperplane (b) An inside view

Figure 3.2: Spun trefoil knot

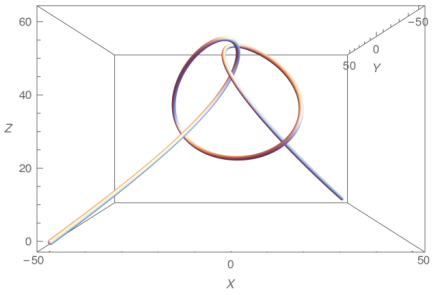

Figure 3.3: Knotted arc of long figure eight knot

Example 3.1.3. (Spun figure eight knot): Using the parametrization for the long figure eight knot given in [**ANB**] (Figure 3.3) and following the same procedure as above, we obtain a polynomial parametrization of the spun figure eight knot given by $\phi : [a, b] \times [0, 2\pi] \to \mathbb{R}^4$ where

$$\Phi(t, s) = (f(t), g(t), h(t)\, C(s), h(t)\, S(s))$$

$$\text{where,} \qquad f(t) = \frac{2}{5}\left(t^2 - 7\right)\left(t^2 - 10\right) t,$$
$$g(t) = \frac{1}{10} t \left(t^2 - 4\right)\left(t^2 - 9\right)\left(t^2 - 12\right),$$

$$h(t) = (20 - 13t^2 - t^4).$$

and $C(s)$, $S(s)$ are the Chebyshev approximations of $\cos s$ and $\sin s$ respectively. Figure 3.4 shows the *Mathematica* plot of a projection of the spun figure eight knot on *XZW-plane*.

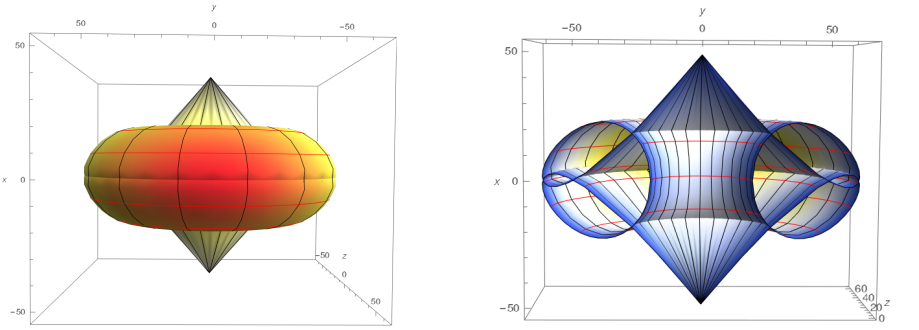

(a) Projection on a hyperplane (b) Inside view of the projection

Figure 3.4: Spun figure eight knot

3.2 Polynomial parameterization of d twist spun knot

Theorem 3.2.1. *Given a classical knot K, there exist polynomials $f(t,\theta)$, $g(t,\theta)$, $h(t,\theta)$ and $p(t,\theta)$ in two variables t and θ such that for some interval $[a,b]$, the image of $[a,b]\times[0,2\pi]$ under the map $\Psi : \mathbb{R}^2 \to \mathbb{R}^4$ defined by*

$$\Psi(t,\theta) = \big(\bar{f}(t,\theta), \bar{g}(t,\theta), \bar{h}(t,\theta), \bar{p}(t,\theta)\big)$$

is isotopic to the d-twist spun of K.

Proof. We start with the parametrization $\phi : [a,b] \to \mathbb{R}^3_+$ of the knotted arc k, given by

$$\phi(t) \to (f(t), g(t), h(t))$$

where $h(a) = 0 = h(b)$ and $h(t) > 0$ for $t \in (a,b)$. The endpoints of k on the boundary $\mathbb{R}^2$ is given by $(f(a), g(a), 0)$ and $(f(b), g(b), 0)$. Now we find an interval $[a', b'] \subset [a,b]$

where all the crossings of K lie.

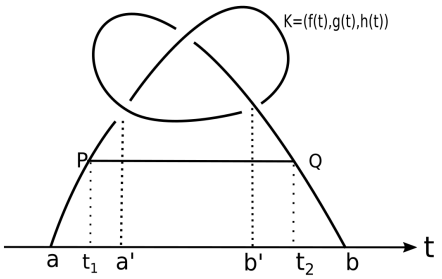

Figure 3.5: Rotating about PQ

In the twist spinning construction, the knotted part of the arc is contained in a 3-ball in $\mathbb{R}^3_+$ and is rotated around the axis of the ball. To achieve this first we choose the axis of rotation as a line segment PQ parallel to the XY plane joining two points on the knotted arc, say $P := (f(t_1), g(t_1), h(t_1))$ and $Q := (f(t_2), g(t_2), h(t_2))$, where $[a', b'] \subset [t_1, t_2]$ and $h(t_1) = h(t_2) = c$ (Figure 3.5). The value of c is chosen so that the knotted part of the arc does not intersect the XY plane while rotating around PQ. By Rodrigues' rotation formula [**Rod**], the rotation around PQ is represented by the following matrix.

$$\mathbf{R'} = \mathbf{T_c} * \mathbf{R} * \mathbf{T_c^{-1}} = \mathbf{T_c} * \mathbf{R} * \mathbf{T_{-c}},$$

where $\mathbf{T_c}$ is the translation matrix along Z axis which will send (x, y, z) to $(x, y, z+c)$ and $\mathbf{R}$ gives the rotation around the line $P'Q'$ on XY plane, parallel to PQ, joining the points $P' = (f(t_1), g(t_1), 0)$ and $Q' = (f(t_2), g(t_2), 0)$ on the knotted arc.

The rotation matrix $\mathbf{R}$ is defined as follows: If $\mathbf{v}$ is a vector in $\mathbb{R}^3$ and $\mathbf{k}$ is a unit vector describing an axis of rotation around which $\mathbf{v}$ rotates by an angle ϕ according to the right-hand rule, the Rodrigues formula for the rotated vector $\mathbf{v_{rot}}$ is given by

$$\mathbf{v}_{rot} = \mathbf{v}\,\cos\phi + (\mathbf{k} \times \mathbf{v})\sin\phi + \mathbf{k} \cdot (\mathbf{k} \cdot \mathbf{v})(1 - \cos\phi).$$

In this case, $\mathbf{k}$ is along the line joining $(f(t_1), g(t_1), 0)$ and $(f(t_2), g(t_2), 0)$. So,

$$\mathbf{k} = \Big(\frac{f(t_2) - f(t_1)}{N}, \frac{g(t_2) - g(t_1)}{N}, 0\Big),$$

where $N = \sqrt{(f(t_2) - f(t_1))^2 + (g(t_2) - g(t_1))^2}$.

For simplification, let us denote

$$f_{21} := f(t_2) - f(t_1)$$

$$g_{21} := g(t_2) - g(t_1).$$

Then

$$\mathbf{k} = \Big(\frac{f_{21}}{N}, \frac{g_{21}}{N}, 0\Big),$$

where $N = \sqrt{f_{21}^2 + g_{21}^2}$.

Then the rotation matrix through an angle ϕ counterclockwise around the axis $\mathbf{k}$ is

$$\mathbf{R} = \mathbf{I} + \sin\phi\ \mathbf{K} + (\mathbf{1} - \cos\phi)\ \mathbf{K^2},$$

where

$$\mathbf{K} = \begin{pmatrix} 0 & -k_z & k_y \\ k_z & 0 & -k_x \\ -k_y & k_x & 0 \end{pmatrix} = \begin{pmatrix} 0 & 0 & \frac{g_{21}}{N} \\ 0 & 0 & -\frac{f_{21}}{N} \\ -\frac{g_{21}}{N} & \frac{f_{21}}{N} & 0 \end{pmatrix}.$$

and the rotation matrix around PQ is given by,

$$\mathbf{R'} = \mathbf{T_c} * \mathbf{R} * \mathbf{T_c^{-1}} = \mathbf{T_c} * \mathbf{R} * \mathbf{T_{-c}},$$

where

$$\mathbf{R} = \begin{pmatrix} \frac{f_{21}^2 \ + \ g_{21}^2 \ \cos\phi}{N^2} & \frac{f_{21}\ g_{21}\ (1 - \cos\phi)}{N^2} & \frac{g_{21}\ \sin\phi}{N} & 0 \\ \frac{f_{21}\ g_{21}\ (1 - \cos\phi)}{N^2} & \frac{f_{21}^2\ \cos\phi \ + \ g_{21}^2}{N^2} & -\frac{f_{21}\ \sin\phi}{N} & 0 \\ -\frac{g_{21}\ \sin\phi}{N} & \frac{f_{21}\ \sin\phi}{N} & \cos\phi & 0 \\ 0 & 0 & 0 & 1 \end{pmatrix}$$

and $\mathbf{T_c}$ is the translation matrix along z-axis which sends (x, y, z) to $(x, y, z + c)$,

given by

$$T_c = \begin{pmatrix} 1 & 0 & 0 & 0 \\ 0 & 1 & 0 & 0 \\ 0 & 0 & 1 & c \\ 0 & 0 & 0 & 1 \end{pmatrix}.$$

Then,

$$\mathbf{R}' = \begin{pmatrix} \dfrac{f_{21}^2 \ + \ g_{21}^2 \ \cos\phi}{N^2} & \dfrac{f_{21}\ g_{21}\ (1-\cos\phi)}{N^2} & \dfrac{g_{21}\ \sin\phi}{N} & -\dfrac{c\ g_{21}\ \sin\phi}{N} \\ \dfrac{f_{21}\ g_{21}\ (1-\cos\phi)}{N^2} & \dfrac{f_{21}^2\ \cos\phi \ + \ g_{21}^2}{N^2} & -\dfrac{f_{21}\ \sin\phi}{N} & \dfrac{c\ f_{21}\ \sin\phi}{N} \\ -\dfrac{g_{21}\ \sin\phi}{N} & \dfrac{f_{21}\ \sin\phi}{N} & \cos\phi & -c\ \cos\phi + c \\ 0 & 0 & 0 & 1 \end{pmatrix}.$$

Thus, the rotation around PQ is given by the parametrization :

$$[a,b] \times [0,2\pi] \longrightarrow \mathbb{R}^4$$

$$(t,\phi) \longrightarrow (f'(t,\phi), g'(t,\phi), h'(t,\phi)) \tag{3.2.1}$$

where

$$f'(t,\phi) = \frac{\left(f_{21}^2 \ + \ g_{21}^2 \ \cos\phi\right)\ \mathbf{f}(\mathbf{t}) + f_{21}\ g_{21}\ (1-\cos\phi)\,\mathbf{g}(\mathbf{t}) + N\ g_{21}\ \sin\phi\,(\mathbf{h}(\mathbf{t}) - c)}{N^2} \tag{3.2.2}$$

$$g'(t,\phi) = \frac{f_{21}\ g_{21}\ (1-\cos\phi)\,\mathbf{f}(\mathbf{t}) + \left(f_{21}^2\ \cos\phi \ + \ g_{21}^2\right)\ \mathbf{g}(\mathbf{t}) + N\ g_{21}\ \sin\phi\,(c - \mathbf{h}(\mathbf{t}))}{N^2} \tag{3.2.3}$$

$$h'(t,\phi) = \frac{-g_{21}\ \sin\phi\ \mathbf{f}(\mathbf{t}) + f_{21}\sin\phi\ \mathbf{g}(\mathbf{t}) + N\ \cos\phi\,\mathbf{h}(\mathbf{t}) + N\,c\,(1-\cos\phi)}{N} \tag{3.2.4}$$

and $N = \sqrt{f_{21}^2 + g_{21}^2}$.

Now, in the twist-spinning construction, there is no rotation outside the 3-ball that contains the knotted part. This is the same as not rotating the knotted arc outside the endpoints of PQ. We achieve this by combining the rotation functions with a bump function. We have, $[a,b] = [a,t_1] \cup [t_1,a'] \cup [a',b'] \cup [b',t_2] \cup [t_2,b]$ (Figure 3.5), where

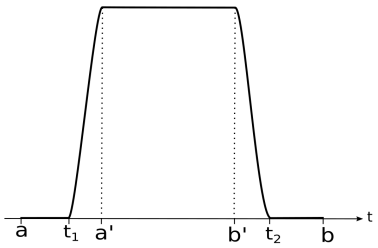

Figure 3.6: Bump function B(t).

1. $[a', b']$ contains all the crossings of the knot.
2. t_1, t_2 corresponds to the endpoints of P and Q. So, $[a, t_1]$ and $[t_2, b]$ correspond to the parts of the arc outside the axis PQ.

Therefore, we define a bump function which takes the value 1 in $[a', b']$ and 0 outside $[t_1, t_2]$. First, consider the function

$$F(t) = \begin{cases} e^{-\frac{1}{t}}, & t > 0 \\ 0, & t \leq 0 \end{cases}.$$

Then define the bump function, $B(t)$ as follows:

$$B(t) = \frac{F(d_1 - t^2)}{F(t^2 - d_2) + F(d_1 - t^2)}$$

where $d_1, d_2 \in \mathbb{R}^+$ are chosen in such a way that

$$B(t) = \begin{cases} 1, & t \in [a', b'] \\ 0, & t \in [a, t_1] \cup [t_2, b] \\ \in (0, 1), & \text{otherwise} \end{cases}.$$

See Figure 3.6.
Then, for $t \in [a, b]$, we define

$$\begin{aligned} \tilde{f}(t, \phi) &= B(t)\, f'(t, \phi) + (1 - B(t))\, f(t) \\ \tilde{g}(t, \phi) &= B(t)\, g'(t, \phi) + (1 - B(t))\, g(t) \\ \tilde{h}(t, \phi) &= B(t)\, h'(t, \phi) + (1 - B(t))\, h(t). \end{aligned}$$

Now, the knotted arc is rotating d times around the PQ axis in $\mathbb{R}^3_+$ while rotating around the XY plane in $\mathbb{R}^4$. Therefore, the rotation angle around PQ is d times the rotation angle around the XY plane i.e. $\phi = d\,\theta$.
Hence, the parameterization for d-twist spun knot is given by $\bar{\Psi} : [a,b]\times[0,2\pi] \longrightarrow \mathbb{R}^4$ where

$$\bar{\Psi}(t,\theta) = \Big(\tilde{f}(t,d\theta)\,,\,\tilde{g}(t,d\theta)\,,\,\tilde{h}(t,d\theta)\,\cos\,\theta\,,\,\tilde{h}(t,d\theta)\,\sin\,\theta\Big)\,. \tag{3.2.5}$$

Now, replacing cosine and sine functions with their corresponding Chebyshev polynomial approximations $C(\theta), S(\theta)$ in $[0,2\pi]$ and $B(t)$ with its Chebyshev polynomial approximations in $[a,b]$, say $B'(t)$, we obtain a polynomial parametrization of d-twist spun knots $\Psi : [a,b]\times[0,2\pi] \longrightarrow \mathbb{R}^4$ given by

$$\Psi(t,\theta) = \big(\bar{f}(t,\theta)\,,\,\bar{g}(t,\theta)\,,\,\bar{h}(t,\theta)\,,\,\bar{p}(t,\theta)\big)\,. \tag{3.2.6}$$

where

$$\begin{aligned}
\bar{f}(t,\theta) &= B'(t)\,f'(t,d\theta) + (1-B'(t))\,f(t),\\
\bar{g}(t,\theta) &= B'(t)\,g'(t,d\theta) + (1-B'(t))\,g(t),\\
\bar{h}(t,\theta) &= (B'(t)\,h'(t,d\theta) + (1-B'(t))\,h(t))\,C(\theta),\\
\bar{p}(t,\theta) &= (B'(t)\,h'(t,d\theta) + (1-B'(t))\,h(t))\,S(\theta).
\end{aligned}$$

This completes the proof.

□

Example 3.2.2 (d-twist spun trefoil)**.** Start with a polynomial representation of the long trefoil knot (Figure 3.7), given by $\phi : \mathbb{R} \to \mathbb{R}^4$ where

$$\phi(t) = (x(t), y(t), z(t))$$

$$\begin{aligned}
x(t) &= t^3 - 3t\\
y(t) &= t^5 - 10t\\
z(t) &= -t^4 + 4t^2 + 16.
\end{aligned}$$

Solving for t_1, t_2 such that $x(t_1) = x(t_2)$ and $y(t_1) = y(t_2)$ we can get the crossing

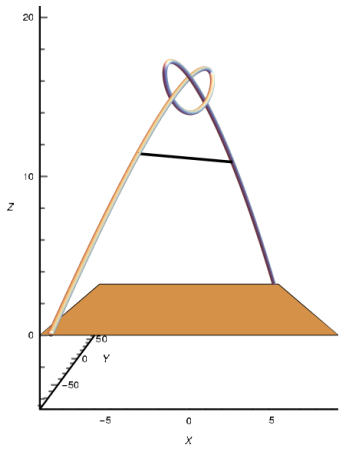

Figure 3.7: knotted trefoil arc with endpoints on XY plane with axis of rotation

data and solving $z(t) = 0$ will give the interval for the arc. Therefore, we have

$$\begin{aligned}
[a, b] &= [-2.54404, 2.54404], \\
[a', b'] &= [-1.946, 1.946], \\
P &= (f[-2.19], g[-2.19], h[-2.19]), \\
Q &= (f[2.19], g[2.19], h[2.19]), \\
c &= h[2.19].
\end{aligned}$$

Hence, $\mathbf{k}$ is along the line joining $(-f[2.19], -g[2.19], 0)$ and $(f[2.19], g[2.19], 0)$. So,

$$\mathbf{k} = \Big(\frac{f[2.19]}{\sqrt{f[2.19]^2 + g[2.19]^2}}, \frac{g[2.19]}{\sqrt{f[2.19]^2 + g[2.19]^2}}, 0\Big)$$

and

$$N = \sqrt{f[2.19]^2 + g[2.19]^2}.$$

This rotation about PQ is given by the parametrization (See Figure 3.8):

$$[-2.54404, 2.54404] \times [0, 2\pi] \longrightarrow \mathbb{R}^4$$

$$(t, \phi) \longrightarrow (f'(t, \phi), g'(t, \phi), h'(t, \phi))$$

where,

$$f'(t,\phi) = \frac{(f[2.19]^2 \ + \ g[2.19]^2 \ \cos\phi)\ \mathbf{f(t)} + f[2.19]\ g[2.19]\ (1-\cos\phi)\,\mathbf{g(t)} + (\mathbf{h(t)} - c)N\ g[2.19]\ \sin\phi}{N^2} \tag{3.2.7}$$

$$g'(t,\phi) = \frac{f[2.19]\ g[2.19]\ (1-\cos\phi)\,\mathbf{f(t)} + (f[2.19]^2 \ \cos\phi \ + \ g[2.19]^2)\ \mathbf{g(t)} + (c - \mathbf{h(t)})N\ g[2.19]\ \sin\phi}{N^2} \tag{3.2.8}$$

$$h'(t,\phi) = \frac{-g[2.19]\ \sin\phi\ \mathbf{f(t)} + f[2.19]\sin\phi\ \mathbf{g(t)} + N\,\mathbf{h(t)}\cos\phi + N\,c\,(1-\cos\phi)}{N} \tag{3.2.9}$$

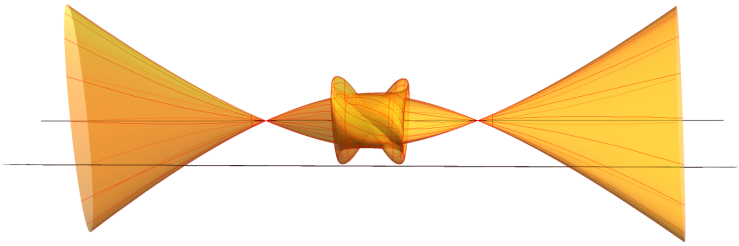

Figure 3.8: Rotating the long trefoil arc about PQ

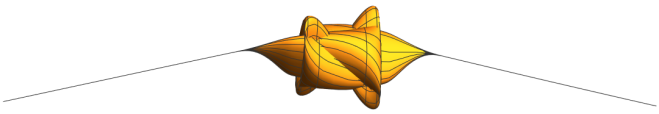

Figure 3.9: $(\tilde{f}(t,\phi), \tilde{g}(t,\phi), \tilde{h}(t,\phi))$ in $[-2.54404, 2.54404]$

Now, the bump function is

$$B(t) = \frac{F(4.8 - t^2)}{F(t^2 - 3.8) + F(4.8 - t^2)}.$$

The restricted rotation about PQ (See Figure 3.9) is given by

$$(t,\phi) \longrightarrow \left\{ \left(\tilde{f}(t,\phi), \tilde{g}(t,\phi), \tilde{h}(t,\phi) \right) \middle| \begin{array}{c} -2.54404 \leq t \leq 2.54404 \\ 0 \leq \phi < 2\pi \end{array} \right\}$$

where

$$\begin{aligned} \tilde{f}(t,\phi) &= B(t)\, f'(t,\phi) + (1 - B(t))\, f(t) \\ \tilde{g}(t,\phi) &= B(t)\, g'(t,\phi) + (1 - B(t))\, g(t)\,. \\ \tilde{h}(t,\phi) &= B(t)\, h'(t,\phi) + (1 - B(t))\, h(t) \end{aligned} \tag{3.2.10}$$

Hence, the polynomial parameterization $\Psi : [-2.54404, 2.54404] \times [0, 2\pi] \longrightarrow \mathbb{R}^4$ for the d-twist spun trefoil knot is given by

$$\Psi(t,\theta) = \left(\tilde{f}(t, d\theta), \tilde{g}(t, d\theta), \tilde{h}(t, d\theta)\, C(\theta), \tilde{h}(t, d\theta)\, S(\theta) \right)$$

The *Mathematica* program for a projection of d-twist spun knot is provided in Appendix A.4. Some of the projections of the d-twist spun trefoil on a hyperplane for the values $d = 0, 1, 2, 5, 10, 20$ are given below. In Figure 3.10(a), it is clear that $d = 0$ represents Artin's spun knot. Figure 3.10(b) and Figure 3.10(d) illustrate the deformation of the knotted arc while rotating around $\mathbb{R}^2$ in the twist spun knot construction, which differs from Artin's spun knot construction.

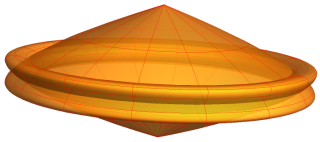

(a) 0-twist spun trefoil

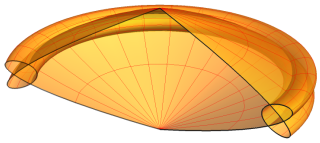

(b) 0-twist spun trefoil: inside view

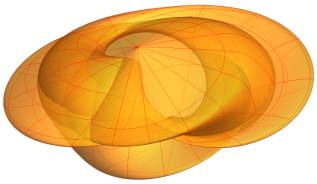

(c) 1-twist spun trefoil

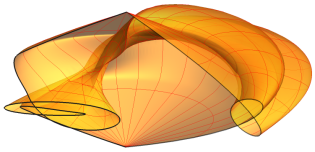

(d) 1-twist spun trefoil: inside view

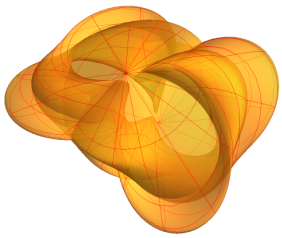

(e) 2-twist spun 2-trefoil

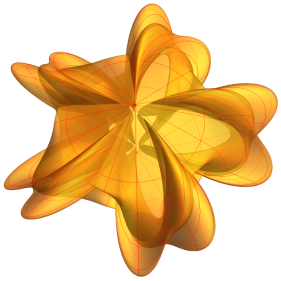

(f) 5-twist spun 2-trefoil

(g) 10-twist spun 2-trefoil

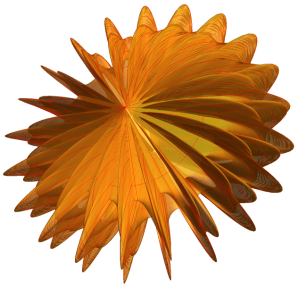

(h) 20-twist spun 2-trefoil

Figure 3.10: d-twist spun 2-trefoil for d=0,1,2,5,10,20

Chapter 4

Non-triviality of welded knots and ribbon torus knots

After discussing the parameterization of knotted spheres, the next surface knot we focus on is knotted torus. Ribbon torus knots are a special type of knotted tori in $\mathbb{R}^4$ which has a projection in $\mathbb{R}^3$ with just ribbon singularities. It was shown in Section 2.5 how a ribbon torus knot T in $\mathbb{R}^4$ can be considered as $Tube(K)$ for a welded knot K, using Satoh's *Tube map* [**Sat00**]. Additionally, $\pi_1(\mathbb{R}^4 \setminus Tube(K)) \cong G(K)$ where $G(K)$ is the fundamental group or the knot group of the welded knot. It is easy to see that tube of a welded unknot is a trivial knotted torus and also the fundamental group of the complement of the trivial surface knot is isomorphic to $\mathbb{Z}$. Before we parameterize the ribbon torus knots, we would like to understand how to choose a welded knot so that the corresponding tube is a non-trivial ribbon torus knot.

In this chapter we discuss about the non-triviality of ribbon torus knots by exploring two welded knot invariants, namely "welded unknotting number" (Section 4.1) and the knot group (Section 4.2). We explicitly compute these invariants for welded knots that are obtained by converting some classical crossings to welded crossings in the standard diagram of two important families of classical knots, namely T_n, the twist knots with n half twists and $K(2, 2n+1)$, the torus knots of type $(2, 2n+1)$. In Section 4.3, we provide results regarding the knot groups of all welded knots that can be obtained from the standard diagrams of all knots up to 6 crossings in Rolfsen's table, by converting classical crossings to welded crossings, .

4.1 Welded unknotting number

Definition 4.1.1. [**GKPV**] For any welded knot diagram D, its *welded unknotting number*, denoted by $u_w(D)$, is defined as the minimum number of classical crossings that need to be changed to welded crossings such that the resultant diagram becomes a trivial diagram.

Then, the *welded unknotting number of* K, denoted by $u_w(K)$, is defined by

$$u_w(K) \coloneqq \min_D\{u_w(D) \mid D \text{ is a diagram of } K\}.$$

Welded unknotting number is clearly an invariant for welded knots and hence for classical knots as well.

Theorem 4.1.2. *For every welded knot K, the welded unknotting number does not exceed the warping degree, i.e., $u_w(K) \leq d(K)$.*

Proof. Let $d(K) = r$. Suppose D_a is an oriented welded knot diagram of K with a base point a that realizes the warping degree of K, i.e. $d(D_a) = r$. It implies that if we follow D_a along its orientation, then we first meet the under-crossings at exactly r number of crossing points of D_a. By transforming these r crossings into welded crossings, we obtain a descending welded knot diagram, which is in fact a trivial welded knot diagram, as by Proposition 2.1.17. Thus $u_w(K) \leq r = d(K)$. □

Theorem 4.1.3. *For every welded knot K, the welded unknotting number does not exceed twice the unknotting number, i.e., $u_w(K) \leq 2\,u(K)$.*

Proof. Let $u(K) = n$. Then there exists a welded knot diagram D representing K with crossings $c_1, c_2, \ldots, c_n$ on D such that by switching all c_i's, we obtain a trivial welded knot diagram, say $\widetilde{D}$. Apply an R_2-move locally in a neighborhood of c_i for each $i = 1, 2, \ldots, n$ to obtain another diagram D' of K, as shown in Figure 4.1. Observe that if we change both c_i and its adjacent crossing to welded crossings, we obtain a diagram that is welded equivalent to $\widetilde{D}$. This implies $u_w(K) \leq u_w(D') \leq 2n = 2\,u(K)$. □

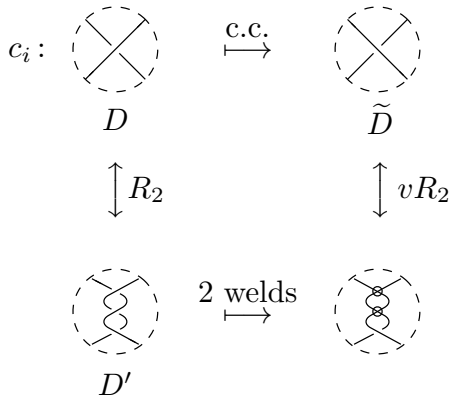

Figure 4.1: Realizing a over/under switch by two classical to welded changes.

In the remaining part of this section we would like to estimate the welded unknoting number for knots from the family of twist knots and the torus knots of type $(2, 2n + 1)$. Let us denote the twist knot with n half-twists by T_n.

(a) $d(D'_a) = 0$.

(b) $d(D_b) = 0$.

Figure 4.2: Twist knots T_1 and T_2 with one welded crossing

Theorem 4.1.4. *T_n has welded unknotting number 1 for all n.*

Proof. Note that T_1 is the trefoil and T_2 is the figure-eight knot. We first prove that converting a single classical crossing to welded, at any position in T_n for $n = 1$ and 2, yields a welded knot equivalent to the unknot. In Figure 4.2(a) and 4.2(b) we can see that the warping degree for trefoil and figure-eight knot with one welded crossing turns out to be zero. Therefore by Corollary 2.1.28 both of these are unknots. Let the standard diagram of twist knot be also denoted by T_n. Denote the welded diagram obtained by converting the left most crossing in T_n by $T_{n,1}$ as shown in Figure 4.3. In the Figure 4.3, we show that $T_{n,1}$ is equivalent to $T_{n-2,1}$ using detour move, F_o

and first Reidemeister move. Applying this process multiple times we get $T_{2,1}$ (if n is odd) or $T_{1,1}$ (if n is even) which are shown to be unknot. □

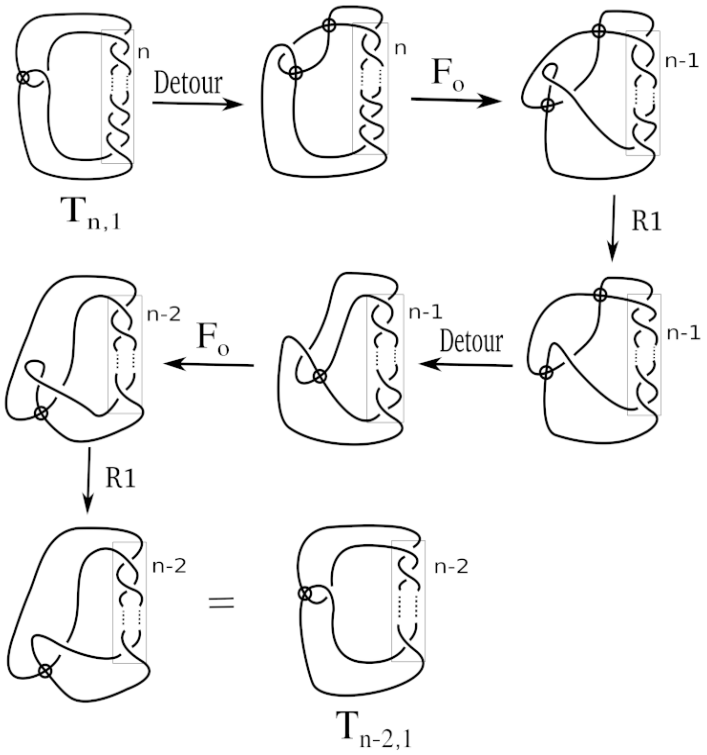

Figure 4.3: Triviality of the twist knot with one weld

Let $K(2, 2n+1)$ denote the torus knot of type $(2, 2n+1)$. Then we have

Theorem 4.1.5. $u_w(K(2, 2n+1)) \leq u(K(2, 2n+1)) = n$.

Proof. We denote the standard oriented diagram of $K(2, 2n+1)$ by $K(2, 2n+1)$ itself. See Figure 4.4(a). The classical unknotting number of $K(2, 2n+1)$ is $\frac{(2-1)(2n+1-1)}{2} = n$, as proved by Kronheimer and Mrowka [**KroMro**]. If we take a base point anywhere on $K(2, 2n+1)$ and go along the diagram following the orientation, we always find n number of undercrossings in alternate positions. Now, covert n number of alternate crossings to welded in $K(2, 2n+1)$ (Figure 4.4(b)) and denote this oriented diagram by D'_n. Then, D'_n be a descending welded knot diagram with respect to any base point on the diagram and by Proposition 2.1.17, it be equivalent to an unknot. Hence the proof. □

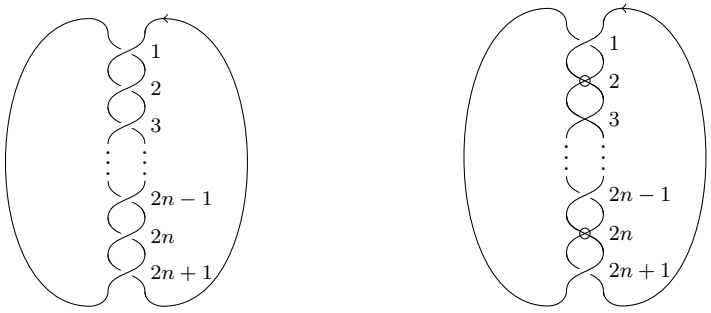

(a) Standard diagram (b) Alternate welded crossings

Figure 4.4: Torus knot $K(2, 2n + 1)$

4.2 Non-trivial ribbon torus knots and fundamental group of welded knots

In this section, we consider the standard diagrams of family of torus knots $K(2, 2n+1)$ and the family of twist knots T_n. We change the crossings from classical to welded one by one and observe how the fundamental group changes. To obtain a non-trivial ribbon torus knots corresponding to the welded knots obtained from these two families, we focus on the cases when the knot group is not isomorphic to $\mathbb{Z}$.

4.2.1 Welded knots arising from $K(2, 2n + 1)$

4.2.1.1 $K(2, 2n + 1)$ with one welding

Let $K_{n,1}$ be the welded knot represented by the diagram shown in Figure 4.5, which is obtained from $K(2, 2n + 1)$ by welding one crossing. Let $G(K_{n,1})$ denotes the fundamental group of $K_{n,1}$.

Theorem 4.2.1. *$G(K_{n,1}) \cong \mathbb{Z}$.*

Proof. The Wirtinger relations at the crossings of the diagram D whose arcs are labeled as shown in Figure 4.5 are given by

$$x_k = \begin{cases} (ba)^{\frac{k+1}{2}} a (ba)^{-\frac{k+1}{2}} & \text{if } k \text{ is odd, } k \leq 2n-3 \\ (ba)^{\frac{k}{2}} b (ba)^{-\frac{k}{2}} & \text{if } k \text{ is even, } k \leq 2n-2 \end{cases}$$

$$
\begin{aligned}
b &= x_{2n-2}x_{2n-3}x_{2n-2}^{-1} \\
&= (ba)^n a (ba)^{-n} \\
a &= bx_{2n-2}b^{-1} \\
&= b(ba)^{n-1}b(ba)^{-(n-1)}b^{-1}.
\end{aligned}
$$

Then a Wirtinger presentation of $G(K_{n,1})$ is given by

$$
G(K_{n,1}) = \left\langle a, b \,\middle|\, b(ba)^n = (ba)^n a,\ ab(ba)^{n-1} = b(ba)^{n-1}b \right\rangle.
$$

Observe that $ab(ba)^{n-1} = b(ba)^{n-1}b = b(ba)^n(ba)^{-1}b = (ba)^n a(ba)^{-1}b = (ba)^n$ implies $ab = ba$, which is a consequence of the relations in $G(K_{n,1})$. Further, $(ba)^n a = b(ba)^n = b(ab)^n = (ba)^n b$ implies $a = b$. Thus $G(K_{n,1}) \cong \langle a : \rangle$, which is isomorphic to $\mathbb{Z}$. □

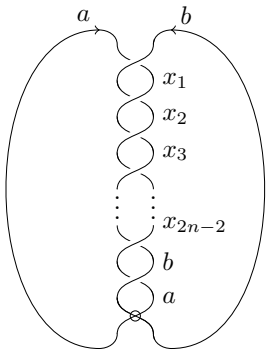

Figure 4.5: $K(2, 2n+1)$ with one welded crosssing.

Thus, it is not certain if the welded knot $K_{n,1}$ or the corresponding tube are trivial or not.

4.2.1.2 $K(2, 2n+1)$ with two weldings

We start with the standard diagram $K(2, 2n+1)$. Two welded crossings divide the diagram in two parts with m_1 and m_2 number of classical crossings as shown in the Figure 4.6. Then, $m_1 + m_2 = (2n+1) - 2 = 2n - 1$. Therefore, the total number of

remaining classical crossings is always odd. We denote this welded knot diagram as $K_{n,2,m_1}$. Now, because of the cyclic nature of the standard diagram of $K(2, 2n+1)$ the following pairs of $\{m_1, m_2\}$ represent the same welded diagram:

$$\{i, j\} \text{ and } \{j, i\} \quad \text{for } i, j = 0, 1, \cdots, 2n-1.$$

So, we only consider the values $m_1 = 0, 1, 2, \cdots, (n-1)$ for $K_{n,2,m_1}$.

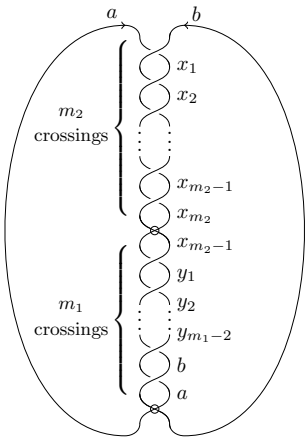

Figure 4.6: $K(2, 2n+1)$ with two welded crossings and arbitrary gap.

Now, $K_{n,2,0}$ is equivalent to the classical knot diagram of $K(2, 2n-1)$ by virtual Reidemeister move vR_2 (Figure 4.7) and the fundamental group of $K(2, 2n-1)$ is not isomorphic to $\mathbb{Z}$. Let $G(K_{n,2,m_1})$ denote the knot group of the welded knot $K_{n,2,m_1}$ where $0 \leq m_1 \leq (n-1)$.

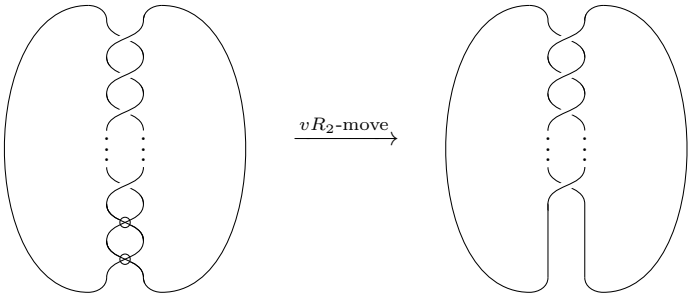

Figure 4.7: $K(2, 2n+1)$ with two welds and zero gap.

Proposition 4.2.2.

$$G(K_{n,2,m_1}) = \langle a, b \mid R1, R2 \rangle \quad \textit{if } m_1 \textit{ is even},$$

$$G(K_{n,2,m_1}) = \langle a, b \mid R3, R4 \rangle \quad \textit{if } m_1 \textit{ is odd},$$

where

$$(ba)^{\frac{m_2}{2}} (ab)^{\frac{m_1-1}{2}} = (ab)^{\frac{m_2-2}{2}} a (ab)^{\frac{m_1-1}{2}} a \tag{R1}$$

$$ab (ba)^{\frac{m_2}{2}} a (ba)^{\frac{m_1-3}{2}} = b (ba)^{\frac{m_2}{2}} (ab)^{\frac{m_1-1}{2}}, \tag{R2}$$

$$b (ab)^{\frac{m_2-1}{2}} b (ab)^{\frac{m_1-2}{2}} = (ab)^{\frac{m_2-1}{2}} (ba)^{\frac{m_1}{2}}, \tag{R3}$$

$$ab (ba)^{\frac{m_2-1}{2}} b (ba)^{\frac{m_1-2}{2}} = b (ba)^{\frac{m_2-1}{2}} b^2 (ab)^{\frac{m_1-2}{2}}. \tag{R4}$$

Proof. To find a presentation of the knot group $G(K_{n,2,m_1})$, let the Wirtinger generators be $x_1, x_2, \cdots, x_{m_2-1}$ and $y_1, y_2, \cdots, y_{m_1-2}, b, a$ (Figure 4.6). Then the Wirtinger relations are

$$x_1 = bab^{-1},$$
$$x_2 = baba^{-1}b^{-1}.$$

By induction, for each $i = 1, 2, \ldots, m_2$

$$x_i = \begin{cases} \underbrace{ba \cdots ba}_{i} b \underbrace{a^{-1}b^{-1} \cdots a^{-1}b^{-1}}_{i} & \text{when } i \text{ is even}, \\ \underbrace{ba \cdots ba}_{i-1} bab^{-1} \underbrace{a^{-1}b^{-1} \cdots a^{-1}b^{-1}}_{i-1} & \text{when } i \text{ is odd} \end{cases}.$$

Therefore,

$$x_{m_2} = \begin{cases} \underbrace{ba \cdots ba}_{m_2} b \underbrace{a^{-1}b^{-1} \cdots a^{-1}b^{-1}}_{m_2} & \text{when } m_2 \text{ is even}, \\ \underbrace{ba \cdots ba}_{m_2-1} bab^{-1} \underbrace{a^{-1}b^{-1} \cdots a^{-1}b^{-1}}_{m_2-1} & \text{when } m_2 \text{ is odd}. \end{cases}$$

- Case I : m_2 is even and therefore m_1 is odd:

$$\begin{aligned} y_1 &= x_{m_2-1} x_{m_2} x_{m_2-1}^{-1}, \\ &= \underbrace{ba \cdots ba}_{m_2} aba^{-1} \underbrace{a^{-1}b^{-1} \cdots a^{-1}b^{-1}}_{m_2}, \\ y_2 &= \underbrace{ba \cdots ba}_{m_2} abab^{-1}a^{-1} \underbrace{a^{-1}b^{-1} \cdots a^{-1}b^{-1}}_{m_2}. \end{aligned}$$

By induction, for each $i = 1, 2, \ldots, m_1 - 2$

$$y_i = \begin{cases} \underbrace{ba\cdots ba}_{m_2}\,\underbrace{ab\cdots ab}_{i}\; a\;\underbrace{b^{-1}a^{-1}\cdots b^{-1}a^{-1}}_{i}\,\underbrace{a^{-1}b^{-1}\cdots a^{-1}b^{-1}}_{m_2} & \text{when } i \text{ is even,} \\ \underbrace{ba\cdots ba}_{m_2}\,\underbrace{ab\cdots ab}_{i-1}\; aba^{-1}\;\underbrace{b^{-1}a^{-1}\cdots b^{-1}a^{-1}}_{i-1}\,\underbrace{a^{-1}b^{-1}\cdots a^{-1}b^{-1}}_{m_2} & \text{when } i \text{ is odd.} \end{cases}$$

Then

$$\begin{aligned} b &= y_{m_1-2}\, y_{m_1-3}\, y_{m_1-2}^{-1}, \\ &= \underbrace{ba\cdots ba}_{m_2}\;\underbrace{ab\cdots ab}_{m_1-1}\; a\;\underbrace{b^{-1}a^{-1}\cdots b^{-1}a^{-1}}_{m_1-1}\;\underbrace{a^{-1}b^{-1}\cdots a^{-1}b^{-1}}_{m_2}, \end{aligned}$$

From this we get the relation R1, given by

$$(ba)^{\frac{m_2}{2}}\,(ab)^{\frac{m_1-1}{2}} = (ab)^{\frac{m_2-2}{2}}\,a\,(ab)^{\frac{m_1-1}{2}}\,a \tag{R1}$$

and

$$\begin{aligned} a &= b\, y_{m_1-2}\, b^{-1} \\ &= b\;\underbrace{ba\cdots ba}_{m_2}\;\underbrace{ab\cdots aba}_{m_1-2}\; b\;\underbrace{a^{-1}b^{-1}\cdots a^{-1}b^{-1}a^{-1}}_{m_1-2}\;\underbrace{a^{-1}b^{-1}\cdots a^{-1}b^{-1}}_{m_2}\; b^{-1}, \end{aligned}$$

From this we get the relation R2, given by

$$ab\,(ba)^{\frac{m_2}{2}}\,a\,(ba)^{\frac{m_1-3}{2}} = b\,(ba)^{\frac{m_2}{2}}\,(ab)^{\frac{m_1-1}{2}}. \tag{R2}$$

Therefore,

$$G(K_{n,2,m_1}) = \langle a, b \mid R1, R2 \rangle \quad \text{if } m_1 \text{ is odd} \tag{4.2.1}$$

- Case II: m_2 is odd and therefore m_1 is even:

$$\begin{aligned} y_1 &= x_{m_2-1}x_{m_2}x_{m_2-1}^{-1} \\ &= \underbrace{ba\cdots ba}_{m_2-1}\; b^2\, a\, b^{-2}\;\underbrace{a^{-1}b^{-1}\cdots a^{-1}b^{-1}}_{m_2-1}, \\ y_2 &= \underbrace{ba\cdots ba}_{m_2-1}\; b^2\, aba^{-1}\, b^{-2}\;\underbrace{a^{-1}b^{-1}\cdots a^{-1}b^{-1}}_{m_2-1}. \end{aligned}$$

By induction, for each $i = 1, 2, \ldots, m_1 - 2$

$$y_i = \begin{cases} \underbrace{ba\cdots ba}_{m_2-1}\, b^2\, \underbrace{ab\cdots ab}_{i-2}\, aba^{-1}\, \underbrace{b^{-1}a^{-1}\cdots b^{-1}a^{-1}}_{i-2} & \\ \qquad\qquad\qquad\qquad\qquad\qquad\qquad\qquad\qquad\qquad\qquad\qquad \text{when } i \text{ is even,} & \\ \qquad\qquad\qquad\qquad\qquad\qquad b^{-2}\, \underbrace{a^{-1}b^{-1}\cdots a^{-1}b^{-1}}_{m_2-1} & \\ \underbrace{ba\cdots ba}_{m_2-1}\, b^2\, \underbrace{ab\cdots ab}_{i-1}\, a\, \underbrace{b^{-1}a^{-1}\cdots b^{-1}a^{-1}}_{i-1} & \\ \qquad\qquad\qquad\qquad\qquad\qquad\qquad\qquad\qquad\qquad\qquad\qquad \text{when } i \text{ is odd.} & \\ \qquad\qquad\qquad\qquad\qquad\qquad b^{-2}\, \underbrace{a^{-1}b^{-1}\cdots a^{-1}b^{-1}}_{m_2-1} & \end{cases}.$$

Then

$$\begin{aligned} b &= y_{m_1-2}\, y_{m_1-3}\, y_{m_1-2}^{-1}, \\ &= \underbrace{ba\cdots ba}_{m_2-1}\, b^2\, \underbrace{ab\cdots ab}_{m_1-2}\, a\, \underbrace{b^{-1}a^{-1}\cdots b^{-1}a^{-1}}_{m_1-2}\, b^{-2}\, \underbrace{a^{-1}b^{-1}\cdots a^{-1}b^{-1}}_{m_2-1}, \end{aligned}$$

From this we get the relation R3, given by

$$b\,(ab)^{\frac{m_2-1}{2}}\, b\,(ab)^{\frac{m_1-2}{2}} = (ab)^{\frac{m_2-1}{2}}\,(ba)^{\frac{m_1}{2}} \tag{R3}$$

and

$$\begin{aligned} a &= b\, y_{m_1-2}\, b^{-1}, \\ &= b\, \underbrace{ba\cdots ba}_{m_2-1}\, b^2\, \underbrace{ab\cdots ab}_{m_1-4}\, aba^{-1}\, \underbrace{b^{-1}a^{-1}\cdots b^{-1}a^{-1}}_{m_1-4}\, b^{-2} \\ &\qquad\qquad \underbrace{a^{-1}b^{-1}\cdots a^{-1}b^{-1}}_{m_2-1}\, b^{-1}, \end{aligned}$$

From this we get the relation R4, given by

$$ab\,(ba)^{\frac{m_2-1}{2}}\, b\,(ba)^{\frac{m_1-2}{2}} = b\,(ba)^{\frac{m_2-1}{2}}\, b^2\,(ab)^{\frac{m_1-2}{2}}. \tag{R4}$$

Therefore,

$$G(K_{n,2,2k}) = \langle a, b \,|\, R3, R4\rangle \quad \text{if } m_1 \text{ is even.} \tag{4.2.2}$$

□

Theorem 4.2.3.

$$\begin{aligned} G(K_{n,2,m_1}) &\cong \mathbb{Z} \quad \textit{when} \quad m_1 = n-1, \\ G(K_{n,2,m_1}) &\ncong \mathbb{Z} \quad \textit{when} \quad 1 \le m_1 < n-1. \end{aligned}$$

Proof. Case 1: $m_1 = (n-1)$ and $m_2 = n$.

- When n is even, from Proposition 4.2.2 we can write,

$$G(K_{n,2,n-1}) = \Big\langle a, b \,\Big|\, (ba)^{\frac{n}{2}} (ab)^{\frac{n-2}{2}} = (ab)^{\frac{n-2}{2}} a (ab)^{\frac{n-2}{2}} a; \\ ab (ba)^{\frac{n}{2}} a (ba)^{\frac{n-4}{2}} = b (ba)^{\frac{n}{2}} (ab)^{\frac{n-2}{2}} \Big\rangle.$$

Substituting the first relation of group the presentation in the second relation we have,

$$\begin{aligned} ab (ba)^{\frac{n}{2}} a (ba)^{\frac{n-4}{2}} &= b (ba)^{\frac{n}{2}} (ab)^{\frac{n-2}{2}}, \\ &= b (ab)^{\frac{n-2}{2}} a (ab)^{\frac{n-2}{2}} a, \\ &= (ba)^{\frac{n}{2}} a (ba)^{\frac{n-2}{2}}, \end{aligned}$$

which gives

$$ab (ba)^{\frac{n}{2}} = (ba)^{\frac{n}{2}} ab. \tag{4.2.3}$$

Substituting (4.2.3) in the first relation on the L.H.S repeatedly,

$$\begin{aligned} (ba)^{\frac{n}{2}} (ab)^{\frac{n-2}{2}} &= (ab)^{\frac{n-2}{2}} a (ab)^{\frac{n-2}{2}} a, \\ (ba)^{\frac{n}{2}} ab (ab)^{\frac{n-4}{2}} &= (ab)^{\frac{n-2}{2}} a (ab)^{\frac{n-2}{2}} a, \\ ab (ba)^{\frac{n}{2}} (ab)^{\frac{n-4}{2}} &= (ab)^{\frac{n-2}{2}} a (ab)^{\frac{n-2}{2}} a. \end{aligned}$$

Canceling ab on both sides we get,

$$\begin{aligned} (ba)^{\frac{n}{2}} (ab)^{\frac{n-4}{2}} &= (ab)^{\frac{n-4}{2}} a (ab)^{\frac{n-2}{2}} a \\ \vdots \qquad & \qquad \vdots \\ (ba)^{\frac{n}{2}} (ab) &= (ab) a (ab)^{\frac{n-2}{2}} a, \\ ab (ba)^{\frac{n}{2}} &= (ab) a (ab)^{\frac{n-2}{2}} a, \\ (ba)^{\frac{n}{2}} &= a^2 (ba)^{\frac{n-2}{2}}, \\ ba &= a^2, \\ b &= a. \end{aligned}$$

This proves that

$$G(K_{n,2,n-1}) \cong \mathbb{Z} \quad \text{when } n \text{ is even.}$$

- When n is odd, from Proposition 4.2.2 we can write,

$$G(K_{n,2,n-1}) = \Big\langle a, b \,\Big|\, b\,(ab)^{\frac{n-1}{2}}\, b\,(ab)^{\frac{n-3}{2}} = (ab)^{\frac{n-1}{2}}\,(ba)^{\frac{n-1}{2}};$$
$$ab\,(ba)^{\frac{n-1}{2}}\, b\,(ba)^{\frac{n-3}{2}} = b\,(ba)^{\frac{n-1}{2}}\, b^2\,(ab)^{\frac{n-3}{2}} \Big\rangle.$$

From the second relation we get

$$\begin{aligned} ab\,(ba)^{\frac{n-1}{2}}\, b\,(ba)^{\frac{n-3}{2}} &= b\,(ba)^{\frac{n-1}{2}}\, b^2\,(ab)^{\frac{n-3}{2}}, \\ &= b\cdot b\,(ab)^{\frac{n-1}{2}}\, b\,(ab)^{\frac{n-3}{2}}, \\ &= b\cdot (ab)^{\frac{n-1}{2}}\,(ba)^{\frac{n-1}{2}} \quad \text{using the first relation} \end{aligned}$$

which gives

$$ab\,(ba)^{\frac{n-1}{2}}\, b = (ba)^{\frac{n-1}{2}}\, b^2\, a. \tag{4.2.4}$$

Substituting (4.2.4) in the first relation repeatedly we have,

$$\begin{aligned} b\,(ab)^{\frac{n-1}{2}}\, b\,(ab)^{\frac{n-3}{2}} &= (ab)^{\frac{n-1}{2}}\,(ba)^{\frac{n-1}{2}}, \\ (ba)^{\frac{n-1}{2}}\, b^2\, a\, b\,(ab)^{\frac{n-5}{2}} &= (ab)^{\frac{n-1}{2}}\,(ba)^{\frac{n-1}{2}}, \\ ab\,(ba)^{\frac{n-1}{2}}\, b\, b\,(ab)^{\frac{n-5}{2}} &= (ab)^{\frac{n-1}{2}}\,(ba)^{\frac{n-1}{2}}, \end{aligned}$$

Canceling ab on both sides,

$$\begin{aligned} (ba)^{\frac{n-1}{2}}\, b\, b\,(ab)^{\frac{n-5}{2}} &= (ab)^{\frac{n-3}{2}}\,(ba)^{\frac{n-1}{2}}, \\ \vdots \qquad & \qquad \vdots \\ (ba)^{\frac{n-1}{2}}\, b^2\, ab &= (ab)^2\,(ba)^{\frac{n-1}{2}}, \\ ab\,(ba)^{\frac{n-1}{2}}\, b^2 &= (ab)^2\,(ba)^{\frac{n-1}{2}}, \end{aligned}$$

which gives

$$(ba)^{\frac{n-1}{2}}\, b^2 = ab\,(ba)^{\frac{n-1}{2}}. \tag{4.2.5}$$

Substituting (4.2.5) in the first relation on the L.H.S repeatedly,

$$\begin{aligned} (ba)^{\frac{n}{2}}\,(ab)^{\frac{n-2}{2}} &= (ab)^{\frac{n-2}{2}}\, a\,(ab)^{\frac{n-2}{2}}\, a, \\ (ba)^{\frac{n}{2}}\, ab\,(ab)^{\frac{n-4}{2}} &= (ab)^{\frac{n-2}{2}}\, a\,(ab)^{\frac{n-2}{2}}\, a, \\ ab\,(ba)^{\frac{n}{2}}\,(ab)^{\frac{n-4}{2}} &= (ab)^{\frac{n-2}{2}}\, a\,(ab)^{\frac{n-2}{2}}\, a, \end{aligned}$$

Canceling ab on both sides,

$$\begin{aligned}
(ba)^{\frac{n}{2}}(ab)^{\frac{n-4}{2}} &= (ab)^{\frac{n-4}{2}} a (ab)^{\frac{n-2}{2}} a, \\
\vdots \qquad & \qquad \vdots \\
(ba)^{\frac{n}{2}}(ab) &= (ab) a (ab)^{\frac{n-2}{2}} a, \\
ab(ba)^{\frac{n}{2}} &= (ab) a (ab)^{\frac{n-2}{2}} a, \\
(ba)^{\frac{n}{2}} &= a^2 (ba)^{\frac{n-2}{2}}, \\
ba &= a^2, \\
b &= a.
\end{aligned}$$

This proves that

$$G(K_{n,2,n-1}) \cong \mathbb{Z} \quad \text{when } n \text{ is even.}$$

Case II: $m_1 \neq (n-1)$.

Let D_n denote the dihedral group of order $2n$. Now, we show that all groups $G(K_{n,2,m_1})\,(1 \leq m_1 < n-1)$ are not isomorphic to $\mathbb{Z}$ by showing that there exists an epimorphism from these groups to some dihedral group.

We take the following presentation for $D_{2(n-m_1)-1}$:

$$\begin{aligned}
D_{2(n-m_1)-1} &= \left\langle r, s \,|\, r^{2(n-m_1)-1} = 1, s^2 = 1, rs = sr^{-1} \right\rangle \\
&\cong \left\langle x, y \,|\, (xy)^{2(n-m_1)}x = (yx)^{2(n-m_1)}y\,,\; x^2 = y^2 = 1 \right\rangle
\end{aligned}$$

where $x = s, y = r^{n-m_1}s$.

Now, we define an epimorphism between the presentations of $G(K_{n,2,m_1})$ and $D_{2(n-m_1)-1}$ by

$$\phi : G(K_{n,2,m_1}) \to D_{2(n-m_1)-1}$$

$$a \mapsto x$$

$$b \mapsto y$$

For the relations (R1), (R2), (R3) and (R4) we check that

$$\phi(R1) = \phi(R2) = \phi(R3) = \phi(R4) = (r^{2n-2m_1-1})^{n-m_1} = 1$$

So, ϕ is well defined. Now, let

$$D_{2(n-m_1)-1} = \Big\{1, r, r^2, \cdots, r^{2(n-m_1)-2}, s, rs, r^2s, \cdots, r^{2(n-m_1)-2}s\Big\}.$$

Then,
$$\begin{aligned}
\phi^{-1}(r^{n-m_1-i}) &= (ab)^{2i-1}, && i = 1, 2, \cdots, n-m_1,\\
\phi^{-1}(r^{2(n-m_1)-(i+1)}) &= (ab)^{2i}, && i = 1, 2, \cdots, n-m_1-1,\\
\phi^{-1}(r^{n-m_1-i}s) &= (ab)^{2i-1}a, && i = 1, 2, \cdots, n-m_1,\\
\phi^{-1}(r^{2(n-m_1)-(i+1)}s) &= (ab)^{2i}a, && i = 1, 2, \cdots, n-m_1-1.
\end{aligned}$$

This shows that ϕ is surjective. Therefore,

$$\frac{G(K_{n,2,m_1})}{\ker\phi} \cong D_{2(n-m_1)-1}.$$

Since, $D_{2(n-m_1)-1}$ is non-abelian, we have

$$G(K_{n,2,m_1}) \ncong \mathbb{Z}.$$

This completes the proof. □

Corollary 4.2.4.

1. *(a)* $\pi_1\big(\mathbb{R}^4 - \text{Tube}(K_{n,2,m_1})\big) \cong \mathbb{Z}$ *if* $m_1 = n-1$.
   (b) $\pi_1\big(\mathbb{R}^4 - \text{Tube}(K_{n,2,m_1})\big) \ncong \mathbb{Z}$ *if* $1 \le m_1 < n-1$.
2. *The number of non-trivial ribbon torus knots obtained from the* $K(2, 2n+1)$ *with two weldings does not exceed* $n-1$.

Proof. The proof follows directly from Theorem 2.5.6, Corollary 2.5.7 and the previous theorem. □

4.2.2 Welded Knots obtained from T_n

4.2.2.1 T_n with one welding:

Let $T_{n,1}$ denote the knot diagram obtained after welding any one crossing in the twist region of the standard twist knot diagram (Figure 4.8(a)) having n real crossings in

the twist regions. We have already seen in Theorem 4.1.4 that $T_{n,1}$ is a trivial welded knot and therefore the knot group is isomorphic to $\mathbb{Z}$. The following theorem verifies this by explicitly by computing the group presentation.

Theorem 4.2.5.

$$G(T_{n,1}) = \left\langle a, b \;\middle|\; \begin{array}{c} (ab^{-1})^{\frac{n-2}{2}} a (ba^{-1})^{\frac{n-2}{2}} b = b(ab^{-1})^{\frac{n-4}{2}} a (ba^{-1})^{\frac{n-2}{2}}, \\ b(ab^{-1})^{\frac{n-2}{2}} = (ab^{-1})^{\frac{n-4}{2}} a \end{array} \right\rangle \cong \mathbb{Z}.$$

Proof. Similar to the proof of the Theorem 4.2.1, this can shown by using Tietz transformations. □

4.2.2.2 T_n with two weldings:

Let $T_{n,2,1}$ denote the knot diagram obtained after welding two crossings with one classical crossing in between in the twist region of the standard twist knot diagram (Figure 4.8(b)).

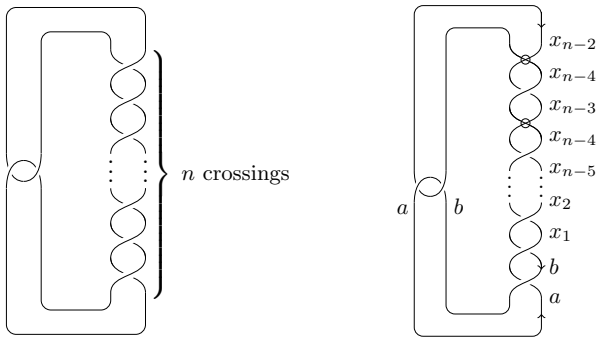

(a) (b)

Figure 4.8: Twist knot T_n and the welded twist knot $T_{n,2,1}$

Theorem 4.2.6. *Let $G(T_{n,2,1})$ be the knot group of $T_{n,2,1}$. Then*

$$G(T_{n,2,1}) \ncong \mathbb{Z} \quad \textit{when } n \textit{ is odd.}$$

Proof. Let $x_1, x_2, \cdots, x_{n-2}$ be the generators for the knot group. The Wirtinger relations are the following. From the twist region:

$$x_1 = b^{-1}\, a\, b,$$

$$x_2 = x_1\, b\, x_1^{-1}.$$
$$x_3 = x_2^{-1}\, x_1\, x_2,$$
$$x_4 = x_3\, x_2\, x_3^{-1}.$$

Then, for $i \leq (n-3)$,

$$x_i = \begin{cases} x_{i-1}\, x_{i-2}\, x_{i-1}^{-1}, & \text{if } i \text{ is even,} \\ x_{i-1}^{-1}\, x_{i-2}\, x_{i-1}, & \text{if } i \text{ is odd,} \end{cases}$$

And

$$x_{n-2} = \begin{cases} x_{n-4}^{-1}\, x_{n-3}\, x_{n-4}, & \text{if } n \text{ is even,} \\ x_{n-4}\, x_{n-3}\, x_{n-4}^{-1}, & \text{if } n \text{ is odd.} \end{cases}$$

From the clasp region:

$$n \text{ even} \begin{cases} x_{n-4} & = a\, x_{n-2}\, a^{-1} \\ a & = x_{n-4}\, b\, x_{n-4}^{-1} \end{cases} \qquad n \text{ odd} \begin{cases} x_{n-2} & = a^{-1}\, x_{n-4}\, a \\ a & = x_{n-4}^{-1}\, b\, x_{n-4} \end{cases}$$

We can write

$$x_1 = b^{-1}\, a\, b,$$
$$x_2 = b^{-1}\, a\, b\, a^{-1}\, b.x_3 \qquad = b^{-1}\, a\, b^{-1}\, a\, b\, a^{-1}\, b,$$
$$x_4 = (b^{-1}\, a)^2\, b\, (a^{-1}\, b)^2.$$

Then, for $i \leq (n-3)$

$$x_i = \begin{cases} \underbrace{b^{-1}\, a \cdots b^{-1}\, a}_{i}\; b\; \underbrace{a^{-1}\, b \cdots a^{-1}\, b}_{i} & \text{if} \quad i \text{ is even} \\ \underbrace{b^{-1}\, a \cdots b^{-1}\, a}_{i-1}\; b^{-1}\, a\, b\; \underbrace{a^{-1}\, b \cdots a^{-1}\, b}_{i-1} & \text{if} \quad i \text{ is odd,} \end{cases}$$

$$x_{n-2} = \begin{cases} \underbrace{b^{-1}\, a \cdots b^{-1}\, a}_{n-4}\; b^{-2}\, a\, b^2\; \underbrace{a^{-1}\, b \cdots a^{-1}\, b}_{n-4} & \text{if} \quad n \text{ is even} \\ \underbrace{b^{-1}\, a \cdots b^{-1}\, a}_{n-3}\; a\, b\, a^{-1}\; \underbrace{a^{-1}\, b \cdots a^{-1}\, b}_{n-3} & \text{if} \quad n \text{ is odd.} \end{cases}$$

Now, clasp region gives the relations for the presentation:
When $n > 3$ is even, $G(T_{n,2,1}) = \left\langle a, b \,\middle|\, R_5, R_6 \right\rangle$ where

$$R_5 : (b^{-1}\,a)^{\frac{n-4}{2}}\, b\, (a^{-1}\, b)^{\frac{n-4}{2}}\, a = a\, (b^{-1}\, a)^{\frac{n-4}{2}}\, b^{-2}\, a\, b^2\, (a\, b^{-1})^{\frac{n-4}{2}}\, a$$
$$R_6 : (a\, b^{-1})^{\frac{n-4}{2}}\, a\, (b\, a^{-1})^{\frac{n-4}{2}} = (b^{-1}\, a)^{\frac{n-4}{2}}\, b\, (a^{-1}\, b)^{\frac{n-4}{2}}$$

When $n > 3$ is odd, $G(T_{n,2,1}) = \left\langle a, b \,\middle|\, R_7, R_8 \right\rangle$ where

$$R_7 : a\, (b^{-1}\, a)^{\frac{n-3}{2}}\, a\, b\, a^{-1}\, (a^{-1}\, b)^{\frac{n-3}{2}} = (b\, a^{-1})^{\frac{n-5}{2}}\, b^{-1}\, a\, b\, (a\, b^{-1})^{\frac{n-5}{2}}\, a$$
$$R_8 : (b^{-1}\, a)^{\frac{n-5}{2}}\, b^{-1}\, a\, b\, (a^{-1}\, b)^{\frac{n-5}{2}}\, a = b\, (b^{-1}\, a)^{\frac{n-5}{2}}\, b^{-1}\, a\, b\, (a^{-1}\, b)^{\frac{n-5}{2}}$$

Let

$$\begin{aligned} D_{2n-7} &= \left\langle r, s \,|\, r^{2n-7} = 1, s^2 = 1, rs = sr^{-1} \right\rangle \\ &\cong \left\langle x, y \,|\, (xy)^{2(n-3)} x = (yx)^{2(n-3)} y\,,\; x^2 = y^2 = 1 \right\rangle. \end{aligned}$$

where $x = s, y = r^{n-3}s$. Now, we define an epimorphism between the presentations of $G(T_{n,2,1})$ $(n > 3, odd)$ and D_{2n-7} by

$$\begin{aligned} \psi : G(T_{n,2,1}) &\to D_{2n-7} \\ a &\mapsto x \\ b &\mapsto y \end{aligned}$$

Therefore,

$$\frac{G(T_{n,2,1})}{\ker \psi} \cong D_{2n-7}$$

which implies

$$G(T_{n,2,1}) \ncong \mathbb{Z}.$$

□

Corollary 4.2.7. *If n is odd, then $\pi_1(\mathbb{R}^4 - \mathrm{Tube}(T_{n,2,1})) \ncong \mathbb{Z}$.*

Proof. The proof follows directly from Theorem 4.2.6. □

Conjecture 4.2.8. *If n is even, then $G(T_{n,2,1}) \ncong \mathbb{Z}$.*

4.3 Knots from Rolfsen's table upto 6 Crossings

In this section, we consider standard diagrams of classical knots with crossing number upto six so that we can observe every case possible. Now, any non-trivial welded knot K satisfies $c(K) \geq 3$, where $c(K)$ is the number of classical crossings (Lemma 2.1.19). Therefore, at most one classical crossing can be changed to a welded crossing in the knots with four crossings (e.g. 4_1), and at most two classical crossings can be changed to a welded crossing in the knots with five crossings (e.g. $5_1, 5_2$).Up to five crossings, all knots belong to the torus or twist families, which are discussed in the preceding sections.

The following tables include the fundamental groups of welded knots obtained by

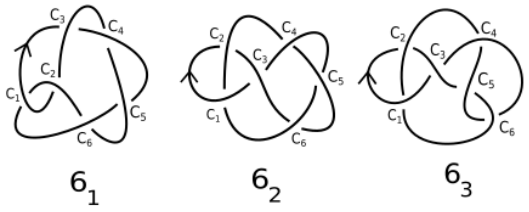

Figure 4.9: Knots with six crossings.

welding at most three crossings of the standard diagrams of the six crossing knots. It is clear that welding more than three crossings lead to the welded unknot (Lemma 2.1.19). In Figure 4.9, the crossings are denoted by $c_i, i = 1, \cdots, 6$.

The first column of each table indicates which crossings are changed to a welded crossing.

$\mathbf{6_1, 6_2, 6_3}$ **one weld**	**Welded knot group** $\mathbf{G(K)}$
$\{c_i,\ \forall i = 1, \cdots, 6\}$	$\cong \mathbb{Z}$

Table 4.1: Six crossing knots with one welded crossing

pair of welded crossings $\{\mathbf{c_i}, \mathbf{c_j}\}$ $i < j$	**Welded knot group** $\mathbf{G(K)}$
$\{c_1, c_j\}, \forall j = 3, 4, 5, 6,\ \{c_2, c_j\}, \forall j = 3, 4, 5, 6$ $\{c_3, c_5\}$,$\{c_4, c_6\}$, $\{c_5, c_6\}$	$\cong \mathbb{Z}$
$\{c_1, c_2\}$	$\cong \mathbb{Z}$ (welded unknot)
$\{c_i, c_{i+1}\}, \forall j = 3, 4, 5$	$\cong \left\langle a, b \middle\| a^{-1}bab^{-1}aba^{-1}b^{-1}ab^{-1} = e \right\rangle \ncong \mathbb{Z}$
$\{c_3, c_6\}$	$\cong \left\langle a, b \middle\| b^{-1}ab = ab^{-1}a \right\rangle \ncong \mathbb{Z}$

Table 4.2: 6_1 with two welded crossings

$\{\mathbf{c_i}, \mathbf{c_j}, \mathbf{c_k}\},\ \mathbf{i < j < k}$	**Welded knot group** $\mathbf{G(K)}$
$\{c_i, c_j, c_k\} \forall\, i, j, k = 1, \cdots, 6$	$\cong \mathbb{Z}$

Table 4.3: 6_1 with three welded crossings

pair of welded crossings $\{\mathbf{c_i}, \mathbf{c_j}\},\ \mathbf{i < j}$	**Welded knot group** $\mathbf{G(K)}$
$\{c_1, c_j\}, \forall j = 3, 4, 5,\ \{c_2, c_j\}, \forall j = 3, 5, 6$	$\cong \mathbb{Z}$
$\{c_3, c_j\}, \forall j = 4, 5, 6\ \{c_4, c_6\}$	$\cong \mathbb{Z}$
$\{c_4, c_2\}$	$\cong \left\langle a, b \middle\| a^2 = b^2, b^{-1}ab = ab^{-1}a \right\rangle \ncong \mathbb{Z}$
$\{c_4, c_5\}, \{c_5, c_6\}$	$\cong \left\langle a, b \middle\| a^{-1}ba^{-1}b^{-1}aba^{-1}bab^{-1} \right\rangle \ncong \mathbb{Z}$
$\{c_2, c_4\}$	$\cong \left\langle a, b \middle\| b^2 = a^2, a^{-1}ba = ba^{-1}b \right\rangle \ncong \mathbb{Z}$
$\{c_5, c_6\}$	$\cong \left\langle a, b \middle\| aba = bab \right\rangle \ncong \mathbb{Z}$

Table 4.4: 6_2 with two welded crossings

$\{\mathbf{c_i}, \mathbf{c_j}, \mathbf{c_k}\},\ \mathbf{i < j < k}$	**Welded knot group** $\mathbf{G(K)}$
$\{c_1, c_3, c_4\}, \{c_1, c_3, c_5\}, \{c_1, c_3, c_6\},$ $\{c_1, c_4, c_5\}, \{c_1, c_4, c_6\}, \{c_1, c_5, c_6\}$	$\cong \mathbb{Z}$
$\{c_1, c_2, c_4\}, \{c_2, c_3, c_5\}, \{c_2, c_3, c_6\}, \{c_2, c_4, c_5\}$ $\{c_2, c_5, c_6\}, \{c_3, c_4, c_5\}, \{c_3, c_4, c_6\}, \{c_4, c_5, c_6\}$	$\cong \mathbb{Z}$
$\{c_1, c_2, c_3\}, \{c_1, c_2, c_5\}, \{c_1, c_2, c_6\}$	$\cong \left\langle a, b \middle\| aba = bab \right\rangle \ncong \mathbb{Z}$
$\{c_2, c_3, c_4\}$	$\cong \left\langle a, b \middle\| a^2 = b^2, a^{-1}ba = ba^{-1}b \right\rangle \ncong \mathbb{Z}$
$\{c_2, c_4, c_6\}$	$\cong \left\langle a, b \middle\| bab^{-1} = aba^{-1} \right\rangle \ncong \mathbb{Z}$

Table 4.5: 6_2 with three welded crossings

pair of welded crossings $\{\mathbf{c_i}, \mathbf{c_j}\},\ \mathbf{i < j}$	**Welded knot group** $\mathbf{G(K)}$
$\{c_1, c_j\}, \forall j = 3, 4, 5, 6,$ $\{c_2, c_j\}, \forall j = 3, 5, 6$	$\cong \mathbb{Z}$
$\{c_3, c_j\}, \forall j = 4, 5, 6$ $\{c_4, c_j\}, \forall j = 5, 6$	$\cong \mathbb{Z}$
$\{c_1, c_2\}$	$\cong \left\langle a, b \middle\| aba^{-1} = b^{-1}ab \right\rangle \ncong \mathbb{Z}$
$\{c_2, c_4\}$	$\cong \left\langle a, b \middle\| b^2 = a^2, a^{-1}ba = ba^{-1}b \right\rangle \ncong \mathbb{Z}$
$\{c_5, c_6\}$	$\cong \left\langle a, b \middle\| aba = bab \right\rangle \ncong \mathbb{Z}$

Table 4.6: 6_3 with two welded crossings

$\{\mathbf{c_i}, \mathbf{c_j}, \mathbf{c_k}\},\ \mathbf{i} < \mathbf{j} < \mathbf{k}$	**Welded knot group** $\mathbf{G(K)}$
$\{c_1, c_2, c_6\}, \{c_2, c_3, c_5\}, \{c_2, c_3, c_6\}, \{c_3, c_4, c_6\}$	$\cong \mathbb{Z}$
$\{c_1, c_2, c_3\}, \{c_1, c_2, c_4\}, \{c_1, c_2, c_5\}, \{c_4, c_5, c_6\}$	$\cong \left\langle a, b \middle\| aba = bab \right\rangle \ncong \mathbb{Z}$
$\{c_2, c_3, c_4\}$	$\cong \left\langle a, b \middle\| a^2 = b^2, ab^{-1}a = b^{-1}ab \right\rangle \ncong \mathbb{Z}$
$\{c_3, c_4, c_5\}$	$\cong \left\langle a, b \middle\| a^2 = b^2, ab^{-1}a = ba^{-1}b \right\rangle \ncong \mathbb{Z}$

Table 4.7: 6_3 with three welded crossings

Chapter 5

Parameterization of ribbon torus knots

In this chapter, we provide a method to parameterize any ribbon torus knot inside $\mathbb{R}^4$. Recall that a ribbon torus knot is isotopic to the tube of some welded knot, where the tube of a welded knot (defined by Satoh) is discussed in Section 2.5. Also, we have seen that a welded knot diagram K can be thought to be obtained from a classical knot diagram in which some crossings are converted as a welded crossing. Thus, to parameterize a tube of a welded knot, we can first find a parameterization of a classical knot projection and then, in the projection, mark the nature of crossings to be either classical (over/under) or welded. This part is easy since we know that all classical knot diagrams can be represented by a trigonometric parameterization [**Kau98**]. To obtain the required ribbon torus knot, we need to construct functions that can create the tube of this welded knot diagram.

In this chapter the main focus is to discuss the tube construction on a welded knot diagram. The *Tube* construction starts with a projection of classical knot K on a plane, say XY plane. Additionally, we provide the crossing information about which crossings are classical and which are welded. Now, placing a circle with a fixed radius at every point of the knot projection in the YZ plane results in a tubular object in $\mathbb{R}^3$, crossing itself at the singular points of the original knot. In order to construct a projection of $Tube(K)$ in $\mathbb{R}^3$ from this tubular object, we need to reduce the radius

of the tube corresponding to the lower arc at a classical crossing so that it penetrates through the tube corresponding to the upper arc of K. On the other hand, the tubes corresponding to the arcs near a welded crossing should be placed side by side so that they do not touch each other. Thus, a suitable function that can shrink the radius of the tube at a point will be required to take care of classical crossings. Similarly, a function that can displace the tube at a crossing will be needed at welded crossings. We prove the existence of such functions in the following.

Theorem 5.0.1. *Given a classical knot K with given trigonometric parameterization $\phi' : [0, 2\pi] \to \mathbb{R}^3$ given by*

$$\phi'(t) = (f(t), g(t), h(t))$$

there exists functions $S_c(t)$ and $S_w(t)$ such that the image of $[0, 2\pi] \times [0, 2\pi]$ under the map $\tilde{\Psi} : \mathbb{R}^2 \to \mathbb{R}^4$ defined by

$$\tilde{\Psi}(t, s) = (f(t),\ (r - d_1 S_c(t))\, g(t) + \cos s,\ (r - d_1 S_c(t))\, g(t) + \sin s + d_2 S_w(t),\ h(t))$$

where $r, d_1, d_2 \in \mathbb{R}^+$, is isotopic to the $Tube(K)$.

Proof. Take the projection of K on XY plane given by $\{f(t), g(t) \,|\, t \in [0, 2\pi]\}$ and let there be n number of classical crossings, denoted by $c_1, c_2, \cdots, c_n$, and m number of welded crossings, denoted by $w_1, w_2, \cdots, w_m$. Additionally, let $\{t_i, s_i\}$ be the pair of values of t where t_i corresponds to the overcrossing point and s_i corresponds to the undercrossing point of c_i respectively for $i = 1, \cdots, n$. Also, let $\{\bar{t}_j, \bar{s}_j\}$ be the pair of values of t where $\bar{t}_j$ corresponds the first encounter of the crossing w_j and $\bar{s}_j$ corresponds the second encounter of the crossing w_j for $j = 1, \cdots, m$.
First, putting a circle with a fixed radius $r \in \mathbb{R}_+$ at each point of the projection is given by

$$\left\{ \big(f(t),\ r\, g(t) + \cos s,\ r\, g(t) + \sin s\big) \,\middle|\, t,\ s \in [0, 2\pi] \right\}.$$

Now, we construct functions for shrinking the radius of the lower tube and displacing the tubes from each other, denoted by $S_c(t)$ and $S_w(t)$ respectively.
Take intervals of the same length, say L, around each t_i and s_i such that no two intervals intersect. Now, we define the bump function with centre c and width w by

$$B(x, c, w) = \begin{cases} \exp\left(-\frac{w^2}{w^2 - (x-c)^2}\right) & \text{if } |x - c| < w \\ 0 & \text{otherwise} \end{cases}$$

The function $S_c(t)$ is defined by summing the functions $B(x, c, \frac{L}{2})$ with centres at the undercrossing points s_i of all the classical crossings. On the other hand, the function $S_w(t)$ is defined by taking an alternating sum of $B(x, c, \frac{L}{2})$ with centres at the welded crossing points $\bar{t}_j$ and $\bar{s}_j$ of all welded crossings. Thus,

$$S_c(x) = \sum_{i=1}^{n} B(x, s_i, \frac{L}{2}),$$
$$S_w(x) = \sum_{j=1}^{m} \left(B(x, \bar{t}_j, \frac{L}{2}) - B(x, \bar{s}_j, \frac{L}{2}) \right)$$

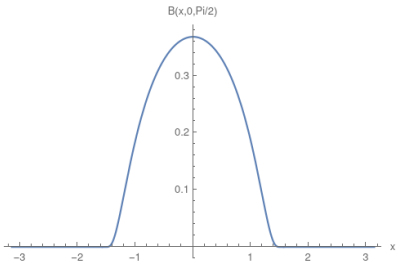

Figure 5.1: The bump function $B(x, c, w)$ with center $c = 0$ and width $w = \frac{\pi}{2}$

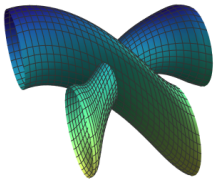

(a) Near classical crossing: lower tube is shrunk

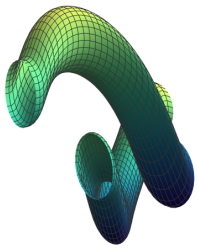

(b) Near welded crossing: upper and lower tubes are displaced

Figure 5.2: Mathematica plot of $Tube(K)$ near the crossings

The parameterization of the ribbon torus $Tube(K)$ is given by

$$\tilde{\Psi} : [0, 2\pi] \times [0, 2\pi] \to \mathbb{R}^4$$

which is defined by

$$\tilde{\Psi}(t, s) = (f(t),\ (r - d_c S_c(t))\, g(t) + \cos(s),\ (r - d_c S_c(t))\, g(t) + \sin(s) + d_w S_w(t),\ h(t))$$

where $r, d_c, d_w \in \mathbb{R}_+$ are the radius of the tube, shrinking factor and the displacement factor, respectively, and $h(t)$ provides the over/under information of the tubes in $\mathbb{R}^4$. This completes the proof. □

Replacing all cosine, sine and bump function with their corresponding Chebyshev approximations, we can get a polynomial parameterization. *Mathematica* plots of the $Tube(K)$ near the classical and welded crossings are shown in Figure 5.2(a) and Figure 5.2(a), respectively.

5.0.1 Example: A non-trivial ribbon torus knot arising from $T(2, 7)$

In this example, we provide explicit parameterization of the Tube of the classical torus knot $T(2, 7)$ with two welded crossings with one gap (Figure 5.3(b)). Let's denote this welded knot as $K_{2,1}$.

(a) Classical $T(2, 7)$ (b) Welded knot $K_{2,1}$

Figure 5.3: Welded knot obtained from $T(2, 7)$

The trignometric parametrization of $T(2, 7)$ (Figure 5.3(a)) is given by

$$\phi'(t) = (f(t), g(t), h(t))$$

where

$$\begin{aligned} f(t) &= \cos(2t)(\cos(7t) + 3) \\ g(t) &= \sin(2t)(\cos(7t) + 3) \\ h(t) &= \sin(7t) \end{aligned}$$

The interval pairs $[t - \frac{L}{2}, t + \frac{L}{2}]$ of equal length $L = \frac{\pi}{7}$ containing the five classical and two welded crossings with over/under information are given in Table 5.1.

$[0,\pi]$	c_1	w_1	c_2	w_2	c_3	c_4	c_5
over	$\left[0,\frac{\pi}{7}\right]$		$\left[\frac{2\pi}{7},\frac{3\pi}{7}\right]$		$\left[\frac{4\pi}{7},\frac{5\pi}{7}\right]$		$\left[\frac{6\pi}{7},\pi\right]$
weld		$\left[\frac{\pi}{7},\frac{2\pi}{7}\right]$		$\left[\frac{3\pi}{7},\frac{4\pi}{7}\right]$			
under						$\left[\frac{5\pi}{7},\frac{6\pi}{7}\right]$	
$[\pi,2\pi]$	c_1	w_1	c_2	w_2	c_3	c_4	c_5
over						$\left[\frac{12\pi}{7},\frac{13\pi}{7}\right]$	
weld		$\left[\frac{8\pi}{7},\frac{9\pi}{7}\right]$		$\left[\frac{10\pi}{7},\frac{11\pi}{7}\right]$			
under	$\left[\pi,\frac{8\pi}{7}\right]$		$\left[\frac{9\pi}{7},\frac{10\pi}{7}\right]$		$\left[\frac{11\pi}{7},\frac{12\pi}{7}\right]$		$\left[\frac{13\pi}{7},2\pi\right]$

Table 5.1: Crossing data of $K_{2,1}$: $[t-\frac{L}{2},t+\frac{L}{2}]$

In this case, we can write

$$S_c(t)=B\left(t,\tfrac{11\pi}{14},\tfrac{\pi}{14}\right)+B\left(t,\tfrac{15\pi}{14},\tfrac{\pi}{14}\right)+B\left(t,\tfrac{19\pi}{14},\tfrac{\pi}{14}\right)+B\left(t,\tfrac{23\pi}{14},\tfrac{\pi}{14}\right)+B\left(t,\tfrac{27\pi}{14},\tfrac{\pi}{14}\right),$$

$$S_w(t)=\left(B\left(t,\tfrac{3\pi}{14},\tfrac{\pi}{14}\right)+B\left(t,\tfrac{7\pi}{14},\tfrac{\pi}{14}\right)\right)-\left(B\left(t,\tfrac{17\pi}{14},\tfrac{\pi}{14}\right)+B\left(t,\tfrac{21\pi}{14},\tfrac{\pi}{14}\right)\right)..$$

Choosing $r=0.7$, $d_c=1$, $d_w=5$, the parametrization of the Tube($K_{2,1}$) is given by

$$\tilde{\Psi}:[0,2\pi]\times[0,2\pi]\to\mathbb{R}^4$$

which is defined by

$$\tilde{\Psi}(t,s)=(f(t),(0.7-S_c(t))g(t)+\cos(s),(0.7-S_c(t))g(t)+\sin(s)+5S_w(t),h(t))$$

where $t\in[0,2\pi], s\in[0,2\pi]$.
Mathematica plot of the projection of Tube($K_{2,1}$) in XYZ hyperspace is shown in Figure 5.4.

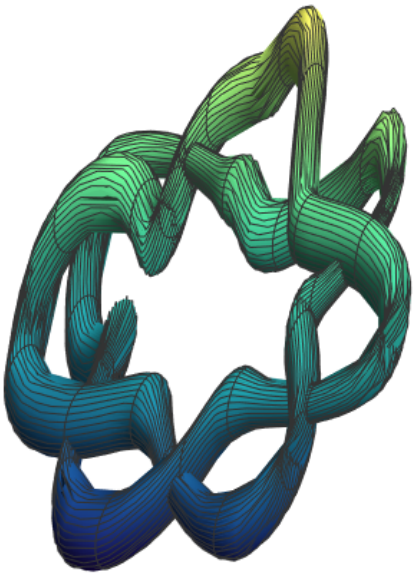

Figure 5.4: Projection of Tube($K_{2,1}$) in XYZ hyperspace

Chapter 6

Parameterization of knotted planes

In this chapter, we discuss about methods for constructing and parameterizing knotted planes using polynomial functions. By a long 2-knot, we mean a proper, smooth embedding of $\mathbb{R}^2$ inside $\mathbb{R}^4$, which is asymptotic outside a compact region. The diagrams for long 2-knots are understood by projecting them on a suitable hyperplane in which the only singularities are the double point curves and the triple points. Then, one provides the extra information at each singularity to see it as an embedding in the four-dimensional space with the help of the fourth coordinate. The simplest situation is when one can find a hyperplane in which the projection has only double point curves as singularity. We call them *simple* long 2 knots. We show that the existence of a long knot ($\mathbb{R}$ in $\mathbb{R}^3$) gives rise to the existence of a simple long 2 knot. We have used a parameterization of a given long knot to construct a parametrization of a simple, long 2 knot. We also show that the properties of the long knot impact the corresponding long 2 knot.

Following the same idea as in [**Shu**], we prove the existence of a polynomial representation for every long 2 knot and show that such a representation is unique up to polynomial isotopy.

Theorem 6.0.1. *Every smooth long* 2*-knot* ($\mathbb{R}^2 \to \mathbb{R}^4$) *has a polynomial representation.*

Proof. Let F be long 2-knot in $\mathbb{R}^4$ given by a smooth embedding $\phi : \mathbb{R}^2 \to \mathbb{R}^4$ defined

by $\phi(t,s) = (\alpha(t,s), \beta(t,s), \gamma(t,s), \delta(t,s))$ such that $\tilde{\phi} \equiv (\alpha, \beta, \gamma) : \mathbb{R}^2 \to \mathbb{R}^3$ is a generic immersion (having finite number of double point sets and triple points as the only singularities). Up to equivalence, we can assume that the Jacobian matrix

$$J = \begin{pmatrix} \frac{\partial \alpha}{\partial t} & \frac{\partial \alpha}{\partial s} \\ \frac{\partial \beta}{\partial t} & \frac{\partial \beta}{\partial s} \\ \frac{\partial \gamma}{\partial t} & \frac{\partial \gamma}{\partial s} \end{pmatrix}$$

has rank 2 outside some closed region $I_1 \times I_1$,where $I_1 = [a, b]$.
Since we have finitely many double point sets or triple points in the image of $\tilde{\phi}$, we can choose another closed region $I_2 \times I_2$, where $I_2 = [c, d]$ such that $\tilde{\phi}(I_2 \times I_2)$ contains all the singularities. $M = [M_1, M_2]$ such that $M \times M$ contains both the rectangles $I_1 \times I_1$ and $I_2 \times I_2$. Let $\phi(M \times M)$ be contained inside a 4-ball of radius R with

$$\|\phi(M_i, M_j)\| = R\,; \quad i, j = 1, 2.$$

Let $N = [N_1, N_2]$ be such that $\phi(N \times N)$ is contained inside a 4-ball of radius $2R$ with

$$\|\phi(N_i, N_j)\| = 2R\,; \quad i, j = 1, 2.$$

By a smooth reparametrization, we can assume that

$$[M_1, M_2] = \left[-\frac{1}{2}, \frac{1}{2}\right] \quad \text{and} \quad [N_1, N_2] = [-1, 1].$$

Thus $\phi\left(\left[-\frac{1}{2}, \frac{1}{2}\right] \times \left[-\frac{1}{2}, \frac{1}{2}\right]\right)$ and $\phi([-1,1] \times [-1,1])$ are contained inside balls of radius R and $2R$ respectively with

$$\left\|\phi\left(\pm\frac{1}{2}, \pm\frac{1}{2}\right)\right\| = R \quad \text{and} \quad \|\phi(\pm 1, \pm 1)\| = 2R$$

and the Jacobian matrix has rank 2 outside $[-\frac{1}{2}, \frac{1}{2}] \times [-\frac{1}{2}, \frac{1}{2}]$. Now, consider the restriction of ϕ to $I_1 \times I_1$ i.e

$$\phi|_{I_1 \times I_1} : I_1 \times I_1 \to \mathbb{R}^4.$$

Since the set of embeddings from a compact Hausdorff manifold to any manifold forms an open set in the set of all smooth maps with C^1-topology, there exists an $\varepsilon_0 > 0$

such that

$$\psi \in N(\phi, \varepsilon_0) \text{ implies that } \psi \text{ is an embedding of } I_1 \times I_1 \text{ in } \quad \mathbb{R}^4,$$

where

$$N(\phi, \varepsilon_0) = \big\{\psi : \sup_{(t,s)\in I_1\times I_1} \{\|\psi(t,s) - \phi(t,s)\|, \|\psi'(t,s) - \phi'(t,s)\|\} < \varepsilon_0\big\}.$$

Let $\varepsilon < \min\{R/2, \varepsilon_0\}$. For this ε, we can take an $\frac{\varepsilon}{2}$-approximation ψ using the Bernstein polynomial [**Sta**] or the Weierstrass' Approximation of two variables inside the square $[-1,1]\times[-1,1]$ [**Sta**]. Let $\psi_1 \equiv (x_1, y_1, z_1, w_1)$ be the approximation,where x_1, y_1, z_1 and w_1 are polynomials in two variables t, s.
Then all the partial derivatives of the polynomials x_1, y_1, z_1 and w_1 are greater than $1 - \frac{\varepsilon}{2}$ in $([-1, -\frac{1}{2}] \cup [\frac{1}{2}, 1]) \times ([-1, -\frac{1}{2}] \cup [\frac{1}{2}, 1])$.
Now, for $\delta_i \in (0, \varepsilon/2), i = 1, 2$, we can choose $N \in \mathbb{Z}^+$ large enough so that

$$\begin{aligned}\psi \equiv &\bigg(x_1 + \frac{\delta_1}{2N+1}t^{2N+1} + \frac{\delta_2}{2N+1}s^{2N+1}, \qquad y_1 + \frac{\delta_1}{2N+1}t^{2N+1} + \frac{\delta_2}{2N+1}s^{2N+1},\\ &z_1 + \frac{\delta_1}{2N+1}t^{2N+1} + \frac{\delta_2}{2N+1}s^{2N+1}, \qquad w_1 + \frac{\delta_1}{2N+1}t^{2N+1} + \frac{\delta_2}{2N+1}s^{2N+1}\bigg)\\ \equiv &(x, y, z, w).\end{aligned}$$

Then ψ is an ε-approximation of ϕ inside $[-1,1]\times[-1,1]$ such that the derivative of ψ is positive outside the square $[-1,1]\times[-1,1]$ as each partial derivative

$$\frac{\partial x}{\partial t}, \frac{\partial x}{\partial s}, \frac{\partial y}{\partial t}, \frac{\partial y}{\partial s}, \frac{\partial z}{\partial t}, \frac{\partial z}{\partial s}, \frac{\partial w}{\partial t}, \frac{\partial w}{\partial s}$$

are positive outside $[-1,1]\times[-1,1]$. Now, inside a compact region, this polynomial map will approximate the knot. Also the presence of large odd degree term with a very small coefficient ensures that the long 2-knot becomes asymptotically flat outside the compact region. It remains to show that $\psi : \mathbb{R}^2 \to \mathbb{R}^4$ is an embedding. Since $\phi : \mathbb{R}^2 \to \mathbb{R}^4$ is embedding implies it is an injective immersion. That means Jacobian $J(\phi; t, s)$ has rank 2. Now, in $[-1,1]\times[-1,1]$

$$\|\psi'(t,s)\| > \|\phi'(t,s)\| - \varepsilon/2$$

which implies that the Jacobian $J(\psi; t, s)$ has rank 2 in $[-1, 1] \times [-1, 1]$. And, outside $[-1, 1] \times [-1, 1]$, all partial derivatives of ψ are positive which implies that the Jacobian $J(\psi; t, s)$ has rank 2 outside $[-1, 1] \times [-1, 1]$ as well. Hence, ψ is an immersion. Since the Jacobian matrix for ψ has rank 2 in and outside $[-1, 1] \times [-1, 1]$, by inverse function theorem it follows that ψ is injective. This completes the proof. □

Definition 6.0.2. Two polynomial embeddings $\psi_0 \equiv (x_0, y_0, z_0, w_0)$, $\psi_1 \equiv (x_1, y_1, z_1, w_1)$ of $\mathbb{R}^2$ in $\mathbb{R}^4$ are said to be polynomially homotopic or P-homotopic if there exists a homotopy $F : \mathbb{R}^2 \times I \to \mathbb{R}^4$ between ψ_0 and ψ_1 such that $F_u := F(t, s, u)$ is a polynomial map for each $u \in [0, 1]$ where $F_0 = \psi_0$ and $F_1 = \psi_1$. If in each $u \in [0, 1]$, F_u is a polynomial embedding, then F is called a P-isotopy, and the embeddings ψ_0 and ψ_1 are said to be polynomially isotopic.

Notation 6.0.3. For $\varepsilon \in \mathbb{R}^+, N \in \mathbb{Z}^+$ and $\phi \equiv (x, y, z, w) : \mathbb{R}^2 \to \mathbb{R}^4$, let $\phi_{\varepsilon,N} : \mathbb{R}^2 \to \mathbb{R}^4$ given by $\phi_{\varepsilon,N}(t, s) = (x(t, s), y(t, s), z(t, s) + \varepsilon t^{2N+1}, w(t, s) + \varepsilon s^{2N+1})$.

We prove the following lemma.

Lemma 6.0.4. *Let $\phi = (x, y, z, w) : \mathbb{R}^2 \to \mathbb{R}^4$ be a polynomial embedding such that the map $(x, y, z) : \mathbb{R}^2 \to \mathbb{R}^3$ is a generic immersion. Then for each $N \in \mathbb{Z}^+, \exists$ an $\varepsilon > 0$ such that ϕ and $\phi_{\varepsilon,N}$ are polynomially isotopic.*

Proof. We have to show that the maps $F_u : \mathbb{R}^2 \to \mathbb{R}^4$ given by

$$F_u(t, s) = (x(t, s), y(t, s), z(t, s) + u\varepsilon t^{2N+1}, w(t, s) + u\varepsilon s^{2N+1})$$

are embedding for each $u \in [0, 1]$.
The Jacobian for each F_u

$$J = \begin{pmatrix} \dfrac{\partial x}{\partial t} & \dfrac{\partial x}{\partial s} \\ \dfrac{\partial y}{\partial t} & \dfrac{\partial y}{\partial s} \\ \dfrac{\partial z}{\partial t} + (2N+1)u\varepsilon t^{2N} & \dfrac{\partial z}{\partial s} \\ \dfrac{\partial w}{\partial t} & \dfrac{\partial w}{\partial s} + (2N+1)u\varepsilon s^{2N} \end{pmatrix}$$

has rank 2 since the Jacobian for ϕ has rank 2. Hence, F_u is an immersion for each $u \in [0, 1]$. Next, we have to show F_u is injective for each $u \in [0, 1]$. Let us use the

notation

$$x(t_i, s_i) = x_{i,i}.$$

Now, consider the set

$$S = \{(t_1, s_1), (t_2, s_2) \in \mathbb{R}^2 \,\Big|\, (x_{1,1}, y_{1,1}) = (x_{2,2}, y_{2,2}) \text{for} (t_1, s_1) \neq (t_2, s_2)\}.$$

Since, ϕ is an embedding,

$$z_{1,1} \neq z_{2,2} \quad \text{when} \quad w_{1,1} = w_{2,2}$$

or,

$$w_{1,1} \neq w_{2,2} \quad \text{when} \quad z_{1,1} = z_{2,2}.$$

We now consider the first case. Now, if we choose an ε such that

$$0 < \varepsilon < \min_{(t_1,s_1),(t_2,s_2)\in S} \left\{ \frac{\left|z_{1,1} - z_{2,2}\right|}{\left|t_1^{2N+1} - t_2^{2N+1}\right|} \right\}.$$

Then, we note that this ε satisfies

$$z_{1,1} + u\varepsilon t_1^{2N+1} \neq z_{2,2} + u\varepsilon t_2^{2N+1}.$$

for all $(t, s) \in S$ and $u \in [0, 1]$. An analogous argument works for the second case. Thus F_u is injective for all $u \in [0, 1]$. This completes the proof. □

This lemma allows us to choose a polynomial embedding with a large odd degree in third and fourth coordinates that keeps the Jacobian positive outside a compact region, say $M \times M$.

Theorem 6.0.5. *Let $\psi_0 \equiv (x_0, y_0, z_0, w_0)$ and $\psi_1 \equiv (x_1, y_1, z_1, w_1)$ be two polynomial embeddings of $\mathbb{R}^2$ in $\mathbb{R}^4$ which represent the isotopic 2-knots. Then ψ_0 and ψ_1 are polynomially isotopic.*

Proof. We can always choose ψ_0 and ψ_1 such that $\tilde{\psi_0} = (x_0, y_0, z_0) : \mathbb{R}^2 \to \mathbb{R}^3$ and $\tilde{\psi_1} = (x_1, y_1, z_1) : \mathbb{R}^2 \to \mathbb{R}^3$ are generic immersions and both ψ_0 and ψ_1 are asymptotic outside a compact region say $M \times M$. Now, let $A \times A$ be the common

compact region inside which both $\tilde{\psi_0}$ and $\tilde{\psi_1}$ have their double curve and triple points. Choose $N \times N \supset (M \times M) \cup (A \times A)$ and image of $N \times N$ under ψ_0 and ψ_1 are $4-$balls of radius R_1 and R_2 respectively. Let $R = \max\{R_1, R_2\}$. We can choose $N \times N = [-\frac{1}{2}, \frac{1}{2}] \times [-\frac{1}{2}, \frac{1}{2}]$. Since ψ_0 and ψ_1 represent the same knot type, there exists an isotopy $F : \mathbb{R}^2 \times I \to \mathbb{R}^4$ such that $F(t, s, 0) = \psi_0(t, s)$ and $F(t, s, 1) = \psi_1(t, s)$. Now consider the restriction of the isotopy map F on $(I_1 \times I_1) \times I$ where $I_1 = [-1, 1]$. Each map $F_u : (I_1 \times I_1) \to \mathbb{R}^4$ is on compact region $(I_1 \times I_1)$ where we can choose a Weierstrass approximation of this map using Bernstein polynomial with two variables inside an ε_0 neighbourhood of F_u for some $\varepsilon_0 > 0$ and adding higher odd order terms to the co-ordinates we can get polynomial embeddings $P_u : (I_1 \times I_1) \to \mathbb{R}^4$ for each $u \in [-1, 1]$ whose derivative is positive outside. Therefore, P_0 and P_1 are polynomially isotopic. Now we can have isotopies between ψ_0 and P_0 defined by $H : \mathbb{R}^2 \times I \to \mathbb{R}^4$ where

$$H(t, s, u) = (1 - u)\psi_0(t, s) + uP_0(t, s).$$

Now each H_u, defined by $H_u(t, s) = (1-u)\psi_0(t, s) + uP_0(t, s)$, is an ε- approximation of ψ_0 inside $I_1 \times I_1$ for our choice of ε and P and $\|H_u\|$ is increasing outside $[-\frac{1}{2}, \frac{1}{2}] \times [-\frac{1}{2}, \frac{1}{2}]$. We can use similar arguments as in Theorem 6.0.1 to prove that H_u is an embedding of $\mathbb{R}^2$ in $\mathbb{R}^4$. Thus, we can define a polynomial isotopy between ψ_0 and P_0. Similarly we can show that ψ_1 and P_1 are polynomially isotopic. Hence ψ_0 and ψ_1 are polynomially isotopic.

□

Definition 6.0.6. A long 2-knot is called a polynomial 2-knot if it is an embedding $\phi : \mathbb{R}^2 \to \mathbb{R}^4$ defined by

$$\phi(t, s) = (f(t, s), g(t, s), h(t, s), p(t, s)),$$

where $f(t, s), g(t, s), h(t, s)$ and $p(t, s)$ are real polynomials.

Theorem 6.0.7. *For every polynomial 2-knot F, there exists a P-homotopy that transforms F to a trivial surface knot.*

Proof. Let F be represented by the the map $\psi : \mathbb{R}^2 \to \mathbb{R}^4$ defined by

$$\phi(t, s) = \big(f(t, s), g(t, s), h(t, s), p(t, s)\big).$$

By Lemma 6.0.4, up to polynomial isotopy we can assume that $p(t,s)$ to be of odd degree and therefore, For $u \in \mathbb{R}$, we define a family of maps $\phi_u : \mathbb{R}^2 \to \mathbb{R}^4$ by

$$(t,s) \to \big(f(t,s), g(t,s), h(t,s), p(t,s) + u^2(t+s)\big).$$

Denote, $p(t,s) + u^2(t+s) = \tilde{p}_u(t,s)$. For each $u \in \mathbb{R}$, the jacobian matrix is

$$\begin{pmatrix} \dfrac{\partial f}{\partial t} & \dfrac{\partial f}{\partial s} \\ \dfrac{\partial g}{\partial t} & \dfrac{\partial g}{\partial s} \\ \dfrac{\partial h}{\partial t} & \dfrac{\partial h}{\partial s} \\ \dfrac{\partial p}{\partial t} + u^2 & \dfrac{\partial p}{\partial s} + u^2 \end{pmatrix}$$

has rank 2 since ψ is an immersion. Since $p(t,s)$ is of odd degree, all partial derivatives of $p(t,s)$, $\frac{\partial p}{\partial t}$ and $\frac{\partial p}{\partial s}$ are even degree polynomials. As shown in [**Mis14**], there exist $R_1, R_2 \in \mathbb{R}$ such that $\frac{\partial p}{\partial t} + R_1 > 0$ and $\frac{\partial p}{\partial s} + R_2 > 0$
Take $R = \max\{R_1, R_2\}$. Therefore

$$\frac{\partial p}{\partial t} + R > 0,$$
$$\text{and} \quad \frac{\partial p}{\partial s} + R > 0.$$

Let $M = \sqrt{R}$.
Therefore, for $u \geq M$,

$$\frac{\partial \tilde{p}_u(t,s)}{\partial t} = \frac{\partial p_u(t,s)}{\partial t} + u^2 > 0,$$
$$\text{and} \quad \frac{\partial \tilde{p}_u(t,s)}{\partial s} = \frac{\partial p_u(t,s)}{\partial s} + u^2 > 0.$$

i.e., $\tilde{p}_u(t,s)$is monotonically increasing for $u \geq M$, ensuring that ϕ_u is a trivial surface knot.
So, we have a homotopy $\phi : \mathbb{R}^2 \times [0,M] \to \mathbb{R}^4$ defined by

$$\phi(t,s,u) = \big(f(t,s), g(t,s), h(t,s), p(t,s) + u^2(t+s)\big)$$

such that $\phi(t,s,0) = \big(f(t,s), g(t,s), h(t,s), p(t,s)\big)$ is the original long 2-knot F and $\phi(t,s,M) = \big(f(t,s), g(t,s), h(t,s), p(t,s) + M^2(t+s)\big)$ presents a trivial long 2-knot. And for each $u \in [0,M]$, $\phi(t,s,u)$ is an immersion.

□

Remark 6.0.8. In Theorem 6.0.7, for each $u \in [0, M]$ we get an immersion ϕ_u in $\mathbb{R}^4$ with same projection as F in $\mathbb{R}^3$. This implies that the singular set is same for each ϕ_u and the one parameter family $\{p(t, s) + u^2(t + s) \mid u \in [0, M]\}$ changes the over/under information through the homotopy ϕ. Therefore, there are finitely many $u \in [0, M]$ for which ϕ_u is an immersion in $\mathbb{R}^4$. Let us refer them as singular long 2-knots. The number of these singular long 2-knots in the homotopy ϕ is called the Singularity Index of the polynomial representation ψ of F.

Definition 6.0.9. *Singularity Index* of a long 2-knot F is defined to be the minimum number of singularity indices over all polynomials ψ presenting F and denoted by *SI(F)*.

Definition 6.0.10. A long 2 knot is said to be *simple* if it has a projection on some $\mathbb{R}^3$ such that a singular set consists of finitely many double point curves only.

Theorem 6.0.11. *Given a polynomial knot K, with the singularity index n there exists a simple polynomial 2-knot P_K with the singularity index less than or equal to n.*

Proof. Let $K : \mathbb{R} \to \mathbb{R}^3$ be a polynomial knot defined as $K(t) = (f(t), g(t), h(t))$ with singularity index n, where $(f(t), g(t))$ is an immersion in $\mathbb{R}^2$ and $h(t)$ is an odd degree polynomial with positive co-efficient [Remark 2.4, [**Mis14**]]. Now, we construct a long 2-knot given by $P_K : \mathbb{R} \times \mathbb{R} \to \mathbb{R}^4$ and defined by

$$P_K(t, s) = (f(t) + s, g(t) + s, s, h(t)).$$

K being an immersion, the jacobian matrix for P_K

$$\begin{pmatrix} \frac{\partial f}{\partial t} & 1 \\ \frac{\partial g}{\partial t} & 1 \\ 0 & 1 \\ \frac{\partial h}{\partial t} & 1 \end{pmatrix}$$

has rank two. Therefore, P_K is an immersion. Let for (t_1, s_1) and (t_2, s_2) we have

$$
\begin{aligned}
f(t_1) + s_1 &= f(t_2) + s_2, \\
g(t_1) + s_1 &= g(t_2) + s_2, \\
s_1 &= s_2, \\
h(t_1) &= h(t_2).
\end{aligned}
$$

This implies

$$
\begin{aligned}
f(t_1) &= f(t_2), \\
g(t_1) &= g(t_2), \\
h(t_1) &= h(t_2).
\end{aligned}
$$

Since, K is an embedding, we have $t_1 = t_2$. Hence, $(t_1, s_1) = (t_2, s_2)$ and therefore P_K is an injective immersion i.e an embedding. The singular set of the long 2-knot contains only double curves, one for each double point of K. If (t_j, t_k) are the values of t for a crossing in the projection of K then the pair (t_j, s) and (t_k, s) will provide a double curve in the projection of P_K in $\mathbb{R}^3$.

By Theorem 6.0.7, we have a continuous map $\Psi : \mathbb{R}^2 \times [0, R] \to \mathbb{R}^4$ such that $\Psi(t, s, 0) = (f(t) + s, g(t) + s, s, h(t))$ is the given knot P_K and $\Psi(t, s, R) = (f(t) + s, g(t) + s, s, h(t) + R^2(t + s))$ is a trivial knot and for each $u \in [0, R]$ the map $\Psi((t, s), u) = (f(t) + s, g(t) + s, s, h(t) + u^2(t + s))$ is an immersion. Now, restriction of this homotopy Ψ on $\mathbb{R} \times [0, R]$, i.e., $\Psi|_{\mathbb{R}\times[0,R]}\mathbb{R} \times [0, R] \to \mathbb{R}^3$ given by

$$
(t, u) \to (f(t) + u, g(t) + u, h(t) + u^2 t),
$$

is the homotopy that transforms the long knot K to a trivial classical knot. Now, K has singularity index n. Therefore, there are at least n values of u, say $u_1, \cdots u_n$ for which $\Psi(t, u_i)$ is a singular knot. For those values of u_i, $i = 1, \cdots, n$,

$$
\begin{aligned}
f(t_a) + u_i &= f(t_b) + u_i, \\
g(t_a) + u_i &= g(t_b) + u_i, \\
h(t_a) + u_i^2 t_a &= h(t_b) + u_i^2 t_b,
\end{aligned}
$$

for all pairs (t_a, t_b) representing the crossing points.

This implies

$$f(t_a) + u_i + s = f(t_b) + u_i + s,$$
$$g(t_a) + u_i + s = g(t_b) + u_i + s,$$
$$h(t_a) + u_i^2 t_a = h(t_b) + u_i^2 t_b,$$

for all the pairs (t_a, s), (t_b, s), representing the double curves.
This suggests that $\Psi(t, s, u_i)$ corresponding to $\Psi(t, u_i)$ for u_i, $i = 1, \cdots, n$ are not embeddings in $\mathbb{R}^4$. This indicates the fact that the long 2-knot P_K is transformed to the trivial surface knot diagram by exchanging over/under information in the set of n number of double curves. Hence, the *Singularity index* of P_K is less or equal to n. □

Example 6.0.12. Here is an example of a long 2-knot (Figure 6.1) constructed from the long trefoil given by the map

$$(t, s) \to (t^3 - 3t + s, t^4 - 4t^2 + s, s, t^5 - 10t).$$

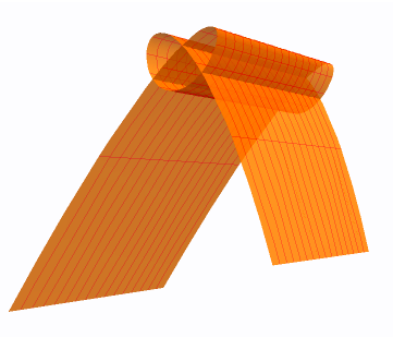

Figure 6.1: Projection of the simple long trefoil 2-knot on a hyperplane

There are many other ways to construct a knotted plane from a given long knot using spun construction. We first prove the following lemma.

Lemma 6.0.13. *For every polynomial K, there exists a knotted disc bounded by $K \sharp K^*$.*

Proof. First, take a knotted arc k of the polynomial knot K in the upper half space $\mathbb{R}^3_+$ with only two endpoints on the boundary $\mathbb{R}^2$. Let the knotted arc be presented by

$\big(f(t), g(t), h(t)\big)$ where $t \in [a, b]$ where $h(a) = 0 = h(b)$ and $h(t) > 0 \quad \text{for}\, t \in (a, b)$. Spinning this arc around $\mathbb{R}^2$ from angle 0 to 2π, results into a semi sphere or a 2-disc in $\mathbb{R}^4$ bounded by $K \sharp K^*$ where K^* is the mirror image of K. Denote it by D. Then D can be parameterized by

$$[a, b] \times [0, \pi] \to \mathbb{R}^4$$

$$(t, s) \to (f(t), g(t), h(t) \sin s, h(t) \cos s)\,,$$

where $s = 0$ and $s = \pi$ will map to the knotted arcs k and k^* on the boundary of D, given by

$$(f(t), g(t), 0, h(t)) \text{ for}\, t \in [a, b],$$

$$(f(t), g(t), 0, -h(t)) \text{ for}\, t \in [a, b]$$

respectively. □

Example 6.0.14. Here is an example of a knotted disc with boundary $K \sharp K^*$ where K is the long trefoil (Figure 6.2), given by

$$[a, b] \times [0, \pi] \to \mathbb{R}^4$$

$$(t, s) \to \big(t^3 - 3t, t^5 - 10t, (-t^4 + 4t^2 + 3) \sin s, (-t^4 + 4t^2) + 3) \cos s\big)$$

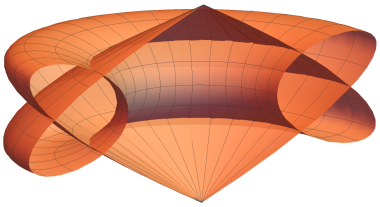

Figure 6.2: Knotted disc with boundary $K \sharp K^*$

Theorem 6.0.15. *For every polynomial knot K, there exists a knotted plane that contains an knotted disc bounded by $K \sharp K^*$.*

Proof. By previous lemma, we have a knotted disc D with boundary $K \sharp K^*$, given by

$$\phi : [a, b] \times [0, 2\pi] \to \mathbb{R}^4,$$

$$(t, s) \mapsto \big(f(t), g(t), h(t) \sin s, h(t) \cos s\big).$$

Now, we construct an annulus A with boundary $K\sharp K^*$ in one end and an unknotted S^1 in the other end by using the P-homotopy map mentioned in Theorem 6.0.11.

For $t \in [a, b]$, $s \in [-\infty, 0]$, we define
$P_K : \psi_1(t, s) = \big(f(t) - s, g(t) - s, s, h(t) + s^2 t\big)$,
$P_{K^*} : \psi_2(t, s) = \big(f(t) + (s - \pi), g(t) + (s - \pi), -(s - \pi), -h(t) + (s - \pi)^2 t\big)$,

where $\psi_1(t, s)$ and $\psi_2(t, s)$ are trivial diagrams for all $s \leq -R$ and $s \geq \pi + R$ by [Lemma 2.7, [**Mis14**]]. Also, we have the following:

- $\psi_1(t, 0) = \phi(t, 0)$, $\psi_2(t, \pi) = \phi(t, \pi)$ presents k and k^* respectively.
- k and k^* are joined at the endpoints $\psi_1(a, 0) = \psi_1(a, 0)$, $\psi_2(b, \pi) = \psi_2(t, \pi)$.
- The values of $\psi_1(a, s)$ for $s \in [-\infty, 0]$ and $\psi_2(b, s)$ for $s \in [\pi, \infty]$ are equal since $h(a) = 0 = h(b)$. Therefore, P_K and P_{K^*} are joined along the lines $\psi_1(a, s)$, $s \in [-\infty, 0]$ and $\psi_2(b, s)$, $s \in [\pi, \infty]$.
- Then the annulus A is obtained by restricting $P_K \cup P_{K^*}$ to $s \in [-R, 0] \cup [0, R]$.
- The other end of the annulus A is a unknotted circle created by $\psi_1(t, -R)$ and $\psi_2(t, \pi + R)$ which are unknotted arcs joined at the endpoints $\psi_1(a, -R) = \psi_1(a, \pi + R)$ and $\psi_2(a, -R) = \psi_2(a, \pi + R)$.
- Outside the interval $s \in [-R, R]$, $\psi_1(t, s) \cup \psi_2(t, s)$ will always be a unknotted S^1.

So, $D \cup A$ joined along the boundary $K\sharp K^*$ gives us an embedding of an open knotted disc with boundary an unknotted S^1. Therefore, extending the interval for s from $[-R, R]$ to $\mathbb{R}$ we get a parameterization of a knotted plane given by

$$\Phi : (a, b) \times \mathbb{R} \to \mathbb{R}^4$$

$$\Phi = \begin{cases} \psi_1 & s \in (-\infty, 0] \\ \phi & s \in [0, \pi] \\ \psi_2 & s \in [\pi, \infty) \end{cases}$$

This completes the proof. □

Remark 6.0.16. This shows that for any knot K, the connected sum of K with its mirror image is a slice knot . By a slice knot, we mean if it is the boundary of a

locally flat disc D^2 embedded into the 4-ball D^4 [**Rol**].

Example 6.0.17. For the long trefoil knot K, we have the knotted plane given by

$$\Phi : (a, b) \times \mathbb{R} \to \mathbb{R}^4,$$

$$\Phi = \begin{cases} \psi_1 & s \in (-\infty, 0], \\ \phi & s \in [0, \pi], \\ \psi_2 & s \in [\pi, \infty), \end{cases}$$

and
$$\begin{aligned} \phi(t,s) &= \big(t^3 - 3t, t^5 - 10t, (-t^3 + 4t^2 + 3)\sin s, (-t^3 + 4t^2 + 3)\cos s\big), \\ \psi_1(t,s) &= \big(t^3 - 3t - s, t^5 - 10t - s, s, (-t^3 + 4t^2 + 3) + s^2 t\big), \\ \psi_2(t,s) &= \big(t^3 - 3t + (s-\pi), t^5 - 10t + (s-\pi), -(s-\pi), (t^3 - 4t^2 - 3) + (s-\pi)^2 t\big). \end{aligned}$$

In Figure 6.3, D is shown in orange color and the annulus A is shown in blue and green for P_k and P_{K^*} respectively.

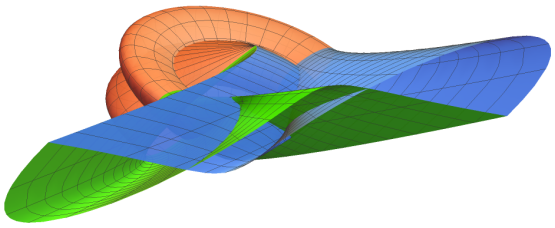

Figure 6.3: Knotted plane with a knotted disc bounded by $K \sharp K^*$.

Theorem 6.0.18. *For a polynomial knot K given by $\big\{(f(t), g(t), h(t)) \,|\, t \in \mathbb{R}\big\}$, there exists a polynomial 2-knot obtained from spinning operation with parameterization given by $\psi' : [a, \infty] \times [0, 2\pi] \to \mathbb{R}^4$ which is defined by*

$$\psi'(t, s) = (f_1(t), g_1(t), h_1(t)\, S(s), h_1(t)\, C(s)) \,.$$

Proof. We start with the knotted arc of K in the upper half space $\mathbb{R}^3_+$. Instead of taking both endpoints of the knotted arc on $\mathbb{R}^2$, we put one endpoint on $\mathbb{R}^2$, and the other end goes to infinity. This happens when $h(t)$ is an odd degree polynomial. If $h(t)$ is an even degree, then we can add a term of a larger odd degree with a very

small coefficient so that the over/under information is not disturbed (Figure 6.4). Let this knotted arc be given by

$$[a, \infty) \to \mathbb{R}^3$$

$$t \to (f_1(t), g_1(t), h_1(t)) .$$

Now, rotating this knotted arc around $\mathbb{R}^2$ results in a knotted plane in S^4 which can be parameterized by

$$[a, \infty) \times [0, 2\pi] \to \mathbb{R}^4$$

$$\big\{\big(f_1(t), g_1(t), h_1(t)\sin s, h_1(t)\cos s\big).$$

Replacing $\cos s$ and $\sin s$ with their corresponding Chebyshev approximations $C(s)$ and $S(s)$, respectively, we get the final polynomial parameterization. This completes the proof. □

Example 6.0.19. An example of a knotted plane obtained from a long trefoil is shown in Figure 6.5.

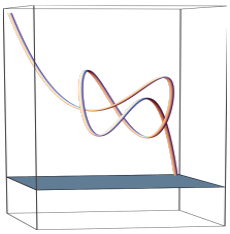

Figure 6.4: Long trefoil arc for $t \in [a, \infty]$

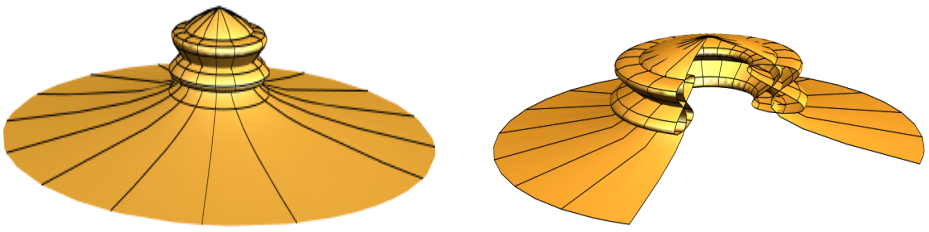

(a) The knotted part inside a compact region

(b) Inside view

Figure 6.5: Knotted plane obtained by spinning

Chapter 7

Concluding remarks and future directions

This chapter summarises our work and discusses a few research problems that can be our potential future projects.

This thesis involved work on parameterizing a few classes of 2- dimensional knots in $\mathbb{R}^4$ and detecting if they are non-trivial. Since the enumeration or classification for knotted surfaces is less understood, we chose specific types of knotted surfaces which are related to some kind of 1-dimensional knot theories so that we could use the parametrization of the 1-dimensional knots to parameterize them. For example, we chose the spun 2-knots and the d-twist spun 2-knots for $d \geq 1$ among knotted spheres. These constructions involve two types of rotation operations: one around a plane in 4-space and another around a line in 3-space. We obtain the required embedding by starting with a polynomial representation of long knots and combining it with these rotation operations. If we approximate these functions by polynomial functions inside a compact domain, we can obtain a polynomial parameterization. Having the desire to parameterize more knotted spheres, we came across a few variations of spinning, for example, *the roll spinning, the super spinning,* and the *deform spinning.* In future, *it will be interesting to understand the geometric operations for these more generalized spinning and then parameterize the corresponding version of spun knots.* For example, Roll spinning was defined by R. H. Fox [**Fox**] with an example, but the

construction is more algebraic. So, the initial challenge would be comprehending and presenting it in terms of geometric operations.

In the knotted torus case, we chose ribbon torus knots to parameterize. Here, Satoh's tube map that connects ribbon torus knots with welded knots has been instrumental for parameterization purposes. This is because a welded knot diagram could be realized as a classical knot diagram in which few crossings have been welded. To do this, we took a parametrization of a classical knot projection in which we can mark the crossings to be either classical or welded. Then, we constructed the functions that provide a circle at every point on the knot projection. We adjust the radius of the tube in such a way that the radius near the under-crossing point is smaller compared to the over-crossing point. This takes care of the map near classical crossings. Similarly, we placed the tubes side by side (not touching each other), corresponding to a welded crossing. For *knotted higher genus surfaces with ribbon singularities*, if we use the fact that they are the connected sum of the torus, we can explore if the connected sum for welded knots makes sense and if the tube operation respects the connected sum. This can be a worthwhile future research project.

While checking the parameterized 2-dimensional knots to be non-trivial, we see that the spun of K and d-twist spun of K ($d > 1$) are non-trivial if the given classical knot K is non-trivial. However, to ascertain a ribbon torus knot to be non-trivial, we have checked that the fundamental group of the corresponding welded knot is not isomorphic to $\mathbb{Z}$. We have worked on the fundamental group for welded knots, which are obtained by welding a few crossings in the standard diagram of $K(2, 2n+1)$ the torus knots of type $(2, 2n+1)$ and T_n the twist knots. We specifically examined the cases for the diagrams of $K(2, 2n+1)$ and T_n with one and two welded crossings. In case only one crossing was welded, it was simpler to write down the group. However, when we wanted to weld two crossings, the number of classical crossings between two welded crossings played an important role. Hence, the diagrams are split into two parts by the welded crossings. Now, if the number of welded crossings increases, the number of partitions also grows, leading to a surge in the number of cases for a fixed number of welding. Consequently, determining the knot group for each case and verifying if they are isomorphic to $\mathbb{Z}$ or not presents a computational challenge. *Therefore, developing a computer program capable of performing this task for each case would be*

an intriguing problem to tackle. We mentioned in Section 2.4.3 that the knot group for welded knots does not detect a welded unknot, and at present, we lack concrete examples of non-trivial welded knots with knot groups isomorphic to Z. *This underscores the critical importance in welded knot theory of finding such examples in future.*

In knot theory, it is essential to determine both upper and lower bounds for any invariant in order to compute it effectively. Typically, we use the relationship of a knot invariant with other invariants to establish these bounds. In this thesis, we focused on the welded knot invariant known as the "welded unknotting number". We explored its connections with two other invariants, namely warping degree and classical unknotting number. Additionally, we calculated its value for the torus family $K(2, 2n+1)$ and the twist family T_n. For $K(2, 2n+1)$, we determined an upper bound, and for T_n, we proved it to be one. However, the generalization of classical invariants for welded knots is limited, and the number of other available invariants is also scarce. It would be beneficial to discover additional properties of the "welded unknotting number", particularly finding a lower bound, which would greatly aid in computation.

In the case of knotted planes, we have constructed and parameterized simple long 2-knots, which are knotted planes with only double point curves as singularities. Our construction involved using slice knots and spun 2-knots. In the future, we can explore parameterizing more complex knotted planes with both double and triple points as singularities. Similar to the 1-dimensional case of long knots, it would be valuable to study a method for finding a general parameterization for long 2-knots. For future work, *other knotted surfaces, orientable and even non-orientable ones, e.g. knotted projective planes are open for exploration.*

We can ask some interesting questions involving the *Tube map.* Virtual surface knot theory has already been introduced as a generalization of virtual knots [**Tak**]. In future, we aim to extend the Tube map to virtual surface knot diagrams to investigate the higher-dimensional knots that can be obtained from this approach. Another question to explore the impact of applying $Tube^n(K)$, i.e. $\underbrace{Tube(\cdots Tube(K))}_{n}$ to a

virtual knot diagram K to obtain a higher dimensional knotted manifolds and analyze how the dimension depends on n.

As the surface knot theory is still evolving, many more interesting questions may emerge.

Appendix A

Mathematica Notebooks

A.1 Chebyshev approximation of cos(dx) and sin(dx) function

```
ClearAll;
d = 1;
n1 = 8;(* degree of chebyshev polynomial for cos[du]*)
n2 = 8; (* degree of chebyshev polynomial for sin[du]*)
a = 0; b = 2 Pi; (*Interval for approximation *)
nd[k_] := N[(a + b) / 2 + (b - a) / 2 * Cos[(2 k - 1) Pi / (2 n1 + 2)]];
nd2[k_] := N[(a + b) / 2 + (b - a) / 2 * Cos[(2 k - 1) Pi / (2 n2 + 2)]];
xk = Array[nd, n1 + 1];

g[u_] := Cos[d * u];
h[u_] := Sin[d * u];
yk1 = g[xk];
yk2 = h[xk];



cof1[j_] := 2 * Sum[yk1[[k]] * Cos[j * (2 k - 1) Pi / (2 n1 + 2)], {k, 1, n1 + 1}] / (n1 + 1);
cof2[j_] := 2 * Sum[yk2[[k]] * Cos[j * (2 k - 1) Pi / (2 n1 + 2)], {k, 1, n1 + 1}] / (n1 + 1);
Co1 = (Sum[yk1[[k]], {k, 1, n1 + 1}]) / (n1 + 1);
Co2 = (Sum[yk2[[k]], {k, 1, n1 + 1}]) / (n1 + 1);
```

```
cappx[x_] := Co1 + Sum[cof1[k] * ChebyshevT[k, x], {k, 1, n1}];
Sappx[x_] := Co2 + Sum[cof2[k] * ChebyshevT[k, x], {k, 1, n1}];

Plot[{g[s], cappx[(s - (a + b) / 2) / ((b - a) / 2)]}, {s, -2, 2 Pi + 2}, PlotLegends → {g[s], "C(s)"}]
Plot[{h[s], Sappx[(s - (a + b) / 2) / ((b - a) / 2)]}, {s, -2, 2 Pi + 2}, PlotLegends → {h[s], "S(s)"}]
```

Out[98]=

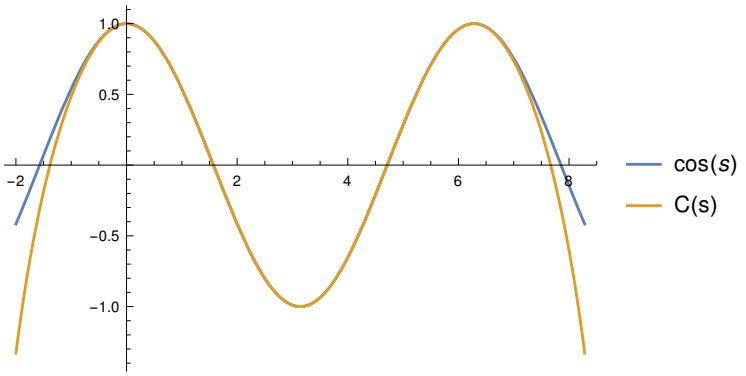

Out[99]=

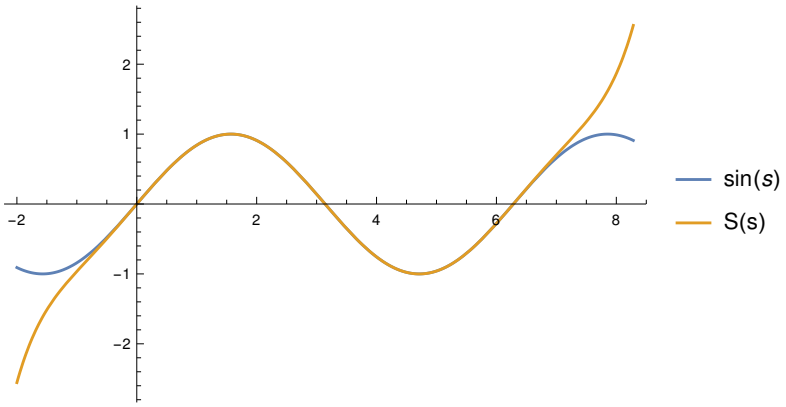

A.2 Spun trefoil 2-knot

In[15]:=
```
ClearAll;
(* Polynomial parameterization of the long knot K given by (f(t), g(t), h(t))*)
f[t_] = t^3 - 3 t;
g[t_] = t^5 - 10 t;
h[t_] = 4 t^2 - t^4;
```

In[19]:=
```
H1[t_] := -(t^4 - 4 t^2) + 3;
Plot[H1[x], {x, -3, 3}]
NRoots[H1[x], x](*This gives the interval [a,b]
 for the knotted arc so that endpoints are on XY plane*)
```

Out[20]=

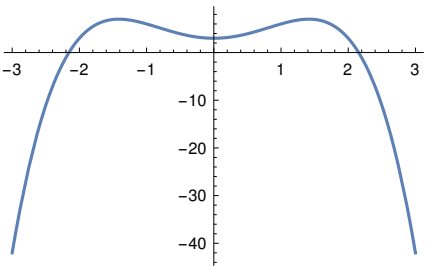

Out[21]= $x == -2.1554 \mid\mid x == 0. - 0.803587\,i \mid\mid x == 0. + 0.803587\,i \mid\mid x == 2.1554$

In[22]:=
```
a = -2.1554;
b = 2.1544;
Show[ParametricPlot3D [{f[t], g[t], H1[t]}, {t, a, b}],
 Graphics3D[InfinitePlane [{2, -2, 0}, {{2, 2, 0}, {-2, 2, 0}}]], ViewPoint -> Front]
```

Out[24]=

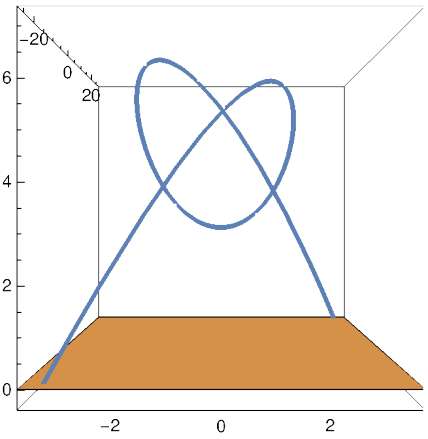

In[25]:=
```
ParametricPlot3D [{f[t], H1[t] * Cos[s], H1[t] * Sin[s]}, {t, a, b}, {s, 0, 2 Pi},
 PlotStyle → Opacity[0.8], ColorFunction → "TemperatureMap ", Mesh → Full,
 MeshStyle -> {Red, Black}, PlotRange → Full, AxesLabel → {x, y, z}]
```

Out[25]=

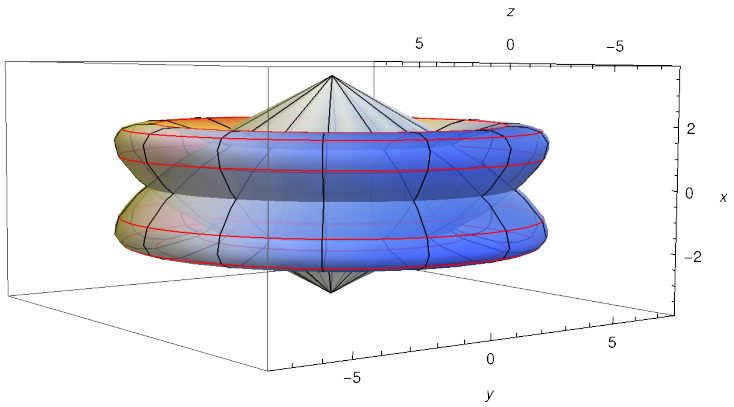

In[26]:=
```
Show[ParametricPlot3D [{f[t], H1[t] * Cos[s], H1[t] * Sin[s]}, {t, a, b}, {s, 0, 2 Pi},
  PlotStyle → Opacity[0.5], ColorFunction → RGBColor[0.96, 0.59, 0.43, 0.5],
  Mesh → Full, MeshStyle -> {Red, Thick}, PlotRange → Full, Boxed → False, Axes → False]]
```

Out[26]=

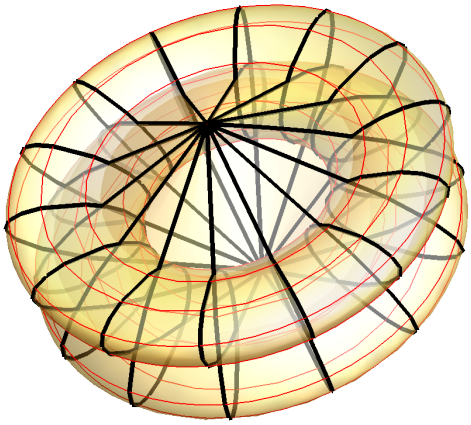

In[27]:=
```
ParametricPlot3D [{f[t], H1[t] × Cos[s], H1[t] × Sin[s]}, {t, a, b}, {s, 0, Pi},
 PlotStyle → Opacity[0.8], ColorFunction → "TemperatureMap ", Mesh → Full,
 MeshStyle -> {Red, Black}, PlotRange → Full, AxesLabel → {x, y, z}]
```

Out[27]=

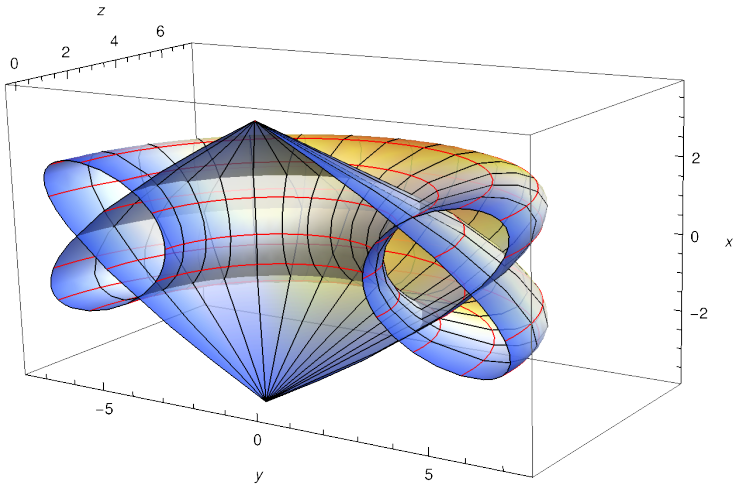

A.3 Spun figure eight 2-knot

In[133]:=
```
ClearAll;
(* Polynomial parameterization of the long knot K given by (f(t), g(t), h(t))*)
f[t_] = 2 (t^2 - 7) (t^2 - 10) t / 5;
g[t_] = t (t^2 - 4) (t^2 - 9) (t^2 - 12) / 10;
h[t_] = -(t^4 - 13 t^2) + 20;
NRoots[h[x], x] (*This gives the interval [a,b]
 for the knotted arc so that endpoints are on XY plane*)
Plot[h[x], {x, -4, 4}]
```

Out[137]=
```
x == -3.7934 || x == 0. - 1.17893 i || x == 0. + 1.17893 i || x == 3.7934
```

Out[138]=

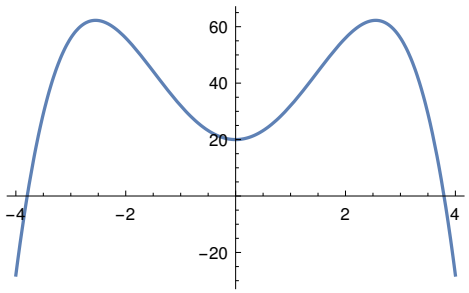

In[141]:=
```
a = -3.7934;
b = 3.7934;
Show[Graphics3D[Tube[Table[{f[t], g[t], h[t]}, {t, a, b, 0.01}], 0.5],
   Boxed → True, Axes → True, AxesLabel → {X, Y, Z}, PlotRange → {All, All, All}],
 Graphics3D[InfinitePlane[{2, -2, 0}, {{2, 2, 0}, {-2, 2, 0}}]], ViewPoint -> Front]
```

Out[143]=

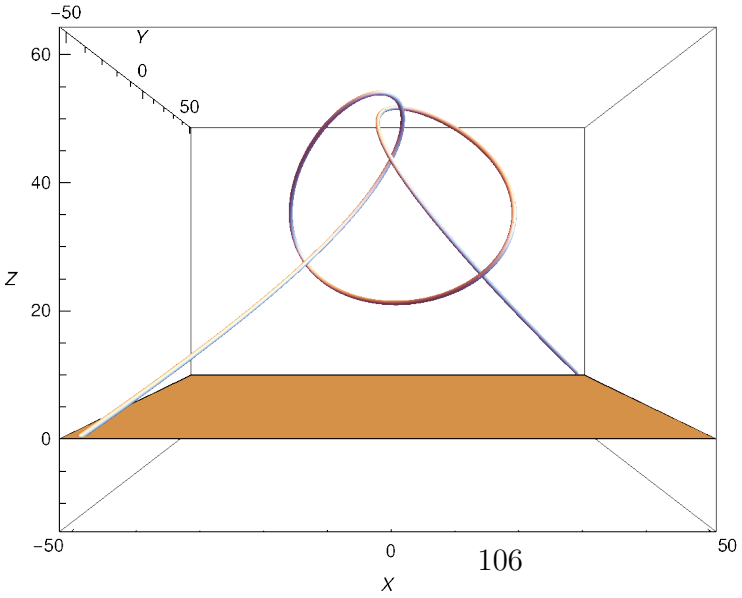

In[151]:=
```
ParametricPlot3D [{f[t], h[t] * Cos[s], h[t] * Sin[s]}, {t, a, b}, {s, 0, 2 Pi},
 PlotStyle → Opacity[0.7], ColorFunction → "TemperatureMap ", Mesh → Full,
 MeshStyle -> {Red, Black}, PlotRange → Full, AxesLabel → {x, y, z}]
```

Out[151]=

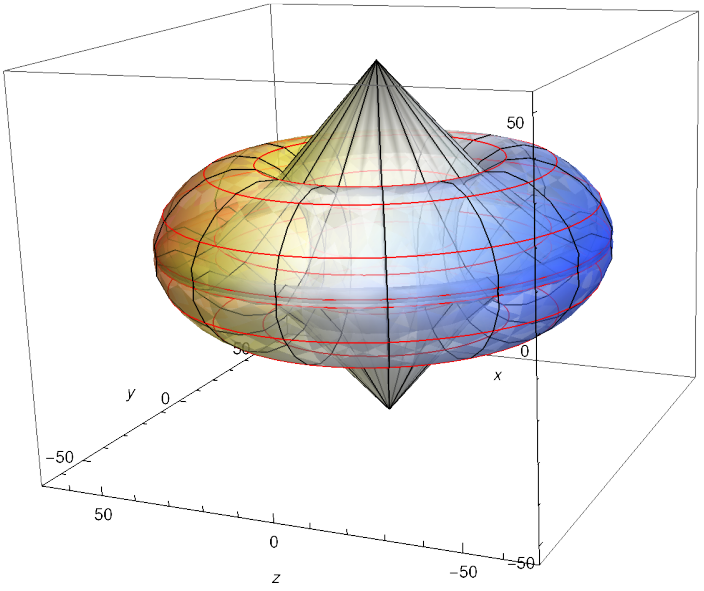

In[152]:=
```
ParametricPlot3D [{f[t], h[t] * Cos[s], h[t] * Sin[s]}, {t, a, b}, {s, 0, Pi},
 PlotStyle → Opacity[0.8], ColorFunction → "TemperatureMap ", Mesh → Full,
 MeshStyle -> {Red, Black}, PlotRange → Full, AxesLabel → {x, y, z}]
```

Out[152]=

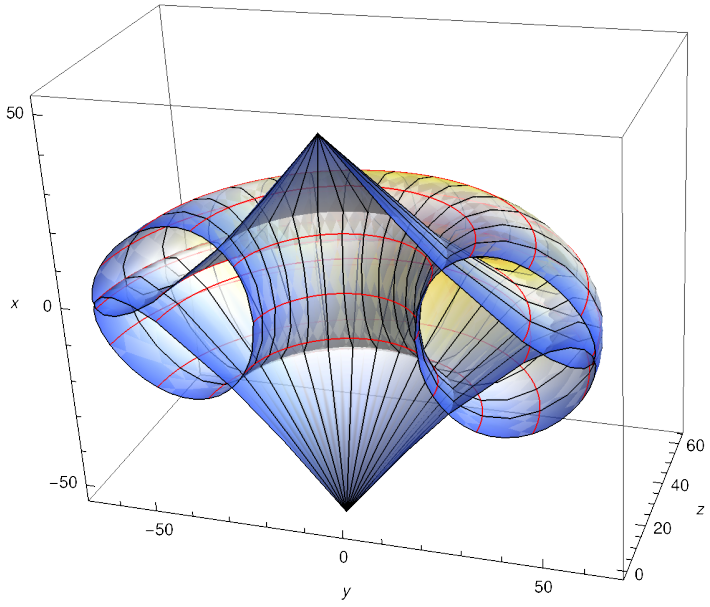

A.4 d-twist spun figure eight knot

```
ClearAll;
(* Polynomial parameterization of the long knot K given by (f(t), g(t), h(t))*)
f[t_] = t^3 - 3 t;
g[t_] = t^5 - 10 t;
h[t_] = 16 + 4 t^2 - t^4;
(*Manipulating z(t) so that while rotating it doesnot intersect xy plane*)
NRoots[h[t], t](*This gives the interval for
 the knotted arc so that endpoints are on xy plane*)
(*[a,b]= interval for the knotted arc with endpoints on XY plane,
t1,t2 corresponds to the endpoints P and Q of the axis PQ,
[a1,b1]= Contains all the crossings of K *)
a = -2.54404;
b = 2.54404;
t1 = -2.19;
t2 = 2.19;
a1 = -1.96;
b1 = 1.96;
Show[Graphics3D[Tube[Table[{f[t], g[t], h[t]}, {t, a, b, 0.005}], 0.2],
  Axes → True, AxesLabel → {X, Y, Z}],
 Graphics3D[{Thickness[0.009], Line[{{f[t1], g[t1], h[t1]}, {f[t2], g[t2], h[t2]}}]}],
 Graphics3D[InfinitePlane[{2, -2, 0}, {{2, 2, 0}, {f[b], g[b], 0}}]], ViewPoint -> Front]
```

Out[ ]= $t == -2.54404 \mid\mid t == 0. - 1.5723\,i \mid\mid t == 0. + 1.5723\,i \mid\mid t == 2.54404$

Out[ ]=

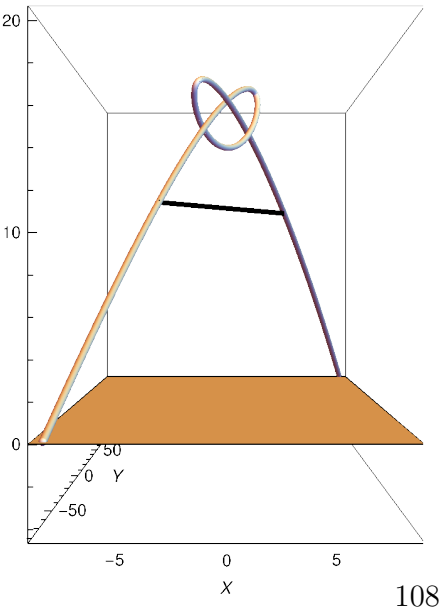

In[ ]:=
```
(*Rotating about the line L joining the points (f[t1],g[t1],h[t1])
 and (f[t2],g[t2],h[t2]) on the knotted arc ,using Rodrigue's formula*)
Clear[t, s];
L =
  Graphics3D[{Thickness[0.001], InfiniteLine[{{f[t1], g[t1], h[t1]}, {f[t2], g[t2], h[t2]}}]}];
 (*axis of rotation for twisting*)
P = Graphics3D[InfinitePlane[{f[-2], g[-2], 0}, {{f[2], g[2], 0}, {f[b], g[b], 0}}]];
(*xy plane *)

Nr = Sqrt[g[t2]^2 + f[t2]^2];
f1[t_, s_] = (1 - (1 - Cos[s]) g[t2]^2 / Nr^2) f[t] +
    (1 - Cos[s]) f[t2] × g[t2] × g[t] / Nr^2 + (h[t] - h[t2]) Sin[s] × g[t2] / Nr;
g1[t_, s_] = (1 - Cos[s]) f[t2] × g[t2] × f[t] / Nr^2 +
    (1 - (1 - Cos[s]) f[t2]^2 / Nr^2) g[t] - (h[t] - h[t2]) Sin[s] × f[t2] / Nr;
h1[t_, s_] = -Sin[s] × g[t2] × h[t2] × f[t] / Nr + Sin[s] × f[t2] × h[t2] × g[t] / Nr +
    h[t2] (1 - Cos[s]) + Cos[s] × h[t];

Show[Graphics3D[{Black, Tube[Table[{f[t], g[t], h[t]}, {t, a, b, 0.005}], 0.3]},
  Axes → False, Boxed → False, AxesLabel → {X, Y, Z}],
 ParametricPlot3D[{f1[t, s], g1[t, s], h1[t, s]}, {t, a, b}, {s, 0, 2 Pi},
  Axes → False, AxesLabel → {X, Y, Z}, ViewPoint → Left, MeshStyle → None,
  Exclusions → None, MaxRecursion → 6, PlotStyle → Opacity[0.6],
  Boxed → False, ImageSize -> Large], L, P, PlotRange -> Full]
```

Out[ ]=

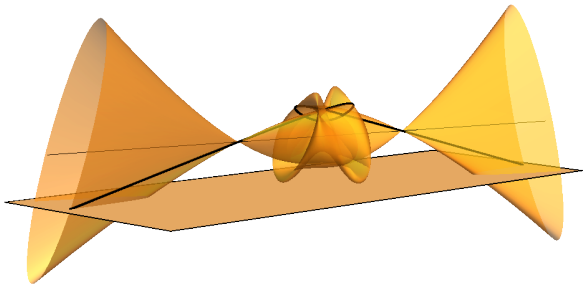

In[ ]:=
```
(*Constructing Bump Function : 1 in [a1,b1],
0 in [a,t1] and [t2,b] and in (0,1) otherwise ,
Choose d1, d2 as follows: d1 > t1+t2 ,
d2< d1 and note that (d1-d2)(>0) decides the slope
  of the bump function when its values are in (0,1)*)
d1 = 4.8;
d2 = 3.8;
F1[t_] = Piecewise[{{Exp[-1/t], t ≥ 0}, {0, t ≤ 0}}];
B[t_] = F1[d1 - t^2]/(F1[d1 - t^2] + F1[t^2 - d2]);
Plot[{B[t]}, {t, a, b}]
```

Out[ ]=

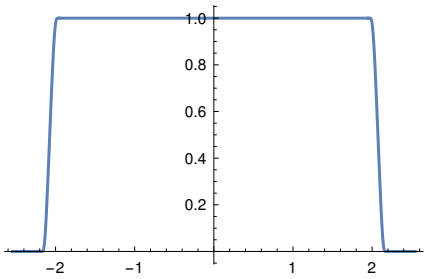

In[ ]:=
```
(*Using Bump function to restrict the rotation in [t1,t2] *)
f2[t_, s_] = f1[t, s] * B[t] + f[t] (1 - B[t]);
g2[t_, s_] = g1[t, s] * B[t] + g[t] (1 - B[t]);
h2[t_, s_] = h1[t, s] * B[t] + h[t] (1 - B[t]);
Show[ParametricPlot3D [{f2[t, s], g2[t, s], h2[t, s]},
  {t, a, b}, {s, 0, 2 Pi}, Exclusions → None , MaxRecursion → 6,
  PlotRange -> Full , Boxed -> False , Axes -> False], P, ViewPoint → Right]
```

Out[ ]=

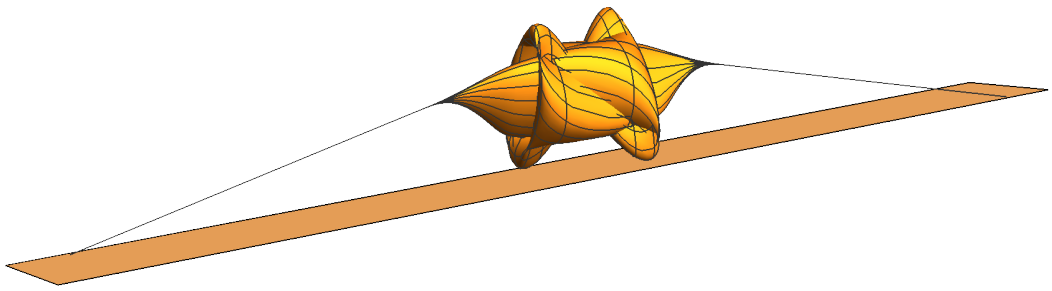

```
(*Spinning about xy plane*)
d = 2;(*twisting d times*)

ParametricPlot3D [{f2[t, d * s], h2[t, d * s] * Cos[s], h2[t, d * s] * Sin[s]},
 {t, a, b}, {s, 0, 2 Pi}, ViewPoint → Top, MeshStyle → Red,
 Exclusions → None, MaxRecursion → 6, PlotStyle → Opacity[0.7],
 ImageSize → Large, Boxed -> False, Axes -> False, PlotRange → Full]
```

Out[ ]=

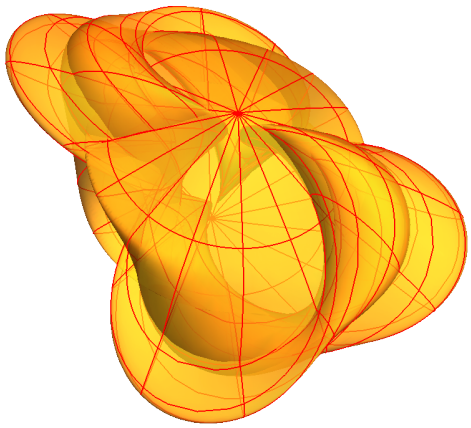

In[ ]:=
```
(*see trefoil twisting while rotating*)
ParametricPlot3D [{f2[t, d * s], h2[t, d * s] * Cos[s], h2[t, d * s] × Sin[s]},
 {t, a, b}, {s, 0, 2 Pi}, ViewPoint → Left , MeshStyle -> {Red, Thick},
 Exclusions → None , MaxRecursion → 6, PlotStyle → Opacity[0.4],
 ImageSize → Large , Boxed -> False , Axes -> False]
```

Out[ ]=

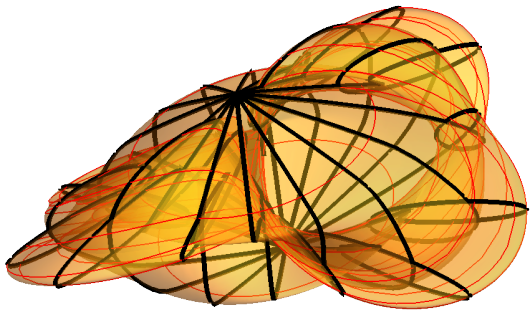

A.5 Ribbon torus knot from two welded $T(2,7)$

In[50]:=
```
(* T(2,7) parametrization *)
x[t_] := Cos[2 t] (3 + Cos[7 t]) ;
y[t_] := Sin[2 t] (3 + Cos[7 t]);
 z[t_] := Sin[7 t];
ParametricPlot [{x[t], y[t]}, {t, 0, 2 Pi}, PlotStyle → Thickness [0.01], Axes → True]
```

Out[53]=

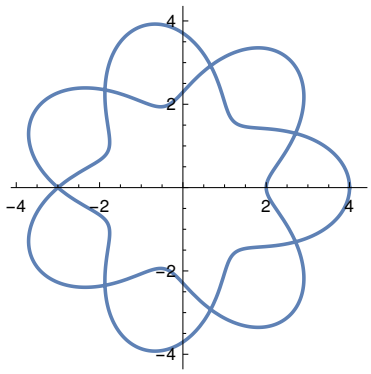

In[54]:=
```
bumpFunction [x_, c_, w_] := Piecewise [{{Exp[-1 / (1 - (x - c) ^ 2 / w ^ 2)], Abs[x - c] < w}}, 0]
(*c=center ,w=width*)
Plot[bumpFunction [x, 0, Pi / 2], {x, -Pi, Pi},
 PlotRange → Full, AxesLabel → {"x", "B(x,0,Pi/2)"}]
Sum1[t_] := Sum[bumpFunction [t, c, Pi / 14], {c, 15 * Pi / 14, 27 * Pi / 14, 4 * Pi / 14}] +
    bumpFunction [t, 11 * Pi / 14, Pi / 14];
Sum2[t_] := Sum[bumpFunction [t, c, Pi / 14], {c, {3 * Pi / 14, 7 * Pi / 14}}] -
    Sum[bumpFunction [t, c, Pi / 14], {c, {17 * Pi / 14, 21 * Pi / 14}}];
```

Out[55]=

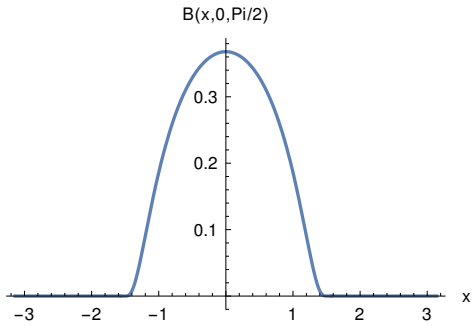

In[58]:=
```
(*At classical crossings we will shrink the lower arc*)Show[
 ParametricPlot3D [{x[t], y[t] + (0.8 - Sum1[t]) * Cos[u], y[t] + (0.8 - Sum1[t]) * Sin[u] + 5 * Sum2[t]},
  {t, 5 Pi / 7, 6 Pi / 7}, {u, 0, 2 Pi}, PlotStyle → Opacity[1],
  ColorFunction → "BlueGreenYellow ", Exclusions → None,
  MaxRecursion → 3, Boxed → False, Axes -> False, Mesh → 30],
 ParametricPlot3D [{x[t], y[t] + (0.8 - Sum1[t]) * Cos[u], y[t] + (0.8 - Sum1[t]) * Sin[u] + 5 * Sum2[t]},
  {t, 12 Pi / 7, 13 Pi / 7}, {u, 0, 2 Pi}, PlotStyle → Opacity[1],
  ColorFunction → "BlueGreenYellow ", Exclusions → None, MaxRecursion → 3,
  Boxed → False, Axes -> False, Mesh → 30], PlotRange -> Full]
```

Out[58]=

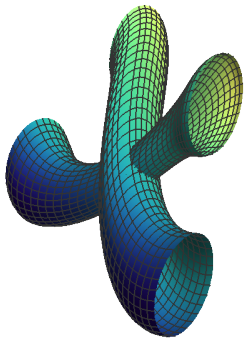

In[59]:=
```
Show[
 ParametricPlot3D [{x[t], y[t] + (0.8 - Sum1[t]) * Cos[u], y[t] + (0.8 - Sum1[t]) * Sin[u] + 5 * Sum2[t]},
  {t, Pi / 7, 2 Pi / 7}, {u, 0, 2 Pi}, PlotStyle → Opacity[1],
  ColorFunction → "BlueGreenYellow ", Exclusions → None,
  MaxRecursion → 3, Boxed → False, Axes -> False, Mesh → 30],
 ParametricPlot3D [{x[t], y[t] + (0.7 - Sum1[t]) * Cos[u], y[t] + (0.7 - Sum1[t]) * Sin[u] + 5 * Sum2[t]},
  {t, 8 Pi / 7, 9 Pi / 7}, {u, 0, 2 Pi}, PlotStyle → Opacity[1],
  ColorFunction → "BlueGreenYellow ", Exclusions → None, MaxRecursion → 3,
  Boxed → False, Axes -> False, Mesh → 30], PlotRange -> Full]
```

Out[59]=

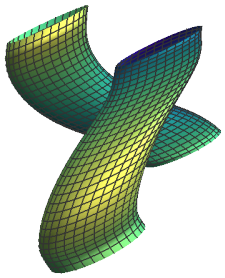

In[60]:=
```
ParametricPlot3D [
 {x[t], y[t] + (0.85 - Sum1[t]) * Cos[u], y[t] + (0.85 - Sum1[t]) * Sin[u] + 5 * Sum2[t]}, {t, 0, 2 Pi},
 {u, 0, 2 Pi}, PlotStyle → Opacity[1], ColorFunction → "BlueGreenYellow ",
 Exclusions → None , MaxRecursion → 3, Boxed → False , Axes -> False , Mesh → 30]
```

Out[60]=

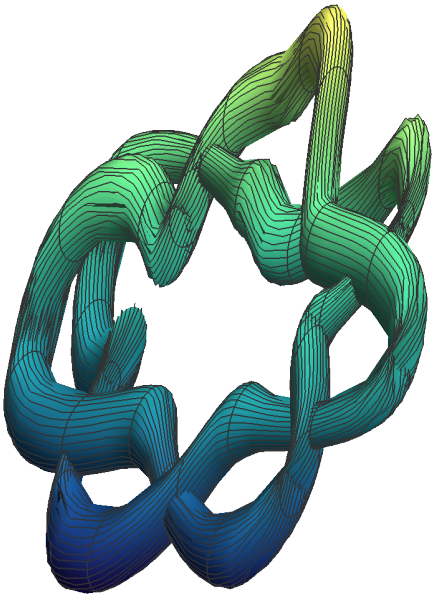

A.6 Knotted plane from long trefoil

```
In[ ]:= ClearAll;
        (* Polynomial parameterization of the long knot K given by (f(t), g(t), h(t))*)
        f[t_] = (t^3 - 3 t);
        g[t_] = t^5 - 10 t;
        h[t_] = -(t^4 - 13 t^2) + 20;

        H[t_] := -(t^4 - 4 t^2) + 3;
        NRoots[H[t], t]
        Show[ParametricPlot3D [{t^3 - 3 t, t^5 - 10 t, H[t]}, {t, -2.1554, 2.1554}],
         Graphics3D[InfinitePlane [{2, -2, 0}, {{2, 2, 0}, {-2, 2, 0}}]], PlotRange -> Full]
```

```
Out[ ]= t == -2.1554 || t == 0. - 0.803587 i || t == 0. + 0.803587 i || t == 2.1554
```

Out[ ]=

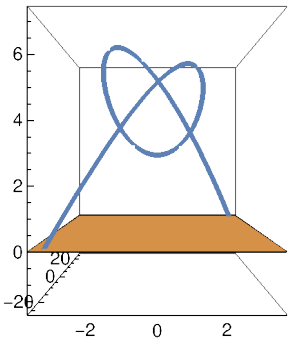


```
In[ ]:= (*Knotted disc D bounded by K # K^* in s in [0,Pi]*)
        P1 = ParametricPlot3D [{(t^3 - 3 t), H[t]* Sin[s], H[t] *Cos[s]}, {t, -2.1554, 2.1554},
          {s, 0, Pi}, PlotStyle → Directive[RGBColor[1., 0.67, 0.5], Opacity[0.9]],
          Exclusions → None, PlotRange -> Full, Boxed -> False, Axes -> False]
```

Out[ ]=

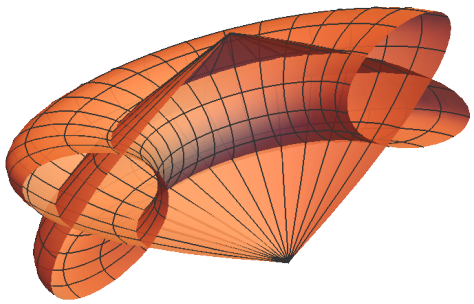

```
(*P_K* for s in [-R,0]*)
P2 = ParametricPlot3D [{(t^3 - 3 t) - s, s, H[t] + s^2 * t}, {t, -2.1554, 2.1554},
    {s, -3, 0}, PlotStyle → Directive[RGBColor[0.42, 0.64, 1.], Opacity[0.9]],
    Exclusions → None, PlotRange -> Full, Boxed -> False, Axes -> False];

(*P_K^*  s in [Pi,Pi+R]*)
P3 =
  ParametricPlot3D [{(t^3 - 3 t) + s - Pi, -(s - Pi), -H[t] + (s - Pi)^2 * t}, {t, -2.1554, 2.1554},
    {s, Pi, Pi + 3}, PlotStyle → Directive[RGBColor[0.33, 0.98, 0.], Opacity[0.9]],
    Exclusions → None, PlotRange -> Full, Boxed -> False, Axes -> False];
(*Annulus A in [*)
Show[P1, P2, P3, PlotRange -> Full, ViewPoint → {0, 0, ∞}]
```

Out[ ]=

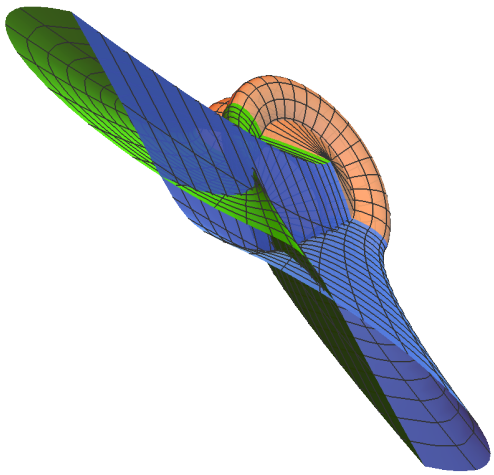

A.7 Knotted plane from long trefoil

In[ ]:=
```
ClearAll;
f[t_] := t^3 - 3 t;
g[t_] := t^4 - 4 t^2;
G1[t_] := -(t + 2) (t + 1.8) (t + 1) t (t - 1) (t - 1.8) (t - 2) + 10;
NRoots[G1[t], t]
Plot[G1[x], {x, -3, 2.2}]
```

Out[ ]=
```
t == -2.00847 - 0.286187 i || t == -2.00847 + 0.286187 i || t == -0.515054 - 0.483818 i ||
  t == -0.515054 + 0.483818 i || t == 1.43 - 0.423988 i || t == 1.43 + 0.423988 i || t == 2.18705
```

Out[ ]=

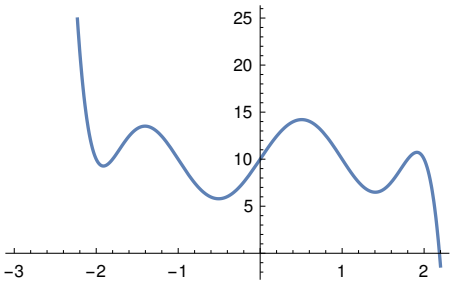

In[ ]:=
```
Show[Graphics3D[Tube[Table[{f[t], g[t], G1[t]}, {t, -2.2, 2.18705, 0.01}], 0.1],
  Boxed → True, Axes → False, AxesLabel → {X, Y, Z}, PlotRange → {All, All, All}],
 Graphics3D[InfinitePlane[{2, -2, 0}, {{2, 2, 0}, {-2, 2, 0}}]]]
```

Out[ ]=

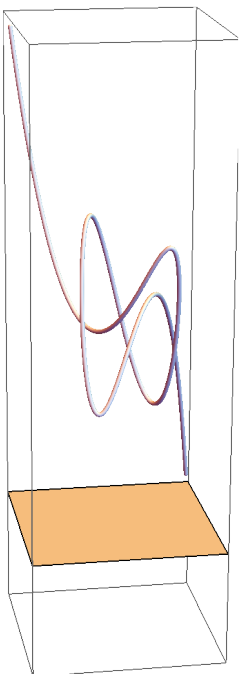

In[ ]:=
```
ParametricPlot3D [{f[t], G1[t] × Cos[s], G1[t] × Sin[s]},
  {t, -2.3, 2.18705}, {s, 0, 2 Pi}, PlotStyle → Opacity[1],
  ColorFunction -> "Monochrome ", Mesh → Full , MeshStyle -> {Black},
  PlotRange → Full , AxesLabel → {x, y, z}, Boxed -> False , Axes -> False]
```

Out[ ]=

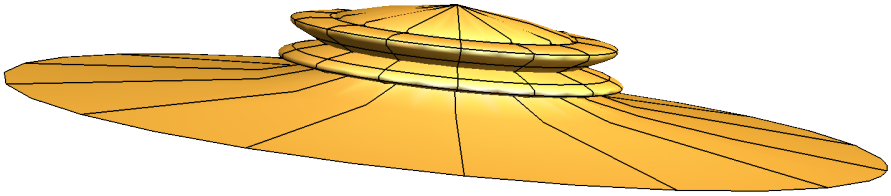

In[ ]:=
```
ParametricPlot3D [{f[t], G1[t] × Cos[s], G1[t] × Sin[s]},
  {t, -2.27, 2.18705}, {s, 0, 3 Pi / 2}, PlotStyle → Opacity[1],
  ColorFunction -> "Monochrome ", Mesh → Full , MeshStyle -> {Black},
  PlotRange → Full , AxesLabel → {x, y, z}, Boxed -> False , Axes -> False]
```

Out[ ]=

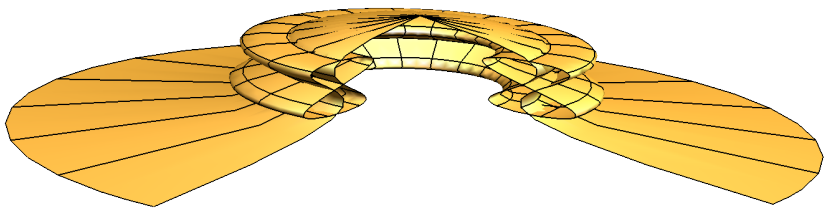

Bibliography

[Abu] M. A. Abutheraa, D. Lester, & C. Ardil (Ed.) *Computable Function Representations Using Effective Chebyshev Polynomial*. In C. Ardil (Ed.), Conference of the World-Academy-of-Science-Engineering-and-Technology (Vol. 25, pp. 103-109). World Academy of Science, Engineering and Technology, (2007).

[Ada] C. C. Adams,*The knot book*. American Mathematical Soc., (1994).

[ANB] A. N. Brown, *Examples of polynomial knots.*(2004).

[Art] E. Artin, *Zur Isotopie zweidimensionaler Flächen imR4*. Abhandlungen aus dem Mathematischen Seminar der Universität Hamburg, 4, 174-177, (1925).

[Bog] M. G. V. Bogle, J. E. Hearst, V. F. R. Jones, and L. Stoilov, *Lissajous Knots* Journal of Knot Theory and Its Ramifications 03:02, 121-140. (1994)

[CarSai] J. S. Carter, & M. Saito, *Knotted Surfaces and Their Diagrams*. Surveys and monographs 55, Amer. Math. Soc.(1998) .

[ConPow] A. Conway and M. Powell. *Embedded surfaces with infinite cyclic knot group*. Geom. Topol. 27(2):739–821, (2023).

[CroFox] R. H. Crowell, and R. H. Fox. *Introduction to Knot Theory.* (1977).

[DurOsh] A. Durfee, & D. O'Shea, *Polynomial knots.*(2006) arXiv preprint math/0612803.

[Dye] H.A. Dye, H.A. . *A*n Invitation to Knot Theory: Virtual and Classical (1st ed.). Chapman and Hall/CRC. (2016) https://doi.org/10.1201/9781315370750

[EMB] E. M. Brown, *Unknotting in M2 × I*, Transactions of the American Mathematical Society , Jun., Vol. 123, No. 2, pp. 480-505. (1966)

[FeRiRo] R. Fenn, R. Rimányi, and C. Rourke. *The braid-permutation group*. Topology 36(1):123–135, (1997).

[Fox] R. H. Fox , *Rolling*, Bulletin of the American Mathematical Society, Bull. Amer. Math. Soc. 72(1.P1), 162-164, (January 1966).

[Fre] M. H. Freedman. *The disk theorem for four-dimensional manifolds*. in: Proc. Internat. Congr. Math. (Warsaw, 1983) Vol. 1,2, pages 647–663, PWN, Warsaw, (1984).

[GKPV] A. Gill, K. Kaur, M. Prabhakar, and A. Vesnin, *An unknotting invariant for welded knots*, Proc. Indian Acad. Sci. Math. Sci., vol. 131, no. 2, Paper No. 47, 17, 2021.

[Glu] H. Gluck, *The embedding of two-spheres in the four-sphere*. Bulletin of the American Mathematical Society, 67, 586-589, (1961).

[HilKaw] J. A. Hillman and A. Kawauchi. *Unknotting orientable surfaces in the* 4*-sphere*. J. Knot Theory Ramifications 4(2):213–224, (1995).

[Ich] A. Ichimori and T. Kanenobu. *Ribbon torus knots presented by virtual knots with up to four crossings*.J. Knot Theory Ramifications 21(13):1240005, (2012).

[Kam] S. Kamada, *Braid and Knot Theory in Dimension Four*, Surveys and monographs 95, Amer. Math. Soc.(2002)

[Kan] T. Kanenobu, *Forbidden moves unknot a virtual knot*.J. Knot Theory Ramifications 10(1):89–96, (2001).

[Kau98] L. H. Kauffman, *Fourier knots*, in Ideal Knots, Vol. 19 in Series on Knots and Everything, ed. by A. Stasiak, V. Katrich, L. Kauffman, World Scientific, (1998).

[Kau99] L. H. Kauffman. *Virtual knot theory*. European J. Combin 20(7):663–690, (1999).

[Kaw] A. Kawauchi, *A Survey of Knot Theory*. Birkhäuser, (2012).

[KroMro] P. B. Kronheimer and T. S. Mrowka. *Gauge theory for embedded surfaces*, I. *Topology* 32(4):773–826, (1993).

[Kui] N. H. Kuiper,*A new knot invariant*. Math. Ann. 278, no. 1-4, 193-209, (1987).

[Kup] G. Kuperberg. *What is a virtual link?* Algebr. Geom. Topol. 3:587–591, (2003).

[LiLeiWu] Z. Li, F. Lei, and J. Wu. *On the unknotting number of a welded knot.* J. Knot Theory Ramifications 26(1):1750004, (2017).

[Lit] R.A. Litherland, *Deforming twist-spun knots*, Trans. Amer. Math. Soc. 250, 311–331, (1979).

[PraMis] R. Mishra, & M. Prabhakar. *Polynomial representation for long knots.* arXiv: Geometric Topology, (2001).

[Man] V. Manturov & V.O.Manturov, *Knot Theory: Second Edition* (1st ed.). CRC Press. https://doi.org/10.1201/9780203402849(2004)

[MAP] The Manifold Atlas Project, *Embeddings in Euclidean space: an introduction to their classification*, `http://www.map.mpim-bonn.mpg.de/Embeddings_of_manifolds_with_boundary:_classification`

[Mis09] R. Mishra, *Minimal Degree Sequence for Torus Knots.* Journal of Knot Theory and Its Ramifications, 759-769, (2009).

[Mis14] R. Mishra, *.Polynomial Unknotting and Singularity Index.* Kyungpook mathematical journal. 54. 271-292. 10.5666/KMJ.2014.54.2.271, (2014).

[Nel] S. Nelson. *Unknotting virtual knots with Gauss diagram forbidden moves.* J. Knot Theory Ramifications 10(6):931–935, (2001).

[Rod] O. Rodrigues, *Des lois géométriques qui régissent les déplacements d'un système solide dans l'espace, et de la variation des coordonnées provenant de ces déplacements considérés indépendamment des causes qui peuvent les produire.* Journal de mathématiques pures et appliquées, 5, 380-440, (1840).

[Rol] D. Rolfsen, *Knots and Links*, isbn=9780821834367, lccn=2003061249,AMS Chelsea Publishing Series, (2003).

[Ros] D. Roseman, *Reidemeister-type moves for surfaces in four-dimensional space.* Banach Center Publications 42.1: 347-380, (1998). ¡http://eudml.org/doc/208817¿.

[Rou] C. Rourke. *What is a welded link?* Intelligence of low dimensional topology 2006, 263–270, Ser. Knots Everything, 40, World Sci. Publ., Hackensack, NJ, (2007).

[Rud] W. Rudin, *Principles of mathematical analysis*, International Series of Pure and Applied Mathematics, (1953).

[Sat00] S. Satoh. *Virtual knot presentation of ribbon torus-knots.*J. Knot Theory Ramifications 9(4):531–542, (2000).

[Sat01] S. Satoh, *Minimal triple point numbers of some non-orientable surface-links*. Pacific Journal of Mathematics, 197, 213-221, (2001).

[Sat09] S. Satoh, *Sheet number and quandle-colored 2-knot*, Journal of the Mathematical Society of Japan, Volume 61, Issue 2, Pages 579-606, Released on J-STAGE July 01, 2009, Online ISSN 1881-1167, Print ISSN 0025-5645, (2009).

[Sat18] S. Satoh. *Crossing changes, delta moves and sharp moves on welded knots*. Rocky Mountain J. Math. 48(3):967–979, (2018).

[Sch] H. Schubert, *Über eine numerische Knoteninvariante*. Math. Z.61, 245–288, (1954).

[Sha] A. R. Shastri,*Polynomial Representation of knots*, Tohoku Math. J. (2) 44, 11-17, (1992).

[Shu] R. Shukla, *On polynomial isotopy of knot-types*. Proc. Indian Acad. Sci. (Math. Sci.) 104, 543–548, (1994).

[Sta] D. D. Stancu, *A Method for Obtaining Polynomials of Bernstein type of two Variables*. The American Mathematical Monthly, 70(3), 260–264, (1963). https://doi.org/10.2307/2313121

[Tak] Y. Takeda, *Introduction to virtual surface-knot theory*(Japan), Journal of Knot Theory and Its Ramifications, 21:14, (2012).

[Vir] O. Ya. Viro, Local knotting of submanifolds, Mathematics of the USSR-Sbornik, Volume 19, Issue 2, 166–176, (1973).

[Win] B. Winter. *The classification of spun torus knots*. J. Knot Theory Ramifications 18:1287–1298, (2009).

[Yaj] T. Yajima. *On the fundamental groups of knotted* 2*-manifolds in the* 4*-space*. J. Math. Osaka City Univ. 13:63–71, (1962).

[Zee61] E. C. Zeeman. *Knotting manifolds*. Bull. Amer. Math. Soc. 67 (1) 117 - 119,(1961).

[Zee] E. C. Zeeman, *Twisting spun knots*. Transactions of the American Mathematical Society, 115, 471-495, (1965).